VOLUME VI APRIL, 1941 NUMBER 2

GEOPHYSICS

A Journal of General and Applied Geophysics

APPLICATION OF THE FOURIER INTEGRAL TO SOME GEOPHYSICAL INSTRUMENT PROBLEMS*

W. T. BORN† AND J. M. KENDALL†

ABSTRACT

This paper considers only the simple part of Fourier Integral theory required for the work in hand. A special type of Henrici rolling sphere harmonic analyzer has been built which makes possible a large reduction in the amount of labor involved in dealing graphically with Fourier Integral operations. Examples of the use of this procedure as applied to several geophysical instrument problems are given.

The availability of a graphical means of dealing with Fourier Intregral analysis provides a direct method of attacking many geophysical problems. This paper discusses the simple part of Fourier Analysis theory required for the work in hand, describes the graphical means used, and gives the results of this application to several geophysical instrument problems.

Before describing the actual work, it will be helpful to compare the Fourier Integral with the Fourier Series, inasmuch as familiarity with the Fourier Series is almost universal.

Any periodically recurring phenomenon $\phi(t)$ may be represented by Fourier Series as the sum of an infinite number of sinusoidal components, $F(in\omega_0)$, whose frequencies are in harmonic ratios. In complex notations:[1]

$$\phi(t) = \sum_{-\infty}^{+\infty} F(in\omega_0)e^{in\omega_0 t}, \qquad (1)$$

* Read at Mid-Year Meeting at Houston, Texas, November 20, 1937. Manuscript received Feb. 18, 1941.

† Geophysical Research Corporation, Tulsa, Oklahoma.

[1] Cf. Carson· *Electric Circuit Theory and Operational Calculus*, McGraw-Hill 1926, p. 174 ff.

where

$$F(in\omega_0) = \frac{1}{T}\int_0^T \phi(\tau)e^{-in\omega_0\tau}d\tau. \tag{2}$$

$$i = \sqrt{-1},$$

$$n = 1, 2, 3, \cdots$$

$F(in\omega_0)$ is the nth harmonic. $\sum_{-\infty}^{+\infty} F(in\omega_0)$ may be considered as being a "line" spectrum, since it contains only the discrete frequencies $(n\omega_0/2\pi)$.

If, on the other hand, a phenomenon $\phi(t)$ is transient, existing only within a definite interval of time, $O<t<T$, then it cannot be described by a Fourier Series. Transients of this sort may however be represented by the Fourier Integral which, in complex notation, may be written:

$$\phi(t) = \int_{-\infty}^{\infty} F(i\omega)e^{i\omega t}d\omega, \tag{3}$$

where

$$F(i\omega) = \frac{1}{2\pi}\int_0^T \phi(\tau)e^{-i\omega\tau}d\tau \tag{4}$$

is the complex value of the sinusoidal component at any ω. $F(i\omega)$ is a continuous spectrum.

There is an obvious similarity between the two equations (1) and (2) on the one hand and Equations (3) and (4) on the other. It is, therefore, not surprising to find a corresponding similarity between the results of the analyses of the two processes, as is shown by the following illustrations of each.

As an illustration of the use of the Fourier Series, we shall consider the analysis of the steady state rectangular wave, shown in Fig. 1(a), which is the $\phi(t)$ of Equation (1).[2] Fig. 1(b), the $F(in\omega_0)$ of Equation (2), shows the various sinusoidal components (harmonics) plotted against frequency. The frequency scale is in terms of a frequency f_0, defined as $1/T$, where T is twice the duration of one pulse. The zero frequency component (d.c.), f_0 (fundamental), $5f_0$, $9f_0$, etc., are plotted as being positive, while $3f_0$, $7f_0$, etc., are plotted as being negative. The negative amplitudes signify that they are 180° out of phase with the

[2] Cf. Shea, *Transmission Networks and Wave Filters*, D. Van Nostrand Co. 1929, p. 401 ff.

positive amplitudes. This plot shows only a few of the most important components. Actually there are an infinite number of components extending to an indefinitely high frequency with the respective amplitudes diminishing with frequency.

As an illustration of the use of the Fourier Integral, we shall consider the analysis of a single rectangular pulse taken out of the above steady state rectangular wave. This single pulse is shown in Fig. 2(a),

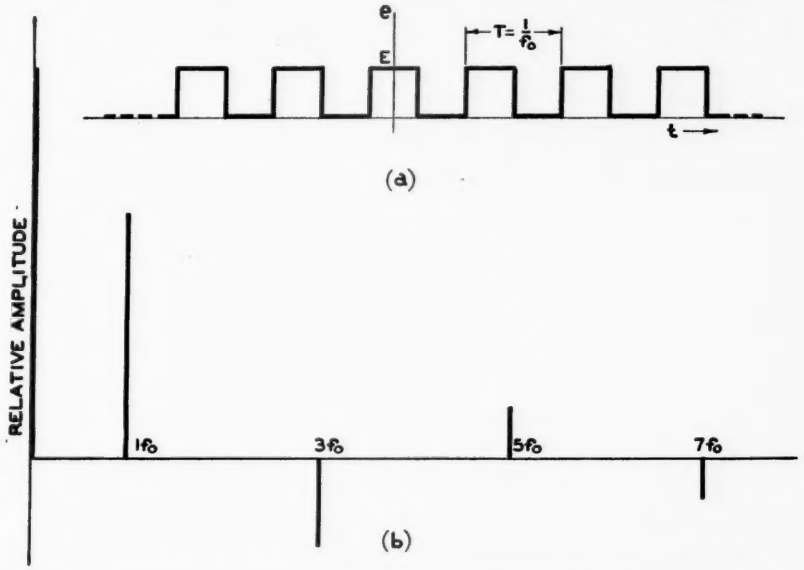

FIG. 1. (a) Steady state rectangular wave. (b) Frequency spectrum (Fourier Series coefficients) of above wave.

which is the $\phi(t)$ of Equation (3). Fig. 2(*b*) shows the $F(i\omega)$ of Equation (4) with its continuous distribution of amplitudes of the steady state sinusoidal components. As before, the negative values are 180° out of phase with the positive values. Likewise, the spectrum extends indefinitely up the frequency scale with diminishing amplitudes. Corresponding to components of Fourier Series given in Fig. 1(b), the components of Fig. 2(b) have their largest amplitudes in the vicinity of f_0, $3f_0$, $5f_0$, $7f_0$, etc. The similarity of these two spectra is quite apparent.

The spectrum of the second illustration above differs in two respects from the general case which is of interest in connection with geophysical problems. In geophysical work, spectra or frequency

characteristics are contained within the interval defined by a low frequency cutoff and a high frequency cutoff. Amplitudes at frequencies existing outside of this "pass band" may be ignored. This circumstance is of great help in dealing with spectra in a manner considered later on in this paper. Another difference from the general case concerns the phase angle. The phase angle in the illustrations given above is either zero, or 180°, because of the simplicity of these special cases.

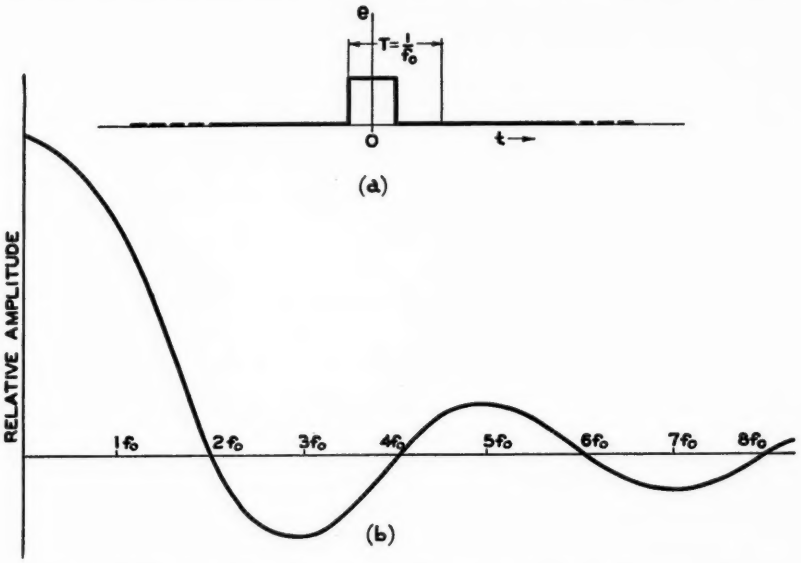

FIG. 2. (a) Single rectangular pulse. (b) Frequency spectrum of above pulse.

In general, however, the phase angle is also an arbitrary function of frequency. Therefore, a second curve, which we shall call the phase curve, must be plotted simultaneously with the amplitude curve to specify a spectrum that is complete. Henceforth, in this paper, the term "spectrum" will include the amplitude together with the associated phase curve, and will be designated $F(i\omega)$.

By performing the analyzing operation specified by Equation (4) on a given transient $\phi(t)$ its spectrum $F(i\omega)$ is obtained. On the other hand, by performing the synthesizing operation specified by Equation (3) on a given spectrum $F(i\omega)$ the corresponding transient $\phi(t)$ is obtained. The practical value of the Fourier Integral concept lies in the fact that the spectrum $F(i\omega)$ may be dealt with exactly as if it were a steady state phenomenon. Thus, if $F(i\omega)$ is modified in some

such manner as by passing it through a system with a frequency characteristic $F_S(i\omega)$, a new spectrum $F(i\omega) \cdot F_S(i\omega)$ is obtained, which, when synthesized, will give the modified transient.

Several examples of application of this procedure to seismic problems may be mentioned. Its use in obtaining the true ground motion by correcting the record for the frequency and phase distortion of the instruments will be presented in detail. Another application is that of determining what the shape of a reflection pulse would have been if the instruments used had different characteristics. In this connection it might be stated further that the Fourier Integral method permits the prediction of the performance of instruments having arbitrarily assigned frequency and phase characteristics, even though these characteristics may be extremely difficult or even physically impossible to obtain.

Tables[3] have been prepared which contain nearly all known analytical solutions of Equations (3) and (4). However, such tables are seldom of assistance in the study of purely arbitrary functions such as are characteristic of geophysical phenomena. It is therefore necessary to fall back upon a more direct method of solution.

In order to use Equations (3) and (4) in the graphical method to be described, these equations must be rewritten to bring them into the real form, thus:

$$\phi(t) = 2\int_0^\infty F(\omega)\left[\cos\theta(\omega)\cos\omega t + \sin\theta(\omega)\sin\omega t\right]d\omega, \tag{5}$$

$$F(i\omega) = \left[F(\omega), \theta(\omega)\right], \tag{6}$$

$$F(\omega) = \frac{1}{2\pi}\left\{\left[\int_0^T \phi(t)\cos\omega t dt\right]^2 + \left[\int_0^T \phi(t)\sin\omega t dt\right]^2\right\}^{1/2},$$

$$\tan\theta(\omega) = \int_0^T \phi(t)\sin\omega t dt \div \int_0^T \phi(t)\cos\omega t dt.$$

$\phi(t)$ exists only in the interval $O<t<T$.

Examination of Equations (5) and (6) shows that if we had a rapid method of evaluating $\int F(x)\sin ax\,dx$ and $\int F(x)\cos ax\,dx$ the most laborious part of the procedure would be eliminated. For this purpose, the junior author has designed a special form of a Henrici rolling

[3] G. A. Campbell, "Practical Applications of the Fourier Integral." Bell System Technical Journal, October, 1928.

sphere analyzer. Fig. 3 shows this device as constructed at the laboratory of the Geophysical Research Corporation. The sphere, which is a large ball-bearing ball, rests on a roller so arranged that when the tracing pointer is traced over the curve representing the transient, the sphere is rotated on a horizontal axis by an amount proportional to the instantaneous amplitude of the curve bing traced. Two integrating cylinders with dial indices rest against the equator of the sphere at points 90° apart. By means of a silk thread on two stepped pulleys,

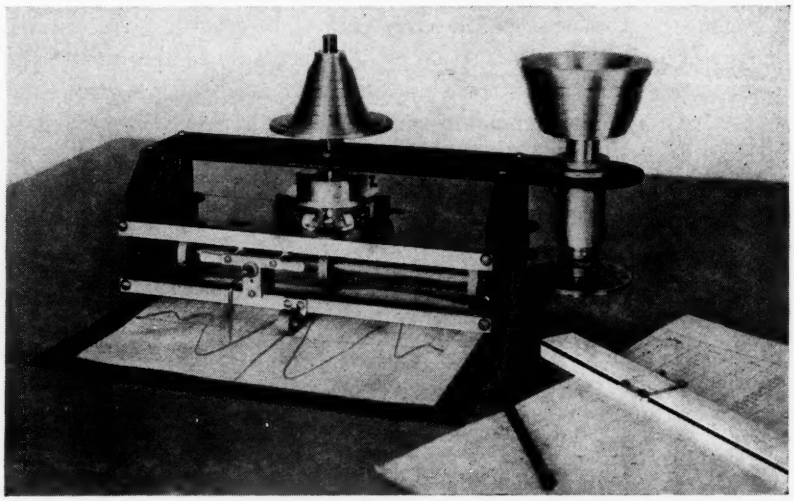

FIG. 3. Fourier Analyzer built at Geophysical Research Corporation Laboratory.

the sphere and the two integrating cylinders are given a rotation about a vertical axis proportional to the movement along the time axis of the curve being traced by the tracing stylus. While the sphere rolls in amplitude and simultaneously rotates, the cylinders take up components of the movement in amplitude which are proportional to the respective sine and cosine components of the spectrum at a particular frequency. The stepped pulleys provided for rotating the cylinders and sphere are arranged to give 100 different ratios. Thus if the transient to be analyzed is contained within the frequency range of 1 c.p.s. to 100 c.p.s., a point on the spectrum curve may be obtained every cycle if desired. The dials connected with the two cylinders read the sine and cosine components respectively, which must be added vectorially to get the magnitude of the spectrum $F(\omega)$ for each frequency. The sine component divided by the cosine component gives the tangent of the

corresponding phase angle $\theta(\omega)$. It should be noted that a single tracing of the pointer over the curve being analyzed, yields but a single point on the frequency spectrum curve and a single point on the phase curve. To obtain the complete frequency spectrum and phase curve for a complicated transient many tracings are required for properly defining the two curves.

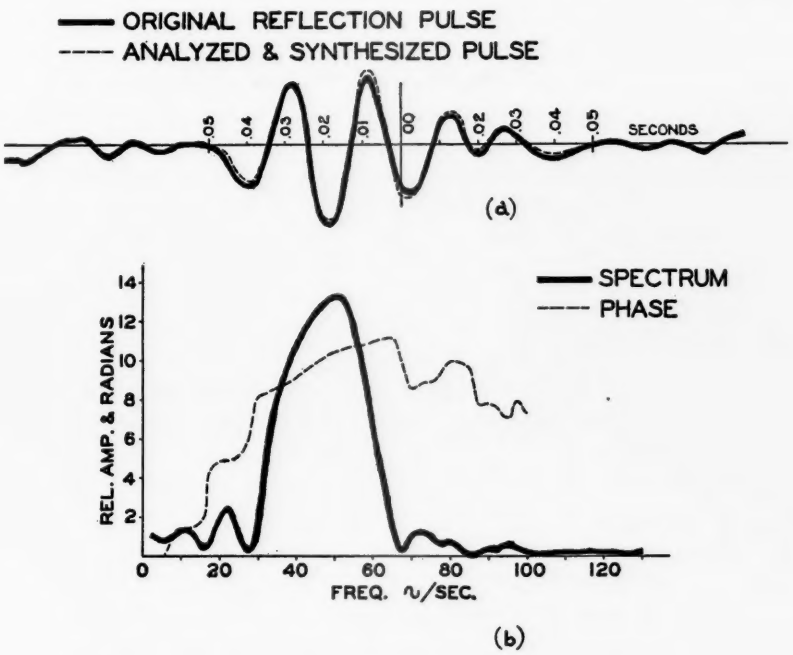

FIG. 4. (a) A selected reflection pulse as taken from a record.
(b) Spectrum and phase curve of above pulse.

Fig. 4 shows a selected reflection pulse of a typical shape, and below it, the spectrum obtained by analyzing it in the fashion just described for approximately 50 points. This spectrum contains exactly the same information as does the transient itself but, so to speak, the information is expressed in a different language. As a check of the accuracy of the analysis, the spectrum was synthesized to give back the transient and the result is shown by the dotted line plotted on top of the original transient.

The relation of the spectrum to the original record may be checked qualitatively by noting that the predominating frequency of the re-

corded pulse is about 50 c.p.s. and that the maximum amplitude of the spectrum comes at this same frequency. Very little energy resides in frequencies below 30 c.p.s. and above 70 c.p.s. The low frequency cutoff may be ascribed principally to the recording system characteristics, but the high frequency cutoff reflects the lack of higher frequencies in the transient itself. The high frequency cutoff of the recording system used was well above 100 c.p.s.

An attempt will now be made to find the true earth motion responsible for this reflection pulse. The procedure for doing this is quite simple. The spectrum of the pulse, which we shall call $F_1(i\omega)$, is divided by the over-all frequency characteristic $F_2(i\omega)$ of the instruments to obtain a new spectrum, $F_3(i\omega)$. That is,

$$\frac{F_1(i\omega)}{F_2(i\omega)} = F_3(i\omega).$$

$F_3(i\omega)$ is the spectrum of the true earth motion. Synthesizing $F_3(i\omega)$ according to Equation (5) should give the true earth motion. This has been done and the result is shown in Fig. 5.

The accuracy of the low frequency end of the corrected spectrum $F_3(i\omega)$ is very poor because of the stringent low frequency discrimination of the recording system used. That is, $F_2(i\omega)$ is very small for low frequencies, while $F_1(i\omega)$ is not small. Therefore, the effect of errors of small absolute amount in the low frequency end of $F_2(i\omega)$ are greatly magnified, and hence the accuracy of $F_3(i\omega)$ is poor. The fundamental difficulty in attempting to calculate true earth motion from an ordinary reflection record by any possible means is the fact that recording systems commonly used have extreme discrimination at low frequencies. The necessary condition to be met in attempting to obtain the true earth motion accurately is that the recording instruments have sufficient band width to pass at least an appreciable percentage of all portions of the spectrum of the true earth-motion pulse. Then, the correction necessary for compensation of the instruments will not be excessive, and therefore, the true earth-motion spectrum may be closely approached.

The synthesis of the true earth-motion spectrum has not been carried out for the entire length of the pulse because the large amplitudes of the low frequencies present in it cause it to stretch out to a great distance in both directions. Presumably the low frequencies are ground roll. A comparison of the true earth-motion character with the recorded character brings out what has been recognized for a long time

—that is, the great improvement in reflection character when the frequencies below 20 c.p.s. are suppressed.

Filters, amplifiers, and other instruments are usually designed to have a specified amplitude-frequency characteristic, but little attention is generally paid to the phase characteristic. This is probably due to difficulties in obtaining an instrument design in which both characteristics are simultaneously specified. However, such a design could

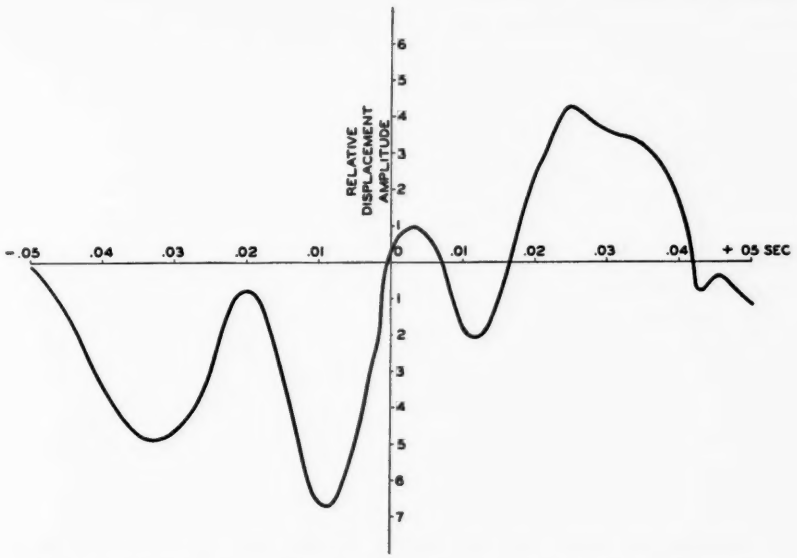

FIG. 5. True earth motion obtained by correcting Fig. 4 (a) for the frequency and phase distortion of the instruments.

be realized approximately if a complicated electrical network were used. In the following example it is assumed that a network having an arbitrarily assigned phase characteristic is added into the recording channel, and its effect on reflection character is investigated. In carrying out this investigation, it was decided to see how Fig. 6(a) would appear if the recording instruments used had been free from phase distortion. In other words, the over-all characteristic of the instruments, $F(\omega)$, $\theta(\omega)$, must be modified to $F(\omega)$, kw, where k is a constant. The phase characteristic, kw, having the constant slope of k throughout, represents a simple time delay. To change $\theta(\omega)$ to kw requires that the special network to be inserted into the recording system will not change the $F(\omega)$ of the instruments, but will add in the negative

of $\theta(\omega)$. This was done as follows: The negative of $\theta(\omega)$ was added to the spectrum and phase characteristic of the pulse of Fig. 6(a) as recorded $F_r(\omega)$, $\theta_r(\omega)$, giving $F_r(\omega)$, $\theta_r(\omega)-\theta(\omega)$. Synthesis of this spectrum yielded the pulse shown in Fig. 6(b).

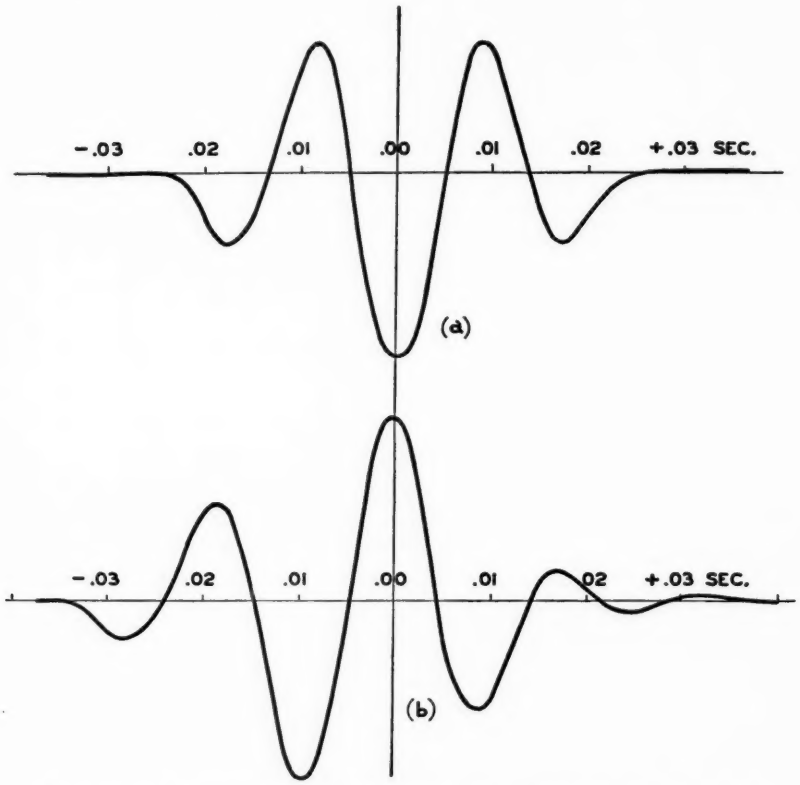

FIG. 6. (a) A symmetrical reflection pulse as recorded. (b) Same pulse corrected for phase distortion.

The particular reflection pulse shown in Fig. 6(a) is perfectly symmetrical and is preceded by a practically dead trace. The shape of this pulse is somewhat unusual because of its perfect symmetry, but such a shape is not extremely rare. The modified pulse Fig. 6(b) is not symmetrical and is of longer duration than the one actually recorded. The explanation of the longer duration lies in the fact that the original pulse is perfectly symmetrical, which is another way of saying that its phase curve $\theta_r(\omega)$ as recorded is already free from phase distortion.

When the phase distortion of the recording system is taken out, the resulting pulse then contains the negative phase distortion of the recording system. This is responsible for the loss of symmetry and the addition of the several small oscillations.

The removal of the instrumental phase distortion, in this particular case, degraded, rather than improved, the appearance of the record. However, it should not be concluded that this particular instrumental phase characteristic $\theta(\omega)$ was the best possible one. It is more probable that the phase characteristics of reflection pulses are random in nature, and that the instrumental characteristic just happened to fit the particular pulse chosen for this illustration.

In concluding, it may be pointed out that the Fourier Integral method of analysis offers the possibility of obtaining frequency characteristic of various instruments when no source of steady state variable frequency excitation is available. The basis of procedure is the substitution of an impulse excitation for the usual oscillator excitation. The spectrum of the impulse excitation must, of course, be known or obtainable. It is almost always a simple matter to devise a system, either electrical or mechanical, which will generate such an impulse. Thus, if no variable frequency oscillator is available for taking a frequency response curve of an amplifier and galvanometer, a sufficiently sharp impulse of voltage may be applied to the amplifier in place of the usual variable frequency voltage. The transient recorded by this procedure may be analyzed for its spectrum, which, in this case, will be the frequency characteristic of the amplifier and galvanometer. Another illustration of this method is the taking of an over-all frequency curve of the instruments from geophone to record without the use of a variable frequency shaking table. The geophone is subjected to a sudden movement, not necessarily an impulse, but one having a known spectrum. The spectrum of the resulting record is corrected for the spectrum of the applied movement. This corrected spectrum is the over-all frequency characteristic sought. Both of these procedures have been carried out in this laboratory with entirely satisfactory results. The frequency curve obtained from the analyzed transient method can be made to agree within one or two per cent with the curve obtained by the usual steady state method.

THE EFFECT OF THE PLACEMENT OF A SEISMOMETER ON ITS RESPONSE CHARACTERISTICS*

HAROLD WASHBURN† AND HAROLD WILEY†

ABSTRACT

A group of experiments were performed to determine the effect of the plant of a seismometer on the motion imparted to it by the ground. It was found experimentally that a seismometer and the ground form a resonant system. The characteristics of this system depend on the type and condition of the ground surface, the method of planting the seismometer and the seismometer weight and base area. Methods were devised for obtaining a satisfactory seismometer plant in areas where ordinary surface plants introduce distortion into seismic records. The mathematical expression of Seismometer Response and Ground Admittance in terms of experimentally measurable quantities is given in the appendix.

INTRODUCTION

In the last few years many difficult field problems in seismic reflection work have been met and at least partially solved by increasing the number of traces and the number of seismometers per trace used for each record. The use of a large number of seismometers has definitely improved the quality of the records and made possible the use of longer spreads. It has also brought into prominence many questions concerning seismometer design and optimum methods of planting them in the field.

Experience shows that with certain types of seismometers it is often necessary to bury them in order to obtain good records. With a small number of seismometers this presents no particular disadvantage. However, as the number is increased it is obvious that seismometers so designed as to give satisfactory records when "planted" on the surface are extremely advantageous.

This paper presents the results of experiments performed with the object of finding out the base area, weight and type of seismometer best suited for a surface "plant." It also includes results of an investigation of various surface conditions met in the field. This investigation was made to insure proper use of seismometers under all conditions.

The technique developed by the authors permits the study of surface conditions without the necessity of a seismic explosion, and

* Presented at the Annual Meeting, Chicago, April 11, 1940.

† United Geophysical Company, Pasadena, California.

thus avoids the many variations which result from size of charge, conditions of the shot hole, depth of shot, etc. The equipment is relatively inexpensive, portable, and requires only one operator.

INSTRUMENTS AND METHODS[1]

A schematic diagram of the measuring apparatus is shown in Fig. 1. The apparatus consists simply of two seismometers whose cases are bolted rigidly together. Both seismometers are of the dynamic type and their moving masses are small compared to their fixed masses.

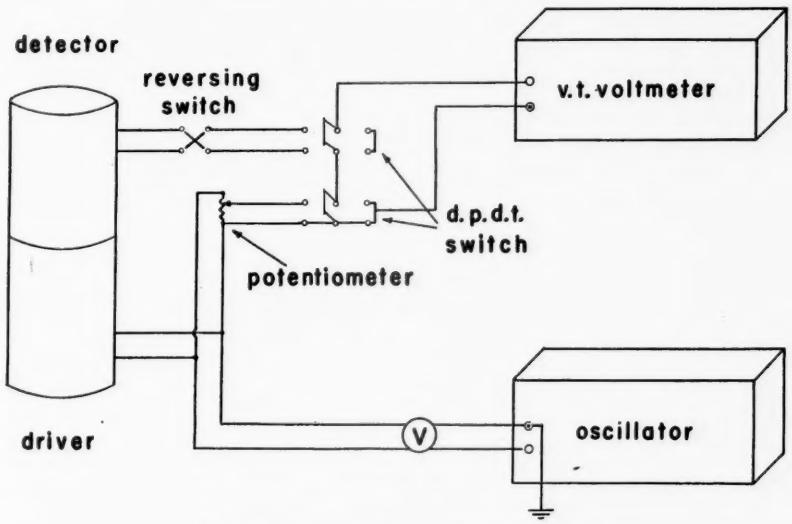

FIG. 1. Diagram of measuring equipment.

One serves as a driver unit to impart motion to the seismometer and ground, the other serves as a detector of the resulting ground velocity. The associated equipment includes a variable-frequency voltage source which actuates the driver-seismometer and a vacuum tube voltmeter for the voltage measurements. By means of the two double-pole double-throw switches and the reversing switch, the operator may quickly read on the vacuum tube voltmeter the detector output voltage, a fraction of the driving voltage, and the vector sum and difference of the two. From these data the phase angle between the detector and driving voltages may be readily computed. A voltmeter

[1] Patent applied for.

in the oscillator circuit indicates the voltage applied to the driver seismometer.

From these data taken with the seismometer planted and with the seismometer freely suspended one can determine the ground admittance and seismometer response.[2] The data for free suspension was obtained by hanging the seismometers on long rubber bands.

Seismometer response is defined in this paper as the ratio of the seismometer motion to the motion of the ground in the absence of the seismometer, expressed as a function of frequency. Ground admittance is defined as the ratio of the ground velocity to the force on the ground. The expression for seismometer response derived in the appendix is developed on the assumption that the portion of the ground whose motion is materially affected by the presence of the seismometer is limited in extent and that it can therefore be approximated by an equivalent electrical circuit containing lumped constants. The experimental justification for this assumption is given in a later section of this article.

EXPERIMENTAL RESULTS

Results of experiments carried out with this apparatus show that the motion of the ground immediately below the seismometer is in some cases very appreciably affected by the presence of the seismometer. Stated in another way, the ground and the seismometer act as a resonant system, and the resonant frequency is sometimes near that of the reflected seismic energy. The seismometer response as defined above will be peaked at this resonant frequency. Hence any differences among individual seismometer plants may introduce serious amplitude and phase distortions on the seismic record, and the careful matching of recording instruments is then vitiated.

The characteristics of this resonant system and the resulting seismometer response depends on many factors—factors contributed by both the ground and the seismometer.[3] The effect of each of these factors on the seismometer response will now be discussed.

EFFECT OF THE BASE AREA OF THE SEISMOMETER ON ITS RESPONSE

Before the experiments were performed it was expected that the peak frequency of the seismometer response would be materially

[2] See Appendix for derivation of expressions used in determining these quantities.

[3] Patents applied for on seismometer designs and field procedures.

higher with a larger seismometer-base area. If this were the case, seismometers of base area large enough to insure a resonant frequency well above the range recorded could be used. With normal methods of planting, however, an increase of seismometer base did not yield the expected result. The largest variation observed showed that a change of base area from 1.3 to 80.0 square inches less than doubled the peak frequency of the plant. In many locations no change in resonant fre-

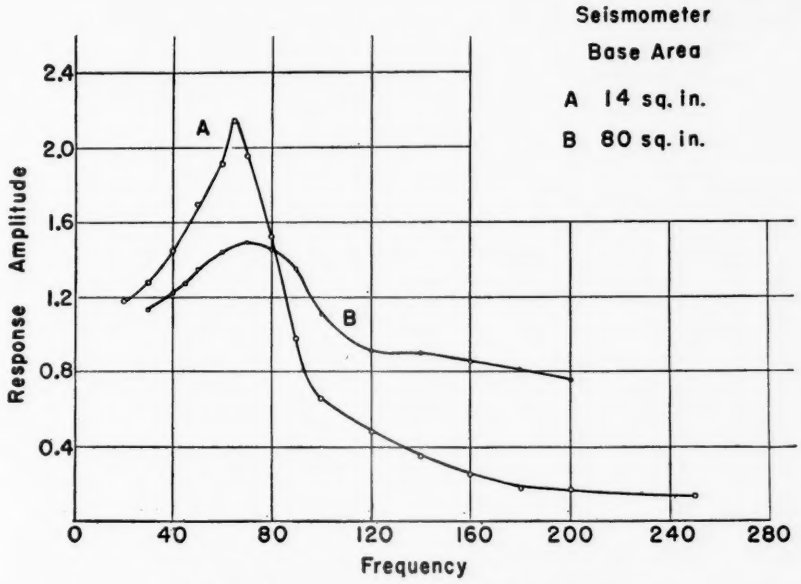

FIG. 2. Seismometer response for two base areas.

quency with base area was observed. The lack of variation of resonant frequency with increased base area was not due to added weight, since the total weight was changed less than ten per cent in making these base area changes.

This absence of frequency change may be due partially to the fact that the area of actual contact between the seismometer and the ground is only a fraction of the base area. It may also be due partially to the fact that with the smaller base areas the ground immediately below the seismometer is subjected to a higher pressure upon planting the seismometer and thus is more highly compacted with a resulting increase in rigidity.

An increase in base area does, however, produce a definite drop

in the peak amplitude of the response and a decrease in the sharpness of resonance. A flatter and more uniform response curve is, obtained, therefore, as shown in Fig. 2. In the figure shown, the seismometer was placed on a wet, muddy surface, giving a peak at approximately 65 cycles per second for a seismometer base area of 14 square inches. An increase in area to 80 square inches changes the peak frequency only 5 cycles per second but broadens the peak and lowers the amplitude

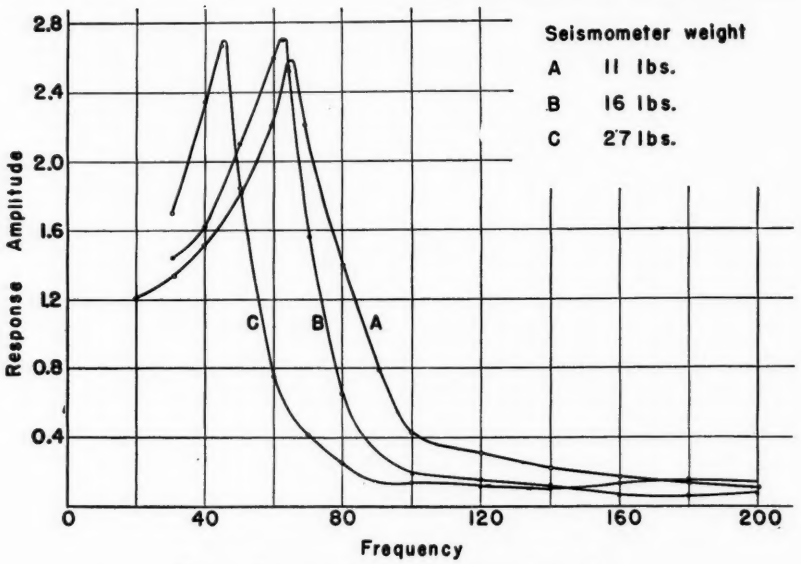

FIG. 3. Response for three seismometer weights.

considerably, thus producing a more uniform response curve. It must be emphasized that when large areas were used much more time and effort was consumed in arranging the seismometer plants than would be possible in field operation. Thus, the increased time necessary to prepare a profile as well as the awkwardness and additional weight of large seismometers make the selection of the optimum base area a compromise between an area large enough to materially flatten the response and an area small enough to facilitate rapid operation.

EFFECT OF WEIGHT OF THE SEISMOMETER ON ITS RESPONSE

Seismometer response curves were obtained for weights ranging from eleven to thirty-four pounds. The results indicate that a reduction in weight raised the peak frequency. The increase in peak frequency resulting from a weight change from thirty-four to eleven

pounds ranged from 20 to 60 per cent, depending on the type of ground surface. These results indicate that seismometers for field work should be light in weight. It is not necessary, however, to go to extremes in this direction, since in areas that give unusually poor surface plants, other practical means such as burying the seismometers may be used to obtain satisfactory records.

Fig. 3 shows the seismometer response curves for seismometer weights of 11, 16, and 27 pounds. The curves are very similar in sharp-

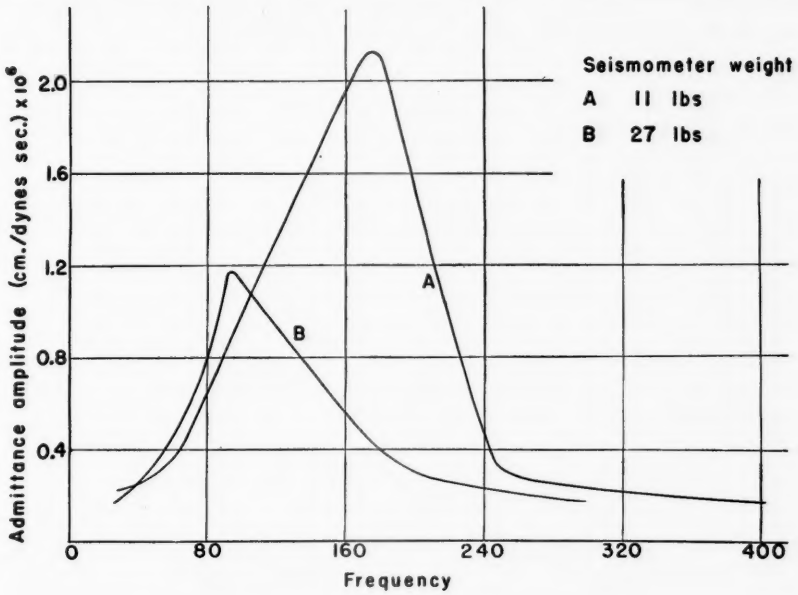

FIG. 4. Ground admittance for two seismometer weights.

ness and amplitude, but the peak frequency is twenty cycles lower in the case of the heaviest seismometer.

The ground admittance curves for two seismometers of different weights in the same region are shown in Fig. 4.

EFFECT OF THE TYPE AND CONDITION OF THE GROUND SURFACE ON SEISMOMETER RESPONSE

The resonant characteristics of a seismometer plant are to a large extent determined by the type and condition of the surface on which the seismometer rests. The peak frequency and the amplitude at the peak of response for surface plants is given in Table I, for several types

of soils and surface conditions. All frequency values given in this Table are for 11 pound seismometers, with a base area of 14 square inches. It is evident from this Table that seismometer plants on moist or wet ground and on plowed ground have low peak frequencies.

TABLE I

RESPONSE PEAK FREQUENCY AND AMPLITUDE FOR DIFFERENT TYPES OF GROUND

Surface	f_0, (*cycles per sec.*)	*Peak Amplitude*
1. Pure dry sand	130	2.0
2. Dry black gumbo	125	1.7
3. Dry sandy clay (plowed)	67	2.9
4. Hard grassy ground	200	3.1
5. Dry sandy clay loam	90 to 130	2.5
6. Damp sticky gumbo (plowed)	68 to 93	1.6
7. Wet sandy mud	61 to 80	2.2
8. Very wet sandy mud	48 to 65	4.6 to 1.8
9. Wet spongy loam	70	2.4
10. Asphalt road	470	1.9

Tests for surface plants taken in February, April and July, shown in Table II, indicate a rise in resonant frequency with the drying of the ground over a long period. These plants were made almost on the same spot and represent the average of many measurements. In February the ground was quite moist from frequent rains, while in July

TABLE II

THE RISE IN PEAK FREQUENCY WITH DRYING OF THE GROUND

Month	f_0
February	120
April	165
July	230

it was dry enough to powder. Thus, the season of the year plays a part in determining the characteristics of a plant in a given region.

Fig. 5 shows the complete response curves for several of the surfaces. It is important to note that those curves which have the highest peak frequency also have the highest amplitude at peak, but in the lower frequency range significant in reflection seismic prospecting they are more nearly flat.

All of the data given so far are for seismometers in which the ratio of moving mass to fixed mass is small. If the moving mass is not small enough to be neglected the response curve becomes more complicated. The moving part of the seismometer becomes closely coupled to the ground, and hence the seismometer frequency and damping become dependent on the plant. The effect of these factors on the response of the seismometer for any given plant will depend to a large extent on

the frequency and damping of the seismometer. In any given case, before attempting to use surface plants with a seismometer having a heavy moving mass, the effect of the plant on the response of the seismometer should be thoroughly investigated.

One particular case was investigated in our laboratory. An equivalent electrical circuit was made which had approximately the same impedance characteristics as the ground for an average surface plant.

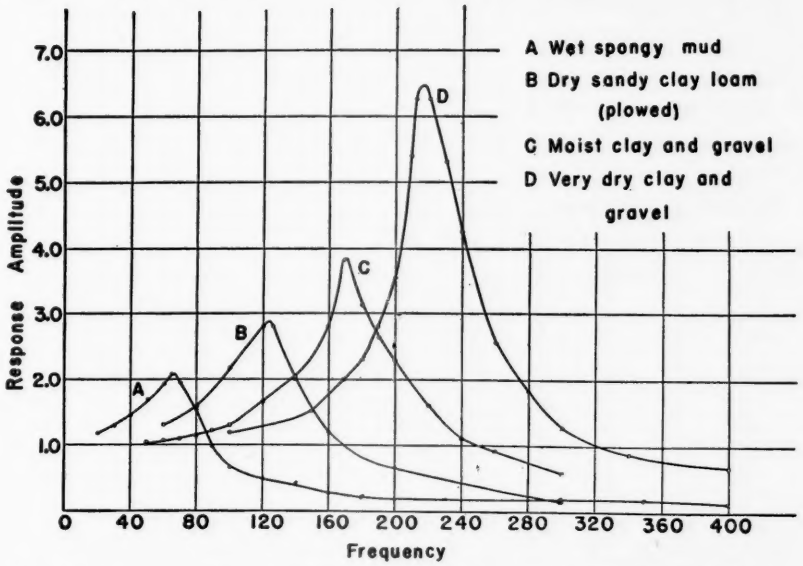

FIG. 5. Seismometer response for several types of ground and surface conditions.

This circuit was connected to an equivalent electrical circuit of a seismometer which in turn was connected to a standard field amplifier and galvanometer. A transient was applied to this combination of equivalent circuits and the output wave form recorded. The seismometer circuit was then altered so that only the ratio between the moving mass and fixed mass was changed. The frequency and damping and plant of the seismometer remained unchanged. The output wave form was recorded. The results of these experiments are shown in Fig. 6. These wave forms show that the recorded output, when using the seismometer with a very light moving mass, is practically unaffected by an average surface plant. On the other hand, the recorded output, when using the seismometers having a heavy moving mass, is materially affected by an average surface plant.

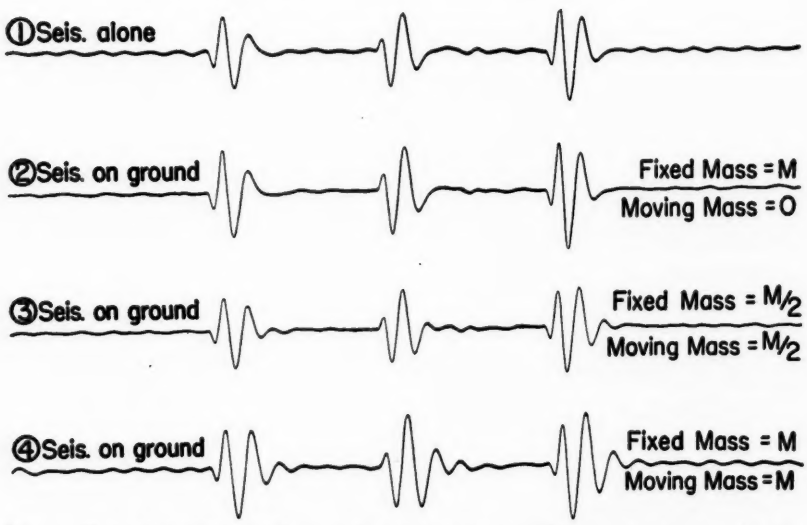

FIG. 6. Transient response of ground, seismometer, amplifier and galvanometer for different weights of seismometer moving element.

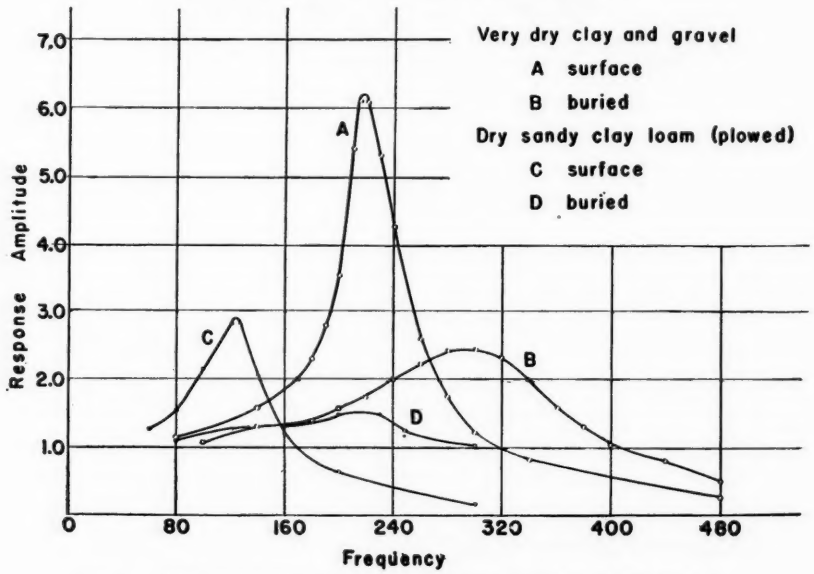

FIG. 7. Seismometer response for surface plant and auger-hole plant.

METHODS OF IMPROVING THE SEISMOMETER PLANT

In regions where a normal plant on the surface has proved unsatisfactory either by direct measurement or by a study of the seismic

records, one of several methods of improving the plant may be used. Perhaps the easiest is to bury the seismometer in an auger hole. This method is effective in many types of surfaces. Fig. 7 shows comparisons between the response curves for surface plants and buried plants for two types of surface. The marked difference between curves *A* and *B*, and between *C* and *D* is apparent. The rather sharp resonance of the surface plants is flattened considerably and the peak frequency raised by burying the seismometer. Merely placing the seismometer in an auger hole produces little change in resonant frequency. The raising of resonant frequency is obtained by thoroughly packing the ground around the seismometer to provide good contact between all of the seismometer and the ground.

This experiment, together with the anomalous results obtained in the base-area experiments, indicates that on all but very wet surfaces the relatively low peak frequency of surface plants is mainly the result of poor contact with the ground. To test this assumption a seismometer was cemented to the ground. An examination of the plant revealed that the cementing material penetrated only slightly below the surface, its main effect being to fill the small irregularities directly under the seismometer, yet the resonant frequency was raised from 220 to 410 cycles per second. This test clearly indicates that the thin layer of soil immediately below the seismometer may largely determine the seismometer response. For some cases, therefore, the approximate representation of the ground by a lumped constant network is fairly accurate.

After these preliminary studies were completed the next problem was to determine just how much effect the improper planting of seismometers would have on the character and accuracy of a record. The location chosen for this test was a very muddy slough surrounded by hard ground. The resonant frequency of the surface plant on the hard ground adjacent to the slough was 200 cycles per second. A surface plant on the muddy ground gave a resonant frequency of about 65 cycles per second for eleven pound and 56 cycles per second for sixteen pound seismometers. Burying the seismometer produced no material change. However, when the seismometers were placed on wooden posts driven about one foot into the mud, the resonant frequency was raised to over 300 cycles per second for an eleven pound seismometer. The response curves for a surface plant and for the seismometer on a post are shown in Fig. 8. The sharp peak of the surface plant and the relative flatness of the plant on the post in the lower frequency range is

easily seen. This is a very interesting result particularly in view of the fact that the mud was quite deep. The posts were easily driven and did not reach hard ground.

Two parallel spreads were set up about five feet apart, each partly on the hard ground and partly on the mud. In one spread the seismometers were placed on posts driven into the ground or mud. In the other spread no posts were used and where mud was encountered the seismometers were pushed down about one inch into the mud.

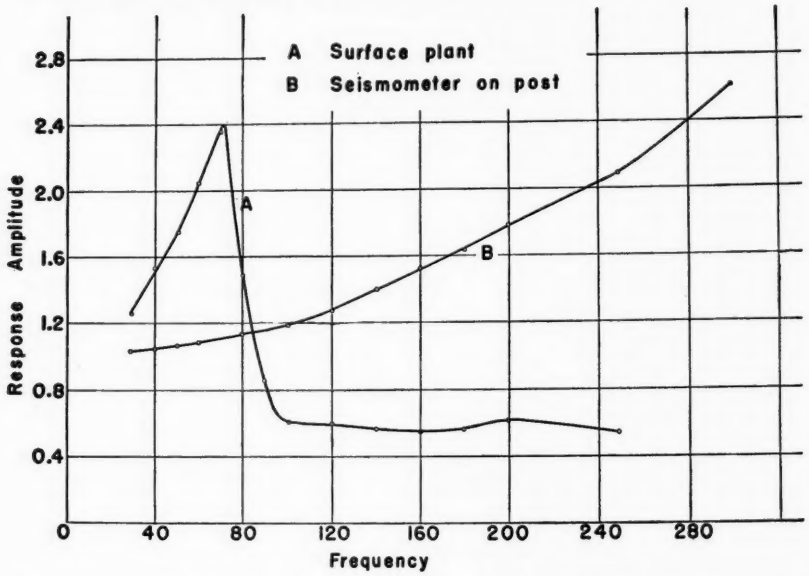

FIG. 8. Response for a seismometer planted on a muddy surface and for a seismometer planted on a short wooden post which was driven into the mud.

Fig. 9 shows two records taken with this setup. The upper half of each record corresponds to the seismometers planted on posts, the lower half to surface plants. Record No. 1, at the top of the figure was taken with six pound seismometers throughout. The surface plants in record No. 2 were 18 pound seismometers. All seismometers had very light moving elements. Traces 1 and 15 are from seismometers planted side by side, traces 2 and 14 from a similar pair, as are traces 3 and 13, 4 and 12, 5 and 11, 6 and 10, and 7 and 9.

The most striking feature of these records is the difference in appearance between the upper and lower halves. The predominant frequency in the lower half of the top record is about 75 cycles per

second. This value agrees closely with the extrapolated resonant frequency measurements made for surface plants on the mud. The predominate frequency in the lower half of record No. 2 is about 50 cycles per second. This value likewise is in agreement with the resonant frequency measurements. These results show that in the case of surface plants the frequency discrimination provided by the resonance

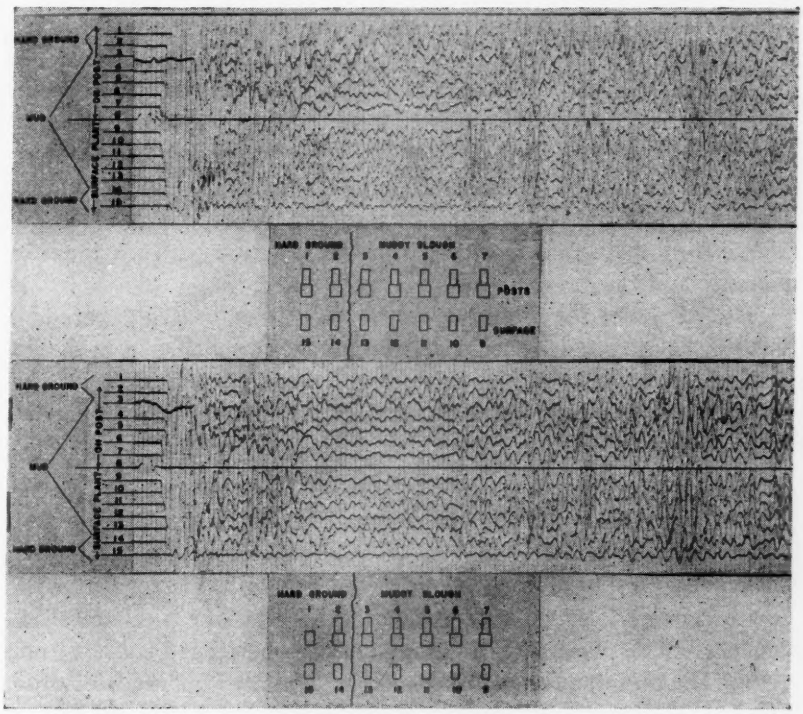

FIG. 9. Records taken to determine character change and error introduced by improper planting of seismometers.

cf the seismometer with the ground is sufficient to materially alter the character of the record.

The change from mud to hard ground comes between traces 2 and 3 and between traces 13 and 14. The records show that for surface plants (lower half of the record) there is a definite change in character in passing from mud to hard ground. A careful study has shown that there is a time error of about .002 of a second resulting from this character change. On the other hand it will be noted that there is little or

no change of character and hence no time error for this transition when the seismometers were planted on posts. This effect was to be expected since the resonant frequency of the plant on the posts is higher than the frequencies passed by the amplifier and oscillograph. Any energy generated at this high frequency is, therefore, not recorded. The absence of any noticeable effect of the resonant frequency of the plant as long as it is sufficiently high is demonstrated by the first two traces of the bottom record. Here the seismometers of the top trace were planted on the ground beside the seismometers of trace No. 2, which were on posts. The similarity of these two traces shows that a 200 cycles per second plant is just as good as a 300 cycles per second plant for the normal seismograph record. In other words, if the resonant frequency of the seismometer plant is sufficiently high so that the response is uniform within the range recorded, the record obtained will be free from distortion resulting from the reaction between the seismometer and the ground.

The results of the experimental work outlined in this paper show that the elastic constants of the ground must be considered in the design of a seismometer. Furthermore, with a seismometer that is properly designed it is permissible to use surface plants in many areas.

APPENDIX

The apparatus used for determining the seismometer response is shown diagrammatically in Fig. 1. The method of determining the seismometer response from the data obtained with this apparatus will now be given. The first assumption used is that the mechanical impedance of the plant may be represented by a lumped constant network. This assumption has been experimentally justified for some cases as explained in the main body of this paper. To simplify the derivation which follows, the mechanical parts of the seismometers and the ground have been represented by equivalent electrical circuits of the inverted type, according to well known methods.[4] The circuit representing the two seismometers bolted together and planted on the ground is shown in Fig. 10.

In Fig. 10:

Z_g = electrical impedance of equivalent circuit of ground and is

[4] F. A. Firestone, The Journal of the Acoustical Society of America, Vol. 4, 1933, p. 249.

H. W. Washburn, GEOPHYSICS, Vol. II, No. 3, July 1937, p. 248.

proportional to the mechanical admittance of ground. (velocity/force)

Z_d = electrical impedance of equivalent circuit of driver seismometer and is proportional to the mechanical admittance of driver seismometer. (velocity/force)

Z_s = electrical impedance of equivalent circuit of detector seismometer and is proportional to the mechanical admittance of detector seismometer. (velocity/force)

E = voltage across terminals 1 and 2 of equivalent electrical circuit and is proportional to the velocity of seismometer cases or velocity of ground.

e_d = voltage applied to driver seismometer.

e_s = voltage produced by detector seismometer.

e_g = voltage applied to equivalent electrical circuit of ground and is proportional to the velocity of ground a short distance below the surface.

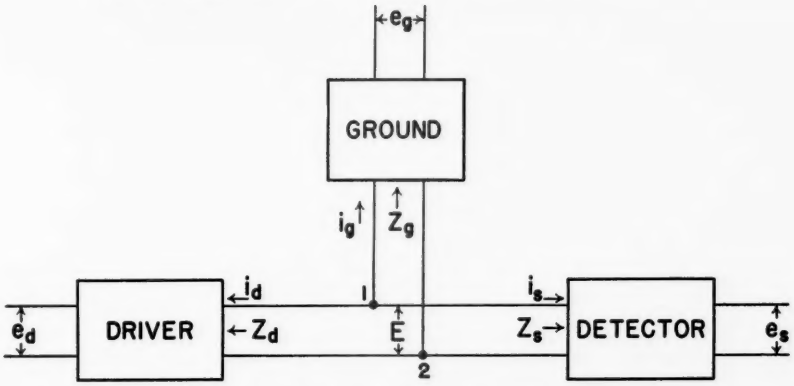

FIG. 10. Equivalent electrical circuit of two seismometers bolted together and planted on the ground.

First Thevenin's theorem[5] will be applied to the circuit for a voltage applied at e_g, Z_d and Z_s being at first disconnected and then connected to terminals 1 and 2. The resulting expression is:

$$\begin{aligned} i_s + i_d &= E_0/\{[Z_s Z_d/(Z_s + Z_d)] + Z_g\} \\ &= E_0/(Z_{sd} + Z_g) \end{aligned} \tag{1}$$

where i_s = current flowing into equivalent circuit of detector seismometer and is proportional to force applied to detector seismometer.

i_d = current flowing into equivalent circuit of driver seismometer and is proportional to force on driver seismometer.

[5] T. E. Shea, *Transmission Networks and Wave Filters*, page 55.

E_0 = voltage across terminals 1 and 2 with Z_d and Z_s disconnected and is proportional to the velocity of ground in the absence of seismometers.

$Z_{sd} = Z_s Z_d/(Z_s + Z_d)$

Equation (1) may be written in the form

$$R = (i_s + i_d)Z_{sd}/E_0 = 1/(1 + Z_g/Z_{sd}) \tag{2}$$

where R = seismometer response

$$= \frac{\text{seismometer velocity}}{\text{velocity of ground in absence of seismometer}}$$

since $(i_s + i_d)Z_{sd}$ = voltage across terminals 1, 2 and is proportional to velocity of seismometer cases.

Now Thevenin's theorem will be applied to the circuit shown in Fig. 10 for a voltage applied at e_d, Z_g being at first disconnected and then connected to terminals 1 and 2. The resulting expression is:

$$\begin{aligned} i_g &= E_0'/\{[Z_s Z_d/(Z_s + Z_d)] + Z_g\} \\ &= E_0'/(Z_{sd} + Z_g), \end{aligned} \tag{3}$$

where i_g = current flowing into equivalent circuit of ground and is proportional to force on ground.

Equation 3 may be written in the form:

$$Z_g/Z_{sd} = i_g Z_g/[E_0' - i_g Z_g], \tag{4}$$

where E_0' = voltage across terminals 1 and 2 with Z_g disconnected and is proportional to velocity of seismometer cases obtained with a given driving voltage e_d and with the seismometers freely suspended (on long rubber bands).

$i_g Z_g$ = voltage across terminals 1 and 2 and is proportional to the the velocity of seismometer cases obtained with the same driving voltage e_d as was used in determining E_0' but with the seismometers planted on ground.

Substituting equation (4) in equation (2) gives:

$$R = 1 - i_g Z_g/E_0'. \tag{5}$$

The quantities $i_g Z_g$ and E'_0 are not measured directly. The detector seismometer voltage e_s, however, is proportional to these quantities for any given frequency. Expression (5) may, therefore, be rewritten in the form:

$$R = 1 - \frac{(Ke_s)_{\text{planted}}}{(Ke_s)_{\text{free}}}$$

$$= 1 - \frac{(e_s)_{\text{planted}}}{(e_s)_{\text{free}}}. \tag{6}$$

In this expression $(e_s)_{\text{planted}}$ and $(e_s)_{\text{free}}$ are vectors. In order to determine the phase angle between these two measured voltage vectors they must be referred to e_d. Since, according to Thevenin's theorem, both $(e_s)_{\text{planted}}$ and $(e_s)_{\text{free}}$ are for the same e_d, expression (6) may be written:

$$R = 1 - \frac{(e_s/e_d)_{\text{planted}}}{(e_s/e_d)_{\text{free}}}. \tag{7}$$

Now for free suspension e_s is proportional to e_d at any given frequency. Consequently the value of R given by expression (7) is independent of the magnitude of $(e_d)_{\text{free}}$. Therefore, it is not necessary to take the free suspension and planted runs at the same voltage.

The data for determining response of any given plant is determined by finding the amplitude and phase of e_s/e_d at several different frequencies with the seismometers freely suspended and with the seismometers planted. The response is then calculated from equation (7). In determining the phase angle of e_s/e_d care should be taken in choosing the proper quadrant since the data taken at any single frequency does not in itself determine the quadrant.

If instead of the response it is desired to determine the ground admittance, equation (4) may be expressed as:

$$Z_g = \frac{Z_{sd}}{\dfrac{(e_s/e_d)_{\text{free}}}{(e_s/e_d)_{\text{planted}}} - 1} \tag{8}$$

where $Z_{sd} \cong 1/j\omega M_{sd}$

M_{sd} = mass of seismometer cases.

This approximation is good for a properly damped seismometer having a moving mass which is small compared with the fixed mass.

The ground admittance may be determined from equation (8) and data taken as described above for seismometer response.

THE ATTENUATION CONSTANT OF EARTH MATERIALS*

W. T. BORN†

ABSTRACT

This paper discusses briefly the nature of viscous losses and solid friction losses, both of which may cause sound waves to be attenuated as they travel through a physical medium. A simple experimental technique for determining the nature and magnitude of the loss factor in small rock samples is described, and data are given which indicate that solid friction losses are primarily responsible for the observed attenuation of the seismic waves employed in the seismic reflection method.

A method of estimating the attenuation factor of earth materials from seismic reflection records is outlined and it is shown that the values so obtained are not inconsistent with the laboratory data.

Frequency characteristic curves of seismic wave paths are derived on the basis of the experimental data.

INTRODUCTION

It is known from observation that plane sound waves traveling through any physical medium are attenuated, that is, their amplitude gradually decreases with distance traveled. It follows that the medium must, in some manner, extract energy from a sound wave passing through it. The amount of energy lost per unit distance of travel will, in general, be different for different media, and the mechanism of energy loss may differ in various media.

Even though the nature of the losses in a particular material may be unknown, it is obvious that the amplitude of a plane sound wave traveling through any continuous attenuating medium must decrease exponentially with distance. Expressed in mathematical symbols:

$$A_x = A_0 e^{-\alpha x} \tag{1}$$

where A_0 = Amplitude of wave at an arbitrary reference point.
A_x = Amplitude at distance, x, from reference point.
α = An attenuation factor.
e = Base of natural logarithms.

This equation simply states that, for each unit of distance traveled, the sound wave suffers the same percentage reduction in amplitude.

The problem involved in determining the attenuation characteristic of earth materials is therefore simply that of evaluating the loss factor, α.

* Presented at the Annual Meeting, Chicago, Illinois, April 11, 1940.

† Geophysical Research Corporation, Tulsa, Oklahoma.

By making the assumption that the losses are viscous in nature, that is, that they are proportional to the particle velocity of the wave disturbance, an expression for the attenuation factor can be simply derived. It is not surprising, therefore, to find in the literature of theoretical seismology a number of treatises on the absorption of seismic waves based on this assumption, the assumption being made simply for mathematical convenience.[1,2]

As early as 1890 Lord Kelvin performed some experiments on the torsional vibration of steel rods and showed that the results obtained were not in accord with a viscous-elastic theory. His results were later confirmed by other investigators, particularly by Kimball and Lovell.[3] By experiment, it has been found that the losses in a number of solid materials are not viscous losses but are of an entirely different type which is commonly called solid friction.[4]

Since the materials of the earth's surface layers are solids, it is rather surprising that the implications of the experimental work done with other solid materials have not been given much consideration by seismologists. The earliest paper in which the earth is considered to be other than an viscous-elastic material seems to be a theoretical paper by B. Derjagin published in 1931.[5]

The present paper describes an experimental method whereby the nature of the losses in small samples of consolidated earth materials may be directly determined and discusses the application of the results obtained to the problem of determining the attenuation constant of the surface materials of the earth.

VISCOUS LOSSES AND SOLID FRICTION

The difference between the effect of viscous losses and that of solid friction losses may be visualized by considering the stress-strain relationships existing when a cyclic stress is applied to an elastic material in which losses exist. In Fig. 1 is shown a stress-strain diagram drawn by plotting applied stress against the resulting strain. If the losses in

[1] N. M. Hosali, "On Seismic Waves in a Visco-Elastic Earth," Proc. Roy. Soc. (A), 104, 1923, p. 271.

[2] K. Sezawa, "On the Decay of Waves in Visco-Elastic Solid Bodies," Bull. Earthquake Res. Inst., Tokio, Vol. 3, 1927, p. 19; also ibid., Vol. 4, 1928, p. 107.

[3] A. L. Kimball and D. E. Lovell, "Internal Friction in Solids," Physical Review, Vol. 30, Dec. 1927.

[4] For a further discussion of solid friction see Kimball's book, *Vibration Prevention in Engineering*, John Wiley and Sons, 1932.

[5] B. Derjagin, Journal of Geophysics, Moscow, Vol. 1, No. 1–2, pp. 207–222.

the material are viscous in nature, the stress-strain diagram is an ellipse. The area included in the ellipse represents the energy lost per cycle, the latter being proportional to the frequency of the cyclic stress. For extremely slow motions the energy loss per cycle approaches zero and the ellipse degenerates into a straight line.

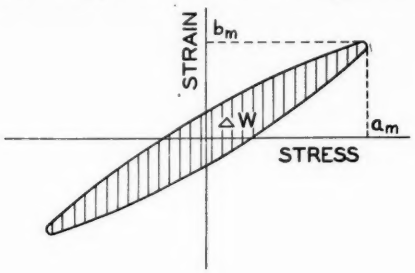

SOLID FRICTION

$$\triangle W = K a_m^2 = K b_m^2 E^2$$

WHERE

K = SOLID FRICTION FACTOR
E = ELASTIC CONSTANT
a_m = MAXIMUM STRESS
b_m = MAXIMUM DISPLACEMENT

VISCOUS DAMPING

$$\triangle W = K' a_m^2 f = K' b_m^2 E^2 f$$

WHERE

K' = VISCOUS LOSS FACTOR
f = FREQUENCY

FIG. 1. Stress-strain diagram.

If, on the other hand, the losses are caused by solid friction, rather than by viscous damping, then the energy lost per cycle is independent of frequency, i.e., the area included within the stress-strain curve is independent of the frequency of the cyclic stress, and depends only upon the nature of the material and the maximum strain amplitude.

The difference between viscous and solid friction losses may be expressed in another way: In an oscillatory system whose damping is caused entirely by internal losses in the elastic member of that system, the decrement of the system, is, if the damping is viscous:

$$\delta = R f_0, \tag{2}$$

where δ = Logarithmic decrement.
R = Constant involving the kinematic viscosity and elastic constant of the system.
f_0 = Natural frequency of the system.

On the other hand, if the damping is caused by solid friction losses, then

$$\delta = R'k \tag{3}$$

where R' = Solid friction constant.
k = Constant of proportionality.

The relationships of decrement to the type of damping present, expressed in Equations 2 and 3, indicate a method whereby the nature of losses in an elastic material may be investigated. It is merely necessary to employ the material in question as the elastic member of an oscillatory system, and to observe the natural frequency and decrement of that system in the absence of other forms of damping. For example, if it is desired to determine the nature of the losses in a piece of wire, the wire may be coiled into a helical spring and attached to a mass to form an oscillatory system. If this system is placed in vacuo to remove the effects of air damping, then the damping will be produced entirely by losses within the spring. If the mass is varied over any desired range, and the natural frequency and decrement corresponding to each mass are observed, it is a simple matter to determine whether the losses in the spring are viscous or due to solid friction. If the former, the decrement will be independent of the natural frequency of the system; if the ~~latter~~ former, it will be proportional to the natural frequency.

EXPERIMENTAL WORK ON ROCK SAMPLES

To determine the type of losses present in a number of earth materials a different technique was employed. A sample of rock, in the form of a bar is supported at its mid-point as shown in Fig. 2. A small

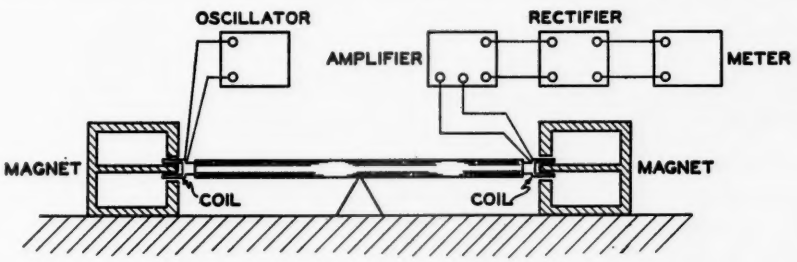

FIG. 2. Arrangement used to determine natural frequency and decrement of bar.

coil of wire is cemented to each end of the bar, and these coils are inserted in a magnetic field. Current from an accurately calibrated variable-frequency oscillator is applied to one coil to drive the bar. The resulting motion at the opposite end of the bar is detected by the

pickup coil, the output of which is amplified, and measured in any suitable manner.

The bar acts as a damped resonant system, the natural frequencies of which are given by:

$$f_n = \frac{nc}{2l} \tag{4}$$

where c = Velocity of longitudinal wave in bar.
l = Length of bar.
n = An integer.

If the driving current is held constant while the frequency of the oscillator is varied, the resonant frequencies may be detected by observing the increased output of the pickup coil. By varying the oscillator frequency in small steps on either side of a resonance frequency and observing the resulting output, data may be obtained from which a resonance curve can be plotted and the decrement of the system determined from the width of the resonance curve in the usual fashion.*

TABLE 1

Material	*Length in Inches*	*Resonant Frequency cycles/sec.*	*Decrement*
Sylvan Shale	(a) 5.5	12,800	.045
(Cut from Core)	(b) 11.0*	6,580	.042
	(c) 21.5*	3,360	.043
Hunton Limestone	(a) 7.4	10,550	.053
(Cut from Core)	(b) 28.6*	2,820	.044
Amherst Sandstone	(a) 33.6	1,260	.057
(Quarry Sample)	(b) 49.0	930	.062

All samples oven-dry

* Fabricated Bars

The viscous theory of damping requires that the observed decrement be directly proportional to the observed resonance frequency. It follows that, the longer the rod of a given material, the smaller should be its decrement. Similarly, if the harmonic modes of vibration are observed, then the decrement of the second harmonic should be two

* Most conveniently, by determining the frequencies, f_1 and f_2, on either side of the resonance frequency, f_r, at which the amplitude is reduced to .707 of its value at resonance. The decrement is then given by

$$\delta = \frac{\pi(f_1 - f_2)}{f_r}.$$

times that of the fundamental, etc. On the other hand, if the losses present are of the solid friction type, then the observed decrement should be independent of the length of the rod and independent of the order of the harmonic observed.

Two methods of observation may, therefore, be employed to ascertain whether the losses in the bar are viscous in nature or are of the solid friction type. One method is to observe the decrement in bars of various lengths cut from the same material; the other, to observe the decrement of the various harmonics in the same bar.

The values of the decrement in a number of rock materials have been determined in the manner described. Many of the specimens of most interest were cut from cores taken while drilling wells and are,

TABLE 2

Material	*Length in inches*	*Harmonic*	*Frequency cycles/sec.*	*Decrement*
Amherst Sandstone	33.6	1	1,260	.057
(Quarry Sample,		2	2,550	.061
oven-dry)		3	3,830	.060
Core from Cockfield-	12.6	1	3,650	.045
Yequa Formation		2	7,060	.047
(Air Dry)		3	10,900	.048

therefore, of limited length. However, it has been found possible to fabricate bars of considerable length by cementing short lengths together end to end and thus to determine the decrement of bars of various lengths. Table 1 shows representative data of this type.

The data shown in the above table indicate that the losses in the samples tested were primarily of the solid friction type; since the observed decrement is practically constant over a wide range of frequencies.

In Table 2 are listed some representative data obtained by determining the decrement of the fundamental and harmonic modes of vibration of bars of several materials.

These data also show that the decrement of the bars is not proportional to the frequency of the vibration but is essentially independent thereof; again leading to the conclusion that the losses present are of the solid friction type.

When experiments of this type were first performed, some difficulty was sometimes experienced in obtaining reproducible data. This difficulty was found to be caused by the effect of slight variations in the moisture content of some samples. To obtain consistent data it

was found desirable to dry the samples at 50°C. for a period of several days and then make the measurements as soon as they had cooled to room temperature. In general, when the previously dried samples were allowed to stand exposed to air, they absorbed moisture, and as they did so, their decrement increased while the velocity of sound in them decreased. A question, therefore, arose regarding the nature of the additional damping produced by the absorbed water: Is it viscous in nature or is it also of the solid friction type?

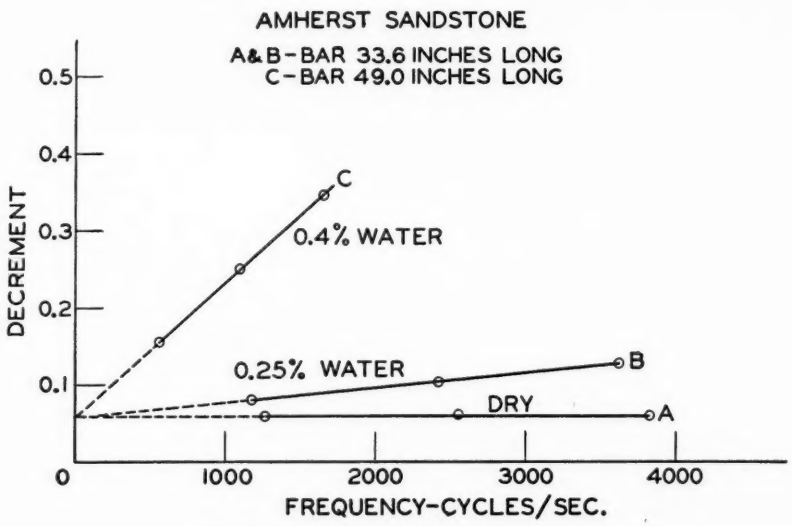

FIG. 3. Decrement of Amherst Sandstone.

To check this point, measurements were made on bars of Amherst Sandstone. This material was chosen because it had previously been found that small changes in the water content of that material produced large changes in its elastic constant.[6] The results of these measurements are shown graphically in Fig. 3, in which the observed decrements are plotted against frequency of the vibration observed. The decrement of the oven-dried bar is essentially independent of frequency as shown by the line *A*. The bars containing moisture show a decrement increasing with frequency. When extrapolated, the lines of the graph intersect near zero frequency. The obvious conclusion

[6] W. T. Born and J. E. Owen, "Effect of Moisture upon Velocity of Elastic Waves in Amherst Sandstone," Transactions Society of Petroleum Geophysicists, Vol. V, page 9.

is that the total decrement is the sum of a decrement which is independent of frequency and a decrement proportional to frequency. Presumably, therefore, both viscous and solid friction losses are present.

Fig. 4 is a graph of other data pointing to the same conclusion. These data* are measurements made on an unusually long core of cap rock, (gypsum and anhydrite) from the dome at Orchard, Texas. This specimen was tested only in an air-dry condition. Because of the long length of this sample, it was found possible to determine the decrement

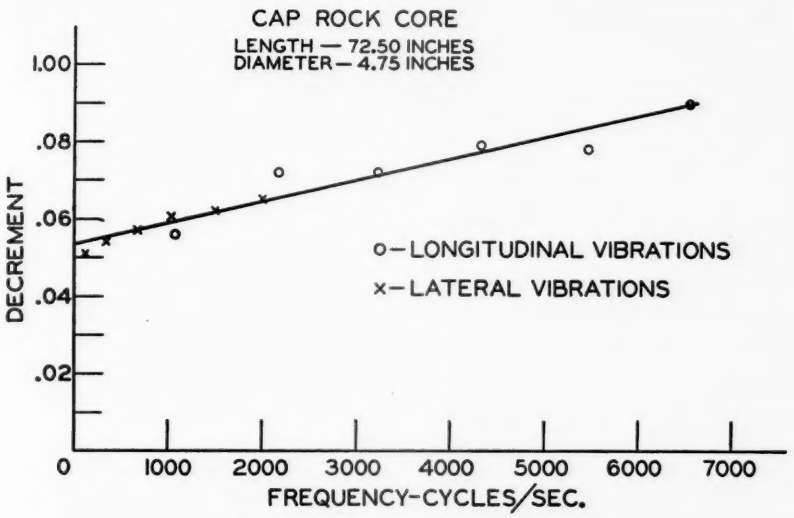

FIG. 4. Decrement of cap-rock core.

of six modes of lateral vibrations of the bar as well as that of six harmonic longitudinal vibrations. The lateral vibrations were excited and detected by cementing the driving and pickup coils to the bar at right angles to its axis. The bar was suspended from two thin wire loops placed at nodes corresponding to the mode of vibration being investigated.

Although the values of decrement observed are somewhat scattered, they definitely indicate that, in this case also, the losses effective at low frequencies are primarily of the solid friction type but that viscous losses are also present and may become of importance at very high frequencies.

* These data have been obtained since this paper was presented in Chicago.

DERIVATION OF THE ATTENUATION FACTOR

Assuming that the rock samples investigated are representative of the bulk of materials traversed by the sound waves employed in seismic prospecting, it would seem that the effect of viscous losses is inappreciable over the range of frequencies employed, that is below 150 cycles per second. The form of the attenuation factor, α, in equation 1, will, therefore, be derived from a consideration of the conditions existing in a vibrating bar in which only solid friction losses are present.

The general form of the propagation equation has been given as

$$A_x = A_0 e^{-\alpha x} \tag{1}$$

or

$$\log_e A_0/A_x = \alpha x. \tag{1a}$$

To apply this to a bar oscillating longitudinally at its fundamental frequency, we consider x in the above equation to be one wave length of the waves in the bar, that is

$$x = 2l = c/f \qquad \text{(From 4)}$$

A_x and A_0 are then identified with the amplitudes of two successive cycles of the vibration. But, by definition

$$\delta = \log_e \frac{A_0}{A_x}.$$

So

$$\delta = \alpha x = \frac{\alpha c}{f}$$

or

$$\alpha = \frac{\delta f}{c}. \tag{5}$$

Substituting in (1)

$$A_x = A_0 e^{-\delta f x/c}. \tag{6}$$

Which may also be written

$$A_t = A_0 e^{-\delta f t} \tag{7}$$

where t = travel time between points at which amplitudes A_t and A_0 are measured.

Equation 7 is the propagation equation applicable to longitudinal waves traveling in a bar of unlimited length. It will, however, apply equally well to the propagation of plane waves in a bulk medium provided the appropriate changes are made in the numerical values of c and δ. Obviously the value of c must be changed from the bar velocity to the corresponding bulk velocity. It is also obvious that the value of δ must be changed by a factor which involves Poisson's ratio, and that the decrement of the material in bulk must be less than that of the same material in bar form. This follows because a longitudinal wave in a bar produces lateral deformation which is absent when a plane wave travels through the material in bulk. At the present time, the mechanism of solid friction is not understood, so that the exact relation between the decrement of a material in bar form and the decrement in bulk cannot be derived on a physical basis. However, by making the assumption that solid friction losses are negligible for pure dilation which is not accompanied by shear, a relationship between the two values of decrement may be obtained. This is done by considering the elastic constants to be complex quantities; a procedure based on the tacit assumption that the stress-strain relationship existing in the medium may be graphically represented by an ellipse. The assumptions lead to the following relationship:*

$$\delta_{bar} = \delta_{bulk}\left(\frac{1 - \sigma^2}{1 - 2\sigma}\right) \tag{8}$$

where σ = Poisson's Ratio.

Taking 0.28 as a reasonable value for Poisson's ratio we have

$$\delta_{bar} = 2.1\delta_{bulk}$$

Having observed values of decrements ranging from .04 to .06 in bar samples of representative sedimentary rocks, we may, therefore, expect the decrement of the same materials in bulk to be approximately .02 to .03.

LABORATORY AND FIELD OBSERVATIONS

The application of data obtained by laboratory experiments on small samples of a few materials, to the problem of determining the attenuation factor of the bulk of the earth's surface materials must necessarily be subject to great uncertainties. The samples tested were

* This equation was derived by Dr. Alfred Wolf.

all well-consolidated materials, so there is no assurance that the results obtained are applicable to semi-consolidated sediments. Furthermore, all the data were obtained at room temperature and atmospheric pressure, whereas sedimentary rocks at even moderate depths are subject to considerable pressure at elevated temperatures. However, it seems quite reasonable to suppose that the effect of both pressure and temperature will be to alter the magnitude, rather than the nature, of the attenuation constant. It also seems reasonable to suppose that, while unconsolidated sediments near the surface may exhibit plastic behavior, and hence produce appreciable viscous losses; the sediments at some depth may be sufficiently compacted by the pressure of overburden so that they behave essentially like solids and exhibit losses of the solid friction type. All this is admittedly speculation, but the writer feels that sufficient evidence is at hand to adopt, as a working hypothesis, the view that the observed attenuation of seismic waves employed in seismic prospecting is in most cases produced by solid friction damping, with the reservation that in some areas viscous losses may be of some importance. Data obtained from field observations must be used to definitely prove or disprove the validity of this view.

It is possible to show that the laboratory data are at least consistent with some conclusions drawn from a consideration of the relative amplitudes of the various reflections found on a seismograph record. The reasoning is as follows: A wave originating at the shot point, traveling downward to a reflecting horizon, and then back to the surface will be reduced in amplitude by three primary factors, namely

1. Geometric divergence.
2. Partial reflection at acoustic boundaries.
3. Attenuation.

The first factor can be accurately allowed for. The second and third factors both give rise to an exponential decrease of amplitude with distance traveled, hence one can be determined only if the other is known. If we simplify matters by assuming that all the acoustic boundaries encountered by the traveling wave have the same reflection coefficient, we can write the propagation equation for plane waves subject to both reflection losses and attenution as:

$$A_x = A_0[(1 - r)^{nx} + e^{-\delta f x/c}] \tag{9}$$

where A_0 = Amplitude at an arbitrary reference point.

A_x = Amplitude at distance, x, from reference point.
x = Distance.
r = Reflection coefficient of each reflecting horizon.
n = Number of reflecting horizons per unit distance.
δ = Decrement.
f = Frequency of wave.
c = Velocity of wave.

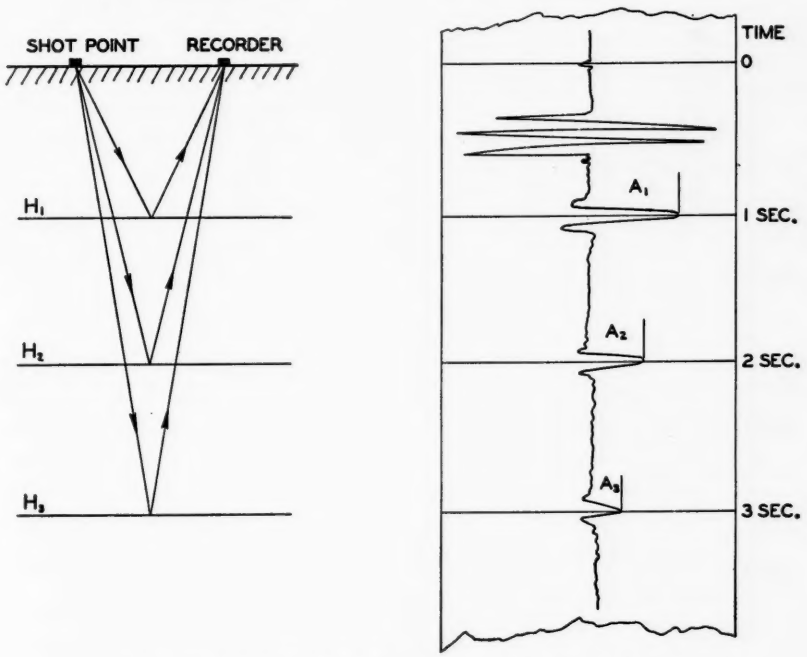

FIG. 5. Idealized reflection paths and reflection record.

If the velocity, c, is the average velocity then

$$x = ct.$$

So we can write*

$$A_t = A_0[(1 - r)^{bt} + e^{-\delta f t}] \qquad (10)$$

where b = Number of reflecting layers traversed in unit time.

To illustrate the application of Equation 10 we may consider the cross section of a simple earth illustrated in Fig. 5. Indicated at the

* It will be noted that the second exponential term of Equation 10 involves frequency, while the first does not. There, therefore, exists the possibility of distinguishing between attenuation, and losses by partial reflection. A discussion of this point is beyond the scope of this paper.

left are a number of reflecting horizons separating homogeneous media, and the paths of waves reflected therefrom. At the right of the figure is a representation of a record showing the resulting reflections. In this case, the number of reflecting horizons is known. If the reflection coefficient is also known, then equation 10 may be used to compute the decrement of the materials traversed by the reflected waves. It is merely necessary to measure the amplitudes of two successive reflections and to determine the time, t, which is simply the difference between the arrival times of the reflections. After correcting the values of observed amplitudes for geometric divergence, these values are substituted in the equation together with the value of the frequency, f, which may also be determined from the record. The value of f must necessarily decrease with the length of path traversed, as will be shown later. However, for this computation it may be taken to be the average frequency of the reflections noted on the record over the interval considered.

If nothing is known concerning the number of reflecting horizons present, or the magnitude of their reflection coefficients, then a maximum value for the decrement of the earth materials can still be determined by neglecting the reflection losses entirely and so assuming that all the losses are caused by attenuation.

Actual reflection records differ from the idealized record just discussed in that they show reflections coming from a multitude of reflecting horizons having widely varying reflection coefficients. It is, however, possible to determine the relative amplitudes of the many reflections and to plot them as a function of arrival time. An average curve drawn through points so plotted will, in effect, minimize the effect of variation in reflection coefficients. In a paper[7] by J. M. Kendall presented at the 1940 Annual meeting of the Society of Exploration Geophysicists, a method of investigating the relative amplitudes of reflections on reflection records was given, and a number of amplitude-time curves were presented. It was shown that, when the amplitudes were corrected for divergence and plotted against time on semi-log paper, the resulting curves were straight lines for a considerable portion of their length, indicating that the amplitude is usually an exponential function of travel time. Through the courtesy of Mr. Kendall, a family of such curves is here reproduced in Fig. 6. In these graphs, the amplitudes plotted have already been corrected for

[7] J. M. Kendall, "The Range of Amplitudes in Seismic Reflection Records," GEOPHYSICS, this number, p. 149.

geometric divergence. For each of the curves, the average frequency of the reflections and the computed value of decrement is given. The

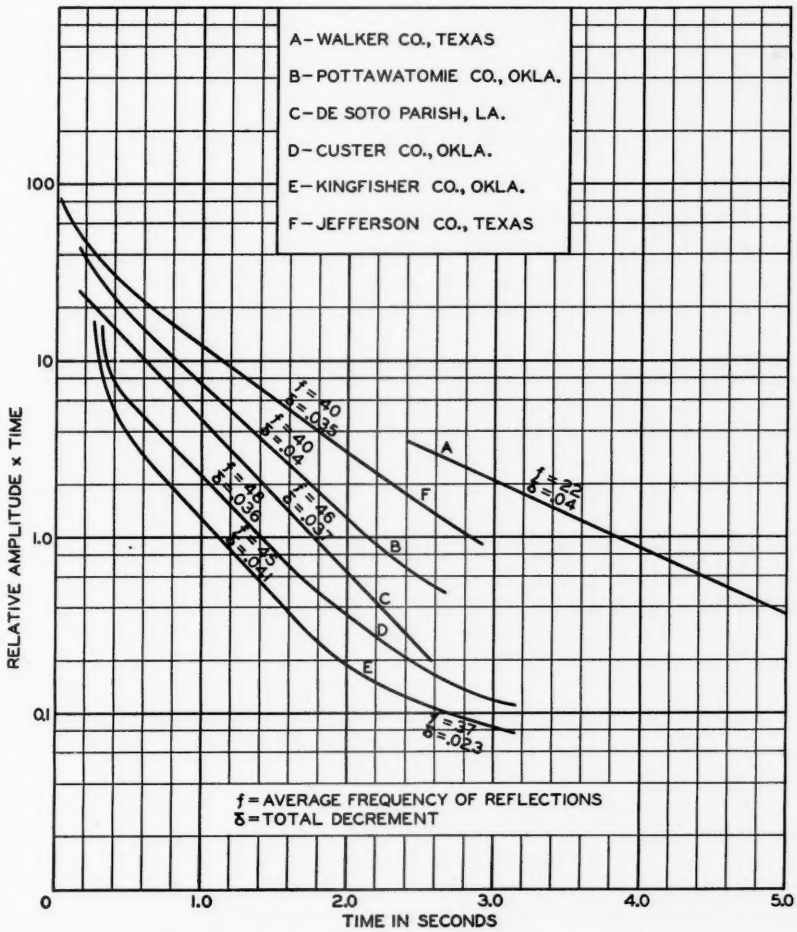

FIG. 6. Amplitude-time graphs of reflection records.

decrement was computed* by neglecting the losses due to partial reflections and assuming the total loss to be caused by solid friction.

* In these computations, the frequency used was the average frequency of the reflected waves over the interval considered. In some records, the variation of frequency with time was appreciable. In those cases the recorded amplitudes were corrected for instrumental characteristics to obtain true amplitude ratios.

The calculated values, therefore, represent a maximum value of total decrement which must necessarily be greater than the true value of the decrement resulting from attenuation alone. The average value of the decrements so computed is 0.036 which may be compared with the values 0.02 to 0.03, which the laboratory experiments indicate to be reasonable values.

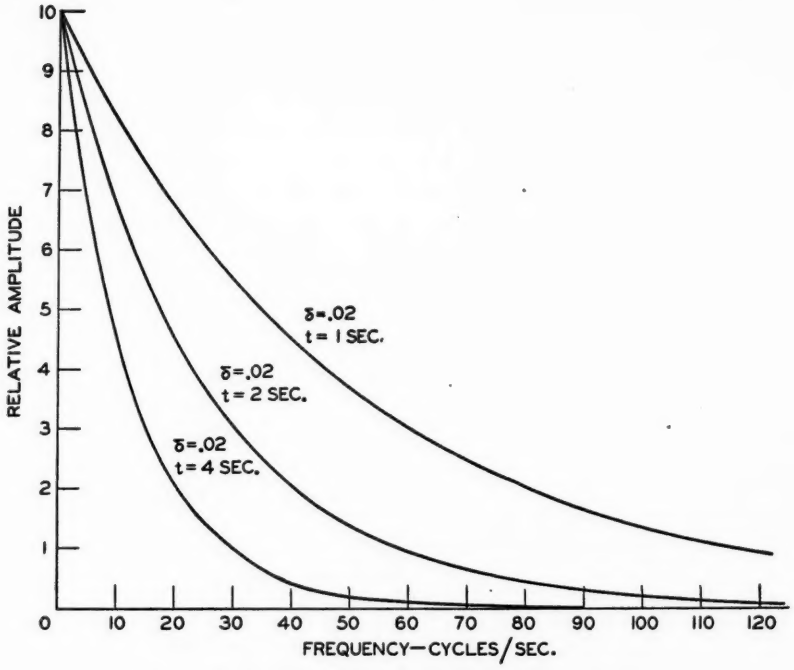

FIG. 7. Frequency characteristics of seismic wave paths.

FREQUENCY CHARACTERISTICS OF SEISMIC WAVE PATHS

If the attenuation factor of the earth is of any form which involves frequency, then the attenuation suffered by a plane wave traveling through the earth will be a function of the frequency of the wave. If the attenuation is entirely caused by solid friction, the attenuation factor has been shown to be

$$\alpha = \frac{\delta f t}{v}$$

The attenuation factor is directly proportional to both f and t so that attenuation will be a function of frequency, and the amplitude-fre-

quency characteristic of a given path in a homogeneous medium will be a function of the length of time required for a sound wave to traverse that path. The characteristic of a given path may be obtained directly from the propagation equation by plotting the ratio of the amplitude at the end of the path to that at the beginning of the path, as a function of frequency. Fig. 7 shows a number of curves of this sort, the frequency characteristics having been computed for the travel times of 1, 2, and 4 seconds, using in each case a value of .02 for the decrement.

These curves show that the earth acts as a low-pass filter. The longer the path of the wave, the greater is the discrimination against high frequencies. If the wave originating at the shot point is a sharp impulse whose frequency spectrum covers a wide band of frequencies, the high frequency components of the impulse will be rapidly attenuated as compared with the low frequency components. This effect is quite noticeable on reflection records taken in many areas, the reflections from the deeper horizons having their energy concentrated in a frequency band definitely lower than that of the reflections from shallow horizons. The same phenomena is also largely responsible for the great difference between the average frequency recorded on seismograms of distant earthquakes and the frequencies recorded on seismic reflection records.

On the basis of the data presented in this paper, the frequency-characteristic curves of Fig. 6 may be considered to be a rough approximation to the frequency characteristics of the earth's surface layers, or could be so considered if the earth were homogeneous. Actually, the frequency characteristic of a layered earth cannot be represented by smooth curves of this type. In such case, these curves must be considered to be in the nature of a "base line" upon which are superimposed numerous peaks and troughs which, under certain conditions, may be of fairly large amplitude. If, for example, the path of a wave traverses a large number of similar reflecting layers, each of approximately the same thickness, a large resonant effect may be superimposed on the basic attenuation curve at a frequency determined by the mean thickness of the layers. On the other hand, if the strata traversed by the wave vary in thickness and acoustic properties in random fashion over wide limits, then the oscillations superimposed upon the basic attenuation curve will be rather like ripples distributed in random fashion and will have no great effect upon the over-all frequency characteristic.

ACKNOWLEDGMENT

The writer wishes to thank Mr. A. R. Denison of the Amerada Petroleum Corporation for supplying some of the cores used in this investigation, and also the Duval Texas Sulphur Co. for supplying the cap rock core.

THE RANGE OF AMPLITUDES IN SEISMIC REFLECTION RECORDS*

J. M. KENDALL†

ABSTRACT

Curves are presented which show the amplitudes of some reflection records, plotted as a function of time, for several widely separated areas. It is shown that amplitude ratios of the order of 1000:1 occur on records in a time interval of two seconds. After correcting for divergence of the recorded waves, it is found that their amplitude decreases exponentially with time. The usable length of record as a function of the size of charge was investigated for one shot hole.

Information concerning the range of amplitudes occurring in reflection records is of practical interest because it is useful in designing amplitude controlling amplifiers. Such information is also interesting

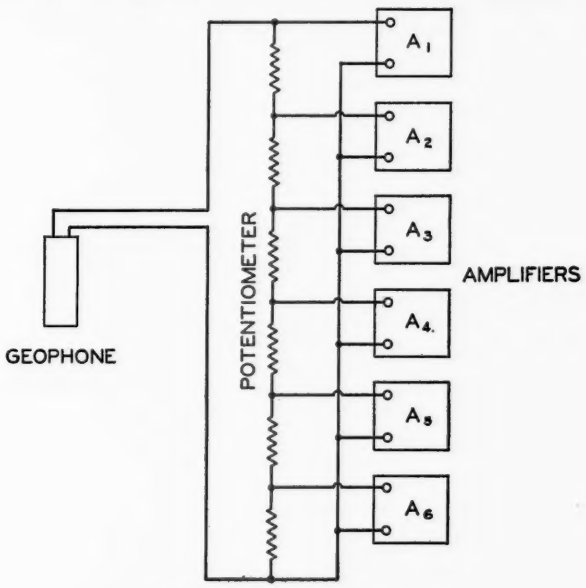

FIG. 1. Instrument layout.

in connection with the study of the wave propagation characteristics of the earth.

Apparatus suitable for determining the range of amplitudes in a reflection record as a function of time is shown in Fig. 1. It consists

* Presented at the Annual Meeting, Chicago, Illinois, April 11, 1940.

† Geophysical Research Corporation, Tulsa, Oklahoma.

of an ordinary set of seismic reflection instruments with the modifications shown in the diagram. Only one geophone is used. The output voltage from the geophone is fed into an attenuating network and is recorded by six amplifiers. The amplifiers are connected at various points in the network and permit a total range of amplitude of 15,000:1 to be recorded. From records obtained with this apparatus, it is possible to plot the relative amplitudes of the incoming waves as

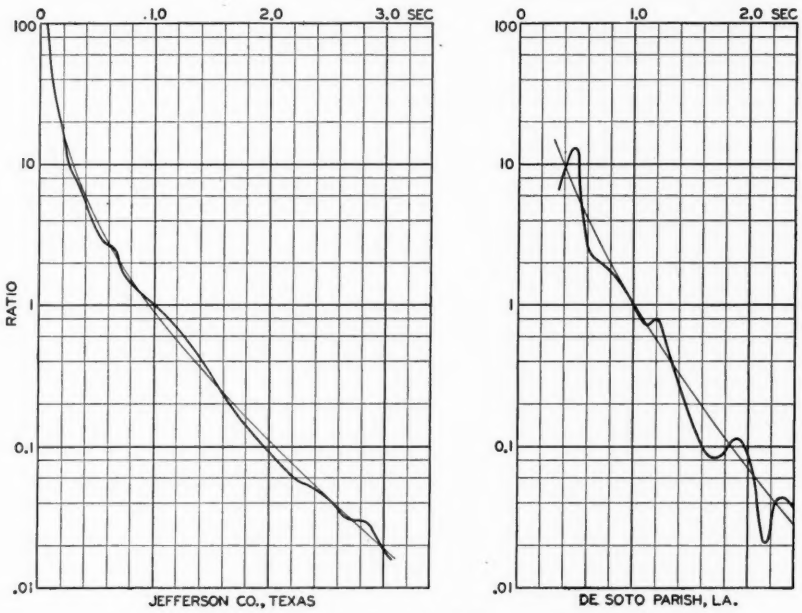

FIG. 2. Time-attenuation curve for Jefferson County, Texas.
FIG. 3. Time-attenuation curve for De Soto Parish, Louisiana.

a function of time. An envelope is drawn through the peaks of the waves in each trace in the record made and this envelope may be considered to be equal to the double amplitude of the record. Such a procedure results in a certain amount of smoothing, which, however, is hardly sufficient to cause an appreciable effect in the over-all result. It is the width of the envelope which is really plotted in the following curves.

Figs. 2 and 3 show two such curves which were plotted from data taken respectively from a setup near Beaumont, Jefferson County, Texas, and De Soto Parish, Louisiana. In the Jefferson County setup the geophone was located only 200 feet from the shot hole. The ampli-

tude of the first burst of energy arriving is, therefore, quite high, but its duration is only about 0.2 seconds. Thereafter, the amplitude dies away at a gradually decreasing rate until it is finally lost in the ground unrest at about 3.0 seconds after the shot goes off. The ratio of the amplitude of the first burst to that of the amplitude at 2 seconds is

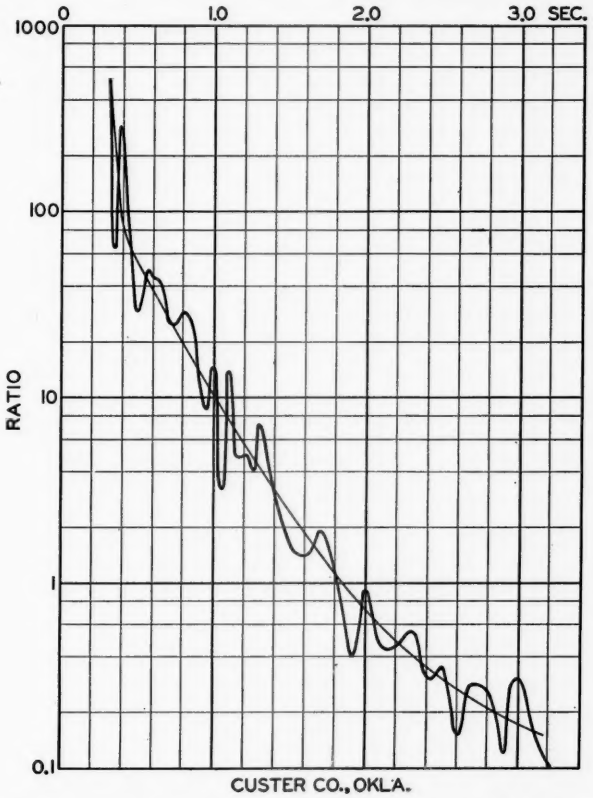

FIG. 4. Time-attenuation curve for Custer County, Oklahoma.

about 1000:1. The Jefferson County record shows very little irregularity in the amplitude-time relation.

The curve for the De Soto Parish setup differs in several respects from the Jefferson County curve. The fact that the geophone was placed 2100 feet away from the shot point accounts for the later time of the first break, as well as for the lesser average slope of the early part of the curve. The greatest amplitude occurring in the record did not occur in the first burst of energy arriving but at about 0.5 seconds

after the shot went off. This circumstance is responsible for the peak present at 0.5 second. The curve shows that the record had greater amplitude irregularities than did the Jefferson County record.

Figs. 4 and 5 show curves for two setups in Oklahoma, one in Custer County and the other in Kingfisher County. These two curves have

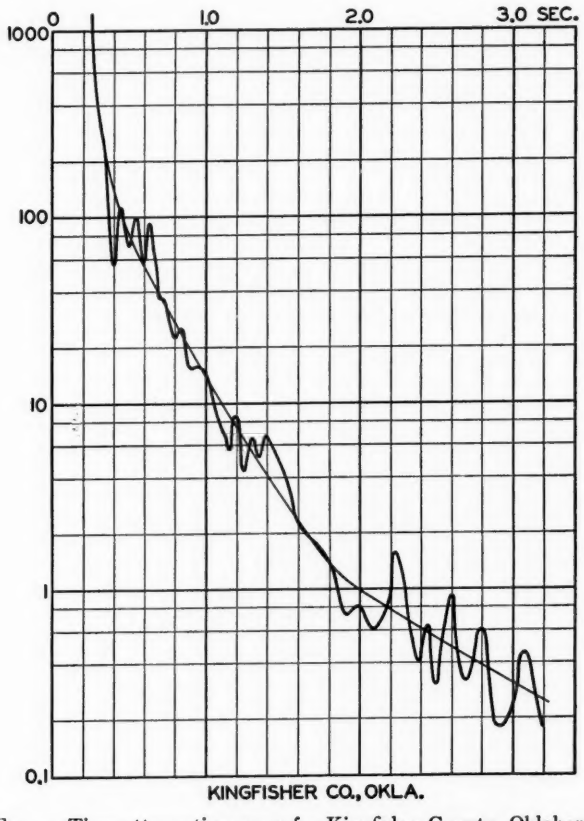

FIG. 5. Time-attenuation curve for Kingfisher County, Oklahoma.

many irregularities, which is tantamount to saying that the records have many reflections. The over-all amplitude ratios are of the order of 3000:1 for a record of about 3 seconds. Incidentally, the greatest amplitude on these records, if the records were taken without the attentuation network and on an amplifier capable of handling the load, would correspond to a galvanometer deflection of about 100 feet double amplitude.

The set of curves shown in Fig. 6 are for three setups in Pottawatomie County, Oklahoma. These curves not only have the same average slope but also show a certain correlation, as might be expected. During the interval 0.4 to 0.9 seconds, several large scale amplitude irregularities occur in each curve. From 0.9 to 1.2 seconds all of the amplitudes are decreasing very rapidly. Then from 1.2 to 1.5 seconds another irregularity occurs which is common to all of the records. From 1.5 to 1.7 occurs another period of rapid decrease. It

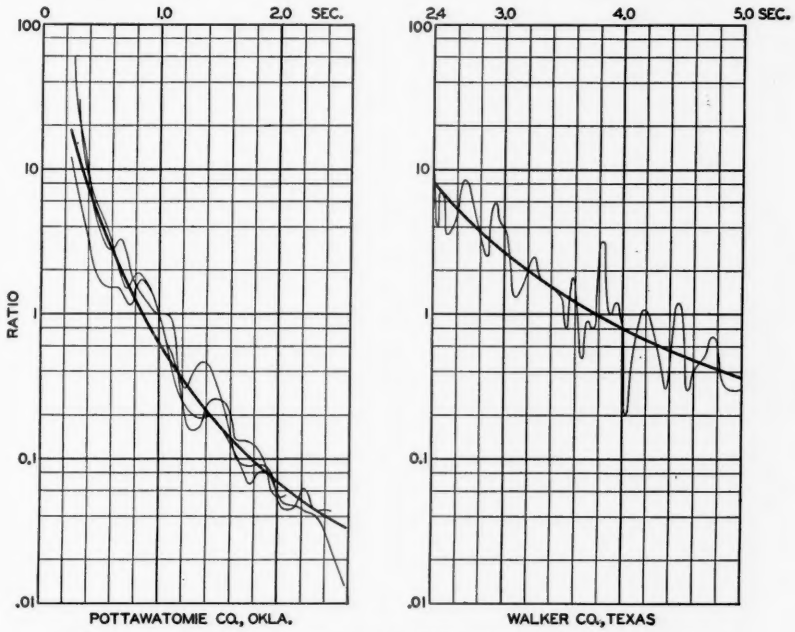

FIG. 6. Time-attenuation curves for Pottawatomie County, Oklahoma.
FIG. 7. Time-attenuation curve for Walker County, Texas.

would seem reasonable to suppose that the intervals, where the amplitude is undergoing a rapid decrease, would correspond to intervals where the earth is relatively homogeneous. On the other hand, the intervals in the curve where the amplitude increases or where it remains stationary, correspond to regions in the earth where much reflection takes place. These time intervals in many cases are so long that they would hardly be seen in records taken with automatic volume control amplifiers, because the automatic adjustment of sensitivity would tend to smooth out these long time irregularities.

The data for the curve, shown in Fig. 7, were taken from a record made in Walker County, Texas, where some very deep reflections were found. The time for this curve starts at 2.4 seconds and runs out to 5 seconds. The amplitude data for the early part of this record are not

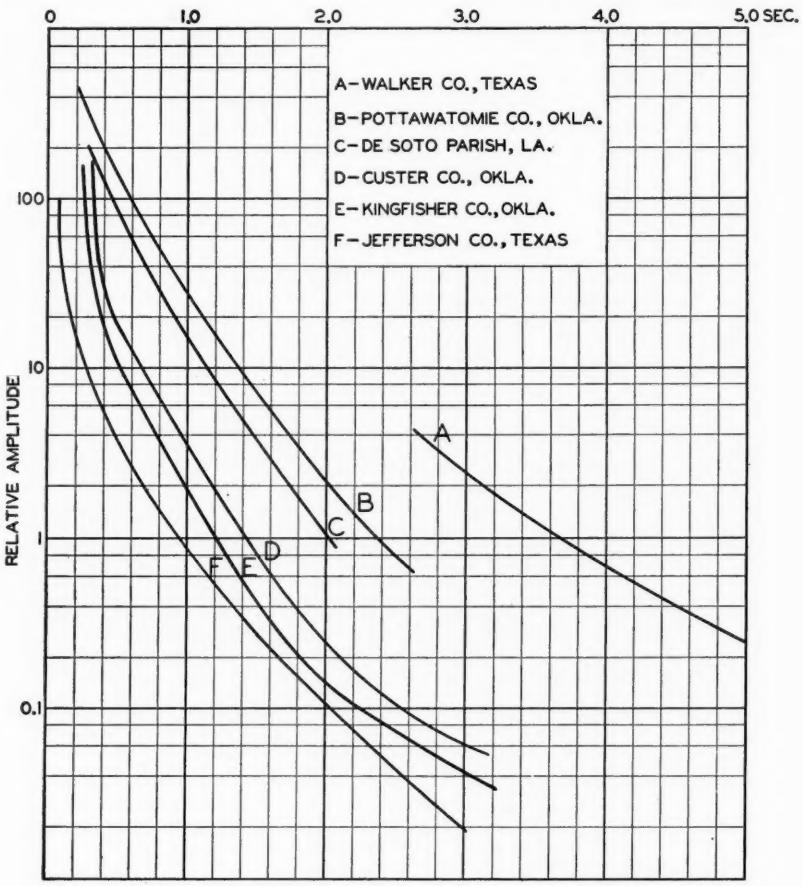

FIG. 8. Summary of smoothed time-attenuation curves.

available. The frequency of reflections present in that portion of the record from which this curve was derived is about 22 cycles per second. Each peak in the curve represents a good reflection in the record. The relatively low frequency of the reflections is believed to account for the small slope of the curve.

Fig. 8 is a summary of the various time-attenuation curves just

shown. Only the smoothed curves are shown here. Since a ratio scale was used for plotting, it is permisible to shift the curves up or down, and this was done to separate the curves from each other. The curves with the least slope are arranged above and those with the greatest

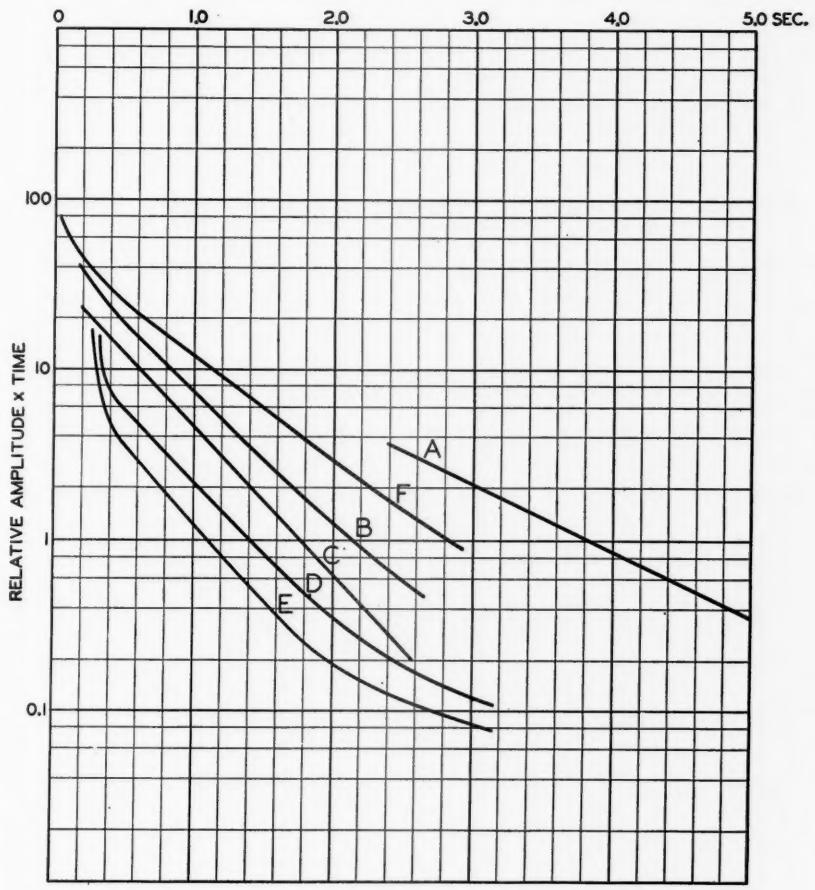

FIG. 9. The curves of Fig. 8 with divergence factor eliminated.

slope are arranged below. As a general feature, the curves have a tendency to be concave upward.

The shape of the curves shown is determined partly by a geometrical consideration. The seismic wave originates at a point source and is therefore a spherical wave whose amplitude decreases directly with

distance because of divergence. Since the distance traveled is approximately proportional to time, the amplitude change caused by divergence may be corrected for by multiplying the amplitude by the travel time. The remaining decrease in amplitude then represents the atten-

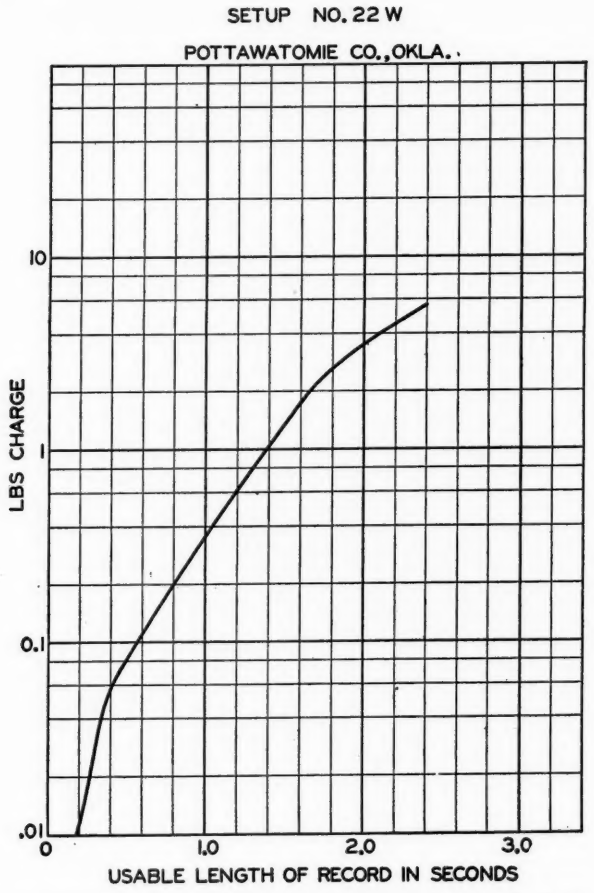

FIG. 10. Curve showing relationship of charge-usable length of record for a shot-hole in Pottawatomie County, Oklahoma.

uation caused by the absorption, scattering, and partial reflection which the wave undergoes while traveling through the earth.

Fig. 9 shows the same curves after each has been multiplied by time for the purpose of eliminating the divergence factor. Allowing for this tends to straighten out the curves. The early parts of some of the

curves, however, still remain concave upward. It seems probable that both reflected and refracted waves are reaching the geophone in the early part of the record and that the combination is responsible for the unduly large amplitude of the first burst of energy. The major portions of all of these curves are straight lines. This would seem to indicate that the earth, throughout the portion from which these reflections, come, is fairly uniform and consists of many reflecting layers of similar characteristics. The sharp breaks in some of the curves may possibly be due to a major change in the propagating characteristics of the earth beginning at the corresponding depth.

It is generally true that the frequency of the waves recorded in reflection records decreases as the record progresses. In plotting the curves shown, no allowance was made for the small change in the recorder sensitivity with decreasing frequency because of the fact that the frequency change which takes place throughout most records is generally not very great.

It does not seem to be commonly realized that a relatively great increase of charge is required to produce even a small increase in the usable length of a record. A curve showing this relationship for one particular location is shown in Fig. 10. This curve is typical for Pottawatomie County, Oklahoma. The data for this curve were obtained by shooting various size charges in a shot-hole. The usable lengths of the resulting records were arbitrarily considered to extend to the points where the double amplitudes fell to three-quarters of an inch. From the curve shown in Fig. 10, it may be seen that the charge must be increased almost exponentially with the usable length. In this case, the charge must be multiplied by a factor of 7 to 10 times in order to increase the usable length by one second.

AVERAGE VERTICAL VELOCITIES FROM REFRACTION AND REFLECTION PROFILES*

W. R. RANSONE† AND FREDERICK ROMBERG†

ABSTRACT

This paper presents data from a combined refraction and reflection profile from which vertical velocities are calculated. The accuracy of velocities so obtained is brought out by checking them with velocities obtained from shooting a well drilled two years after the seismograph work. It is also interesting to note that this method offers a means of identifying reflection horizons with refracting horizons, permitting better correlation between geologic and seismic markers. The method is of particular value in areas where little exploration has been done.

INTRODUCTION

A combined refraction-reflection profile was shot in August, 1937, in the district of Infante, State of Guarico, Venezuela, west of the town of Las Mercedes. A well, Guarico Oil Fields Ltd. Guayabo No. 1, was shot in September, 1939, for vertical velocities. This well was drilled subsequently to the reconnaissance refraction and reflection survey carried out over a large area in the State of Guarico, Venezuela, for the Caracas Petroleum Corporation.

The horizontal refraction velocities obtained from this profile are plotted in the customary form of X-T (time-distance) graph on Fig. 1. These velocities were anticipated from other refraction profiles in the vicinity and are more or less constant over the area. Also plotted on this graph are reflection arrival times for three reflections. It will be noted that one of these becomes tangent to the refraction with an apparent velocity of 16,600 feet per second. This reflecting horizon is present over a large portion of the area and was a key bed on which contour maps were made.

SITE OF PROFILE

Before the profile was shot a location was selected where elevations were as flat as possible, weatherings known to be relatively uniform, and where the profile could be shot along strike. The profile was also shot in the reverse direction, the shorter distances not being used since the expected velocities had been found on the forward profile. That the profile was actually along strike is shown by the fact that the for-

* Manuscript received April, 1940. Published by permission of V. C. Illing of the Caracas Petroleum Corporation.

† Geophysical Service, Incorporated, Dallas, Texas.

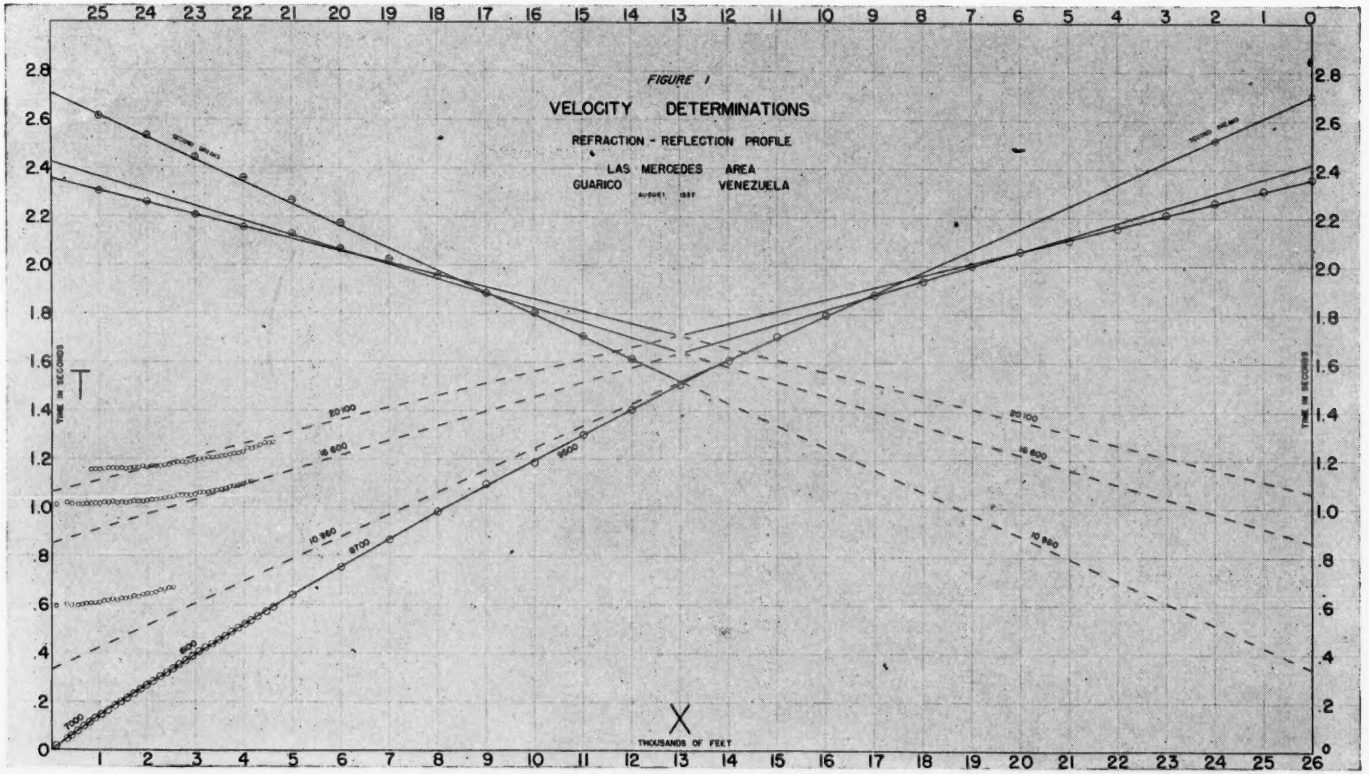

FIG. 1. Time-distance curve (X-T) of refraction and reflection times. Forward and reverse profiles over same ground.

ward and reverse graphs cross exactly in the middle of the profile. It was fortunate that such a location was available in an area of good reflection correlation and also where the profile could be shot in a straight line.

QUALITY OF DATA

The quality of the breaks, both reflection and refraction, is from fair to good, and, as may be seen from the X-T curve, Fig. 1, unusually good second-break refractions occur on many of the records. Fig. 3b illustrates a typical case of the first and second break refractions. Fig. 3a illustrates a short-distance record showing both the refraction first breaks and the reflection events.

It may be seen on the X-T curve, Fig. 1, that a continuous spacing of 45 feet between record traces was carried out to a distance of 5,000 feet. At this point the reflections became poor and a spacing of 500 feet was used out to a distance of 26,000 feet.

Some idea of the charges of dynamite required may be obtained by noting that the short-distance record, Fig. 3a, was obtained with a charge of $\frac{1}{4}$ pound, while the long-distance record, Fig. 3b, required 40 pounds.

VERTICAL REFLECTION VELOCITIES

The average vertical velocities from the reflections were obtained by plotting X^2 against T^2 as seen in the graph, Fig. 2, according to the well-known relationship.[1]

$$\overline{V}^2 = \frac{[X_2^2 - X_1^2]}{[T_2^2 - T_1^2]} = \text{a constant},$$

where $\overline{V}$ = average vertical velocity.
X = distance from shot to recording point.
T = reflection time.

Velocities from three different reflecting horizons were obtained in this manner, as seen in Fig. 2. The irregularity of the points is due in part to the ignoring of small changes in elevation and weathering thickness, and in part to the large scale used in plotting.

The place at which the points deviate from a straight line is the critical point at which the seismic wave follows a refraction rather than a reflection path. This may be checked by noting the value of X^2, and of the X extracted from it. This value of X is the point of tangency

[1] C. H. Green, GEOPHYSICS, Vol. 3, No. 4, October, 1938. p. 295.

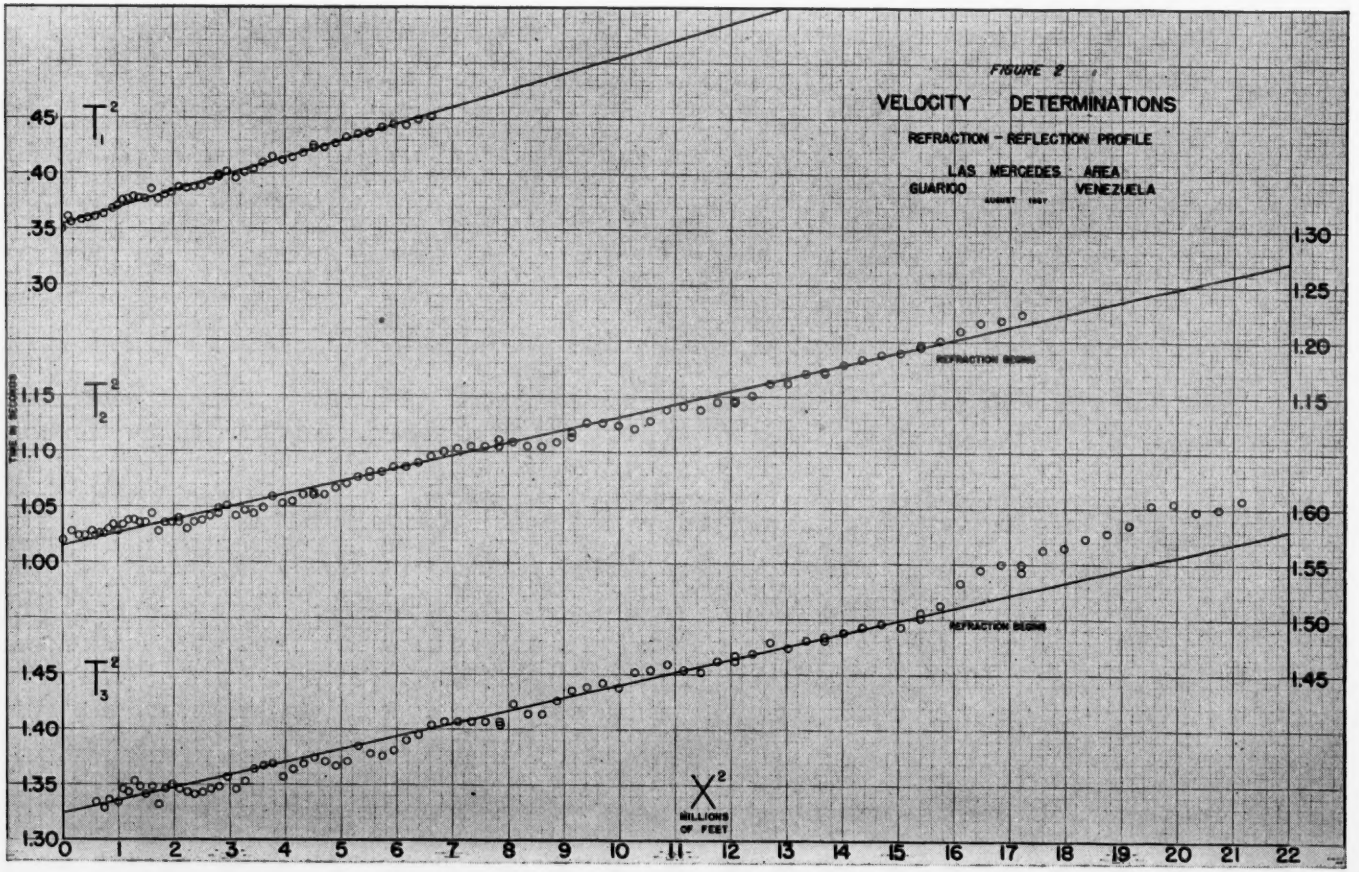

FIG. 2. X^2-T^2 curve of reflections to determine vertical velocities.

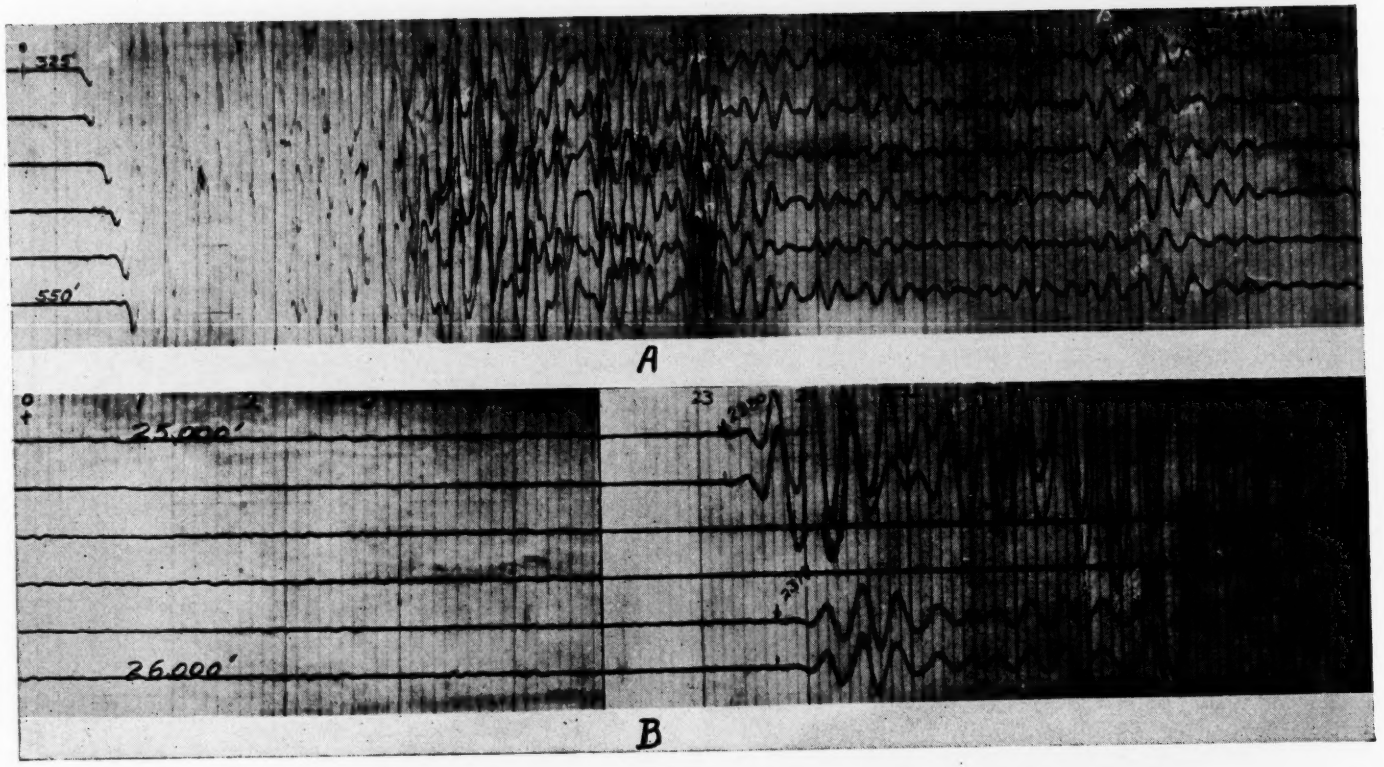

FIG. 3a. Short spread reflection record showing reflection and refraction arrival times.
FIG. 3b. Long spread refraction record showing first and second breaks.

seen between the straight refraction velocity line and the curved reflection line in the X-T graph, Fig. 1. The fact of tangency identifies the reflection horizon with the refraction horizon. The refraction velocity will serve as a rough basis for judging the type of sediment.

The calculations for the reflection velocities are as follows:

$\overline{V}^2 = \dfrac{X_2^2 - X_1^2}{T_2^2 - T_1^2}$	$Z = \overline{V}T/2$
$\overline{V}_1^2 = \dfrac{6 \times 10^6 - 0}{.445 - .354} = \dfrac{6 \times 10^6}{.091}$	$T = \sqrt{.354} = .595$
$\overline{V}_1 = 8120'/\text{sec.}$	$Z_1 = \dfrac{8120[.595]}{2} = 2420'$
$\overline{V}_2^2 = \dfrac{17 \times 10^6 - 0}{1.213 - 1.015} = \dfrac{17 \times 10^6}{.198}$	$T = \sqrt{1.015} = 1.007$
$\overline{V}_2 = 9270'/\text{sec.}$	$Z_2 = \dfrac{9270[1.007]}{2} = 4670'$
$\overline{V}_3^2 = \dfrac{18 \times 10^6 - 0}{1.533 - 1.324} = \dfrac{18 \times 10^6}{.209}$	$T = \sqrt{1.324} = 1.151$
$\overline{V}_3 = 9280'/\text{sec.}$	$Z_3 = \dfrac{9280[1.151]}{2} = 5340'$

VELOCITIES FROM REFRACTIONS

A relation between the velocity and the depth was derived from the X-T curve, Fig. 1, under the assumptions that (1) the rocks are isotropic and (2) the velocity increases continuously with depth. Assumption (2) means that the X-T curve is also continuous, which can be considered true in the present example down to the line representing the velocity of 16,600 feet per second.

If an impulse originating at a shot point S penetrates to a depth z_d and returns to the surface a distance x_d away from S, the equation of its path (Calculus of Variations) will be (see Fig. 4)

$$v\sqrt{1 + z'^2} = A_d$$

where $z' = dz/dx$ for the path.
A_d = a constant characteristic of the path.
v = velocity (true velocity, not average velocity $\overline{V}$).

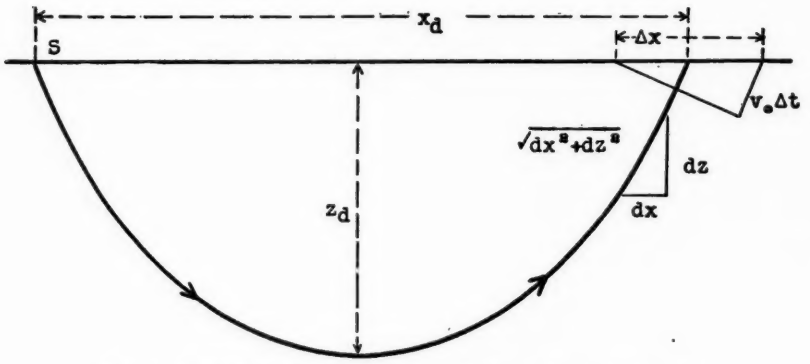

FIG. 4. Path of a refraction, showing relation between inclination of path and surface velocity.

At the lowest point in the path the energy is traveling horizontally, $z'=0$, and we find A_d to be

$$A_d = v_d.$$

At the surface $v=v_0$, and $A_d=v_0\sqrt{1+z'^2}$. From the similar triangles in Fig. 4,

$$v_0\sqrt{1+z'^2} = v_0\frac{\sqrt{dx^2+dz^2}}{dx} = v_0\frac{\Delta x}{v_0\Delta t} = \frac{\Delta x}{\Delta t}$$

or

$$A_d = \Delta x/\Delta t$$

where $\Delta x/\Delta t$ is the horizontal emergence velocity as observed conventionally from the X-T curve, Fig. 1. The travel time for an impulse which leaves S and arrives at x_d will be given by

$$t_d = 2\int_0^{z_d}\frac{\sqrt{1+x'^2}}{v}\,dz$$

and if x' is $1/z'$, and $A=\sqrt{1+z'^2}$, t can be expressed as

$$t_d = 2\int_0^{z_d}\frac{A_d\,dz}{v\sqrt{A_d^2-v^2}}$$

A_d, corresponding to t_d, can be read from the X-T curve at any point. The difficulty is to find from the above integral equation the relation between z and v. The problem can be attacked by solving the integral

equation;[2] a simpler method is to assume a function relating v to z, and integrate for as many t_d's as there are constants in the function. The resulting integrals can be solved as simultaneous equations for the constants.

If, for example, it is assumed that $v=a+bz$, we have immediately that $a=v_0$. Then b can be found by changing the integrating variable to v and writing t_d as

$$t_d = \frac{2A}{b}\int_{v_0}^{v_d} \frac{dv}{v\sqrt{A_d{}^2 - v^2}} = \frac{2}{b}\log\left[\frac{A_d + \sqrt{A_d{}^2 - v_0{}^2}}{v_0}\right]$$

which gives for b

$$b = 2/t \log\left[\frac{A_d + \sqrt{A_d{}^2 - v_0{}^2}}{v_0}\right].$$

The integration can be performed from $z=$ any polynomial in v, including the case commonly written as $v=\sqrt{a+bz}$.

In the example under consideration, the first major discontinuity in the X-T curve (Fig. 1) occurs at $t=1.868$, where a horizontal velocity of 10,960′/sec. intersects one of 16,600′/sec. The surface velocity is observed to be $v_0=7{,}000'$/sec. To find a velocity-depth relation which ought to hold as far down as the 16,600′/sec. horizon, b (in $v=v_0+bz$) can be computed as follows:

$A_d = 10{,}960'$/second; $\quad t_d = 1.868$ second. Then

$$b = \frac{2}{1.868}\log\left[\frac{10{,}960 + \sqrt{[10{,}960]^2 - [7{,}000]^2}}{7{,}000}\right] = 1.091, \text{ so}$$

$$v = 7{,}000 + 1.091z.$$

This v is compared with the velocities from the reflection profiles by converting it to the average velocity $\overline{V}$, thus:

$$\overline{V} = 2z/t = z/\int 1/v\, dz = bz/\log\left[\frac{a+bz}{a}\right].$$

Using Z_1, Z_2, and Z_3 from the reflection profile, we get the following results from $\overline{V}$: ($\overline{V}_3$ is here an extrapolation, since $v=a+bz$ is not supposed to apply deeper than Z_2.)

[2] Louis Slichter, *Physics*, Vol. 6, 1932. p. 273.

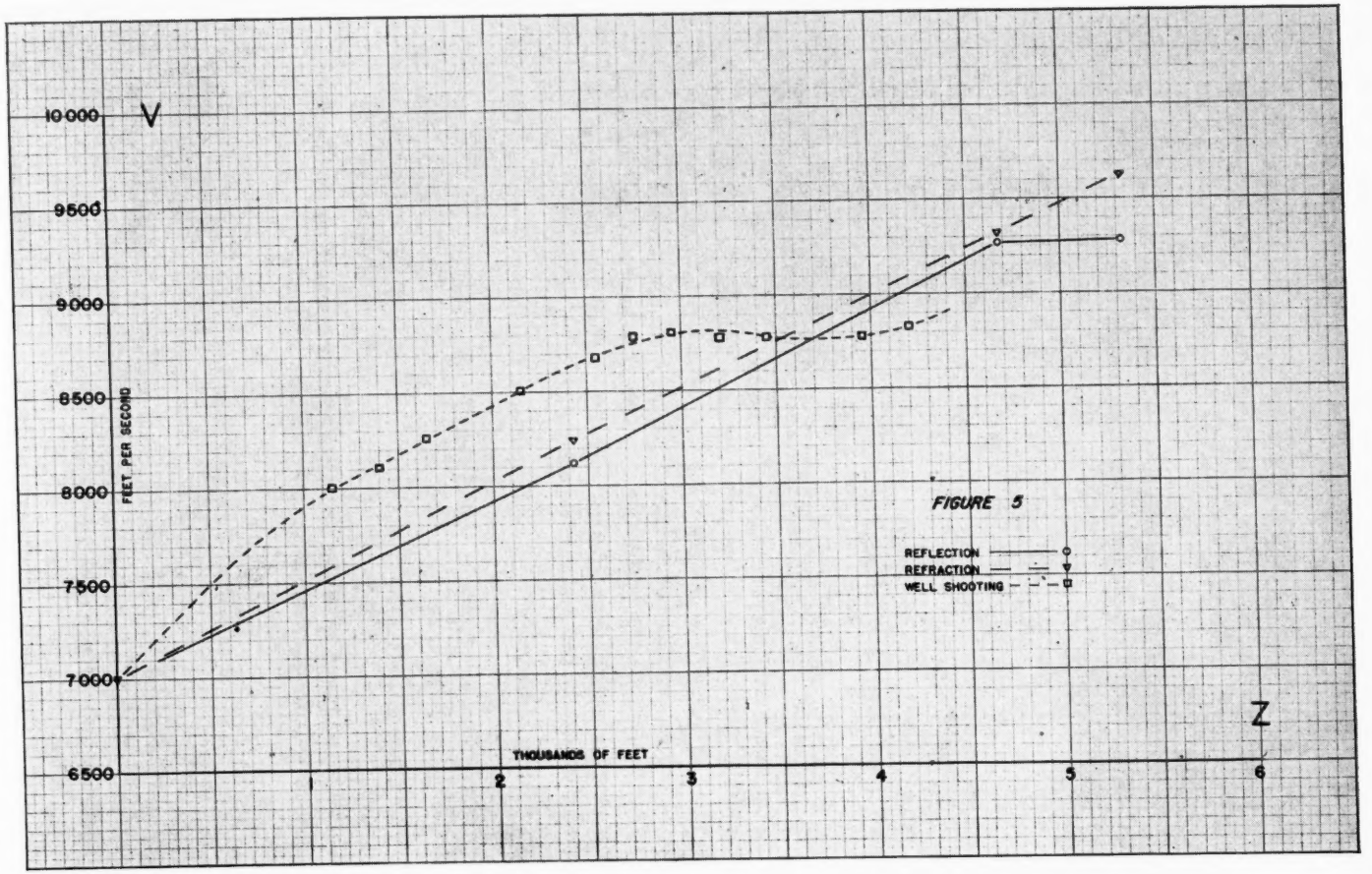

FIG. 5. Comparison between calculated velocities and velocities obtained by actual well shooting.

$$\overline{V}_1 = \frac{1.091 \times 2{,}420}{\log\left[\frac{7{,}000 + 1.091 \times 2{,}420}{7{,}000}\right]}$$

$$= \frac{2{,}640}{\log 1.377} = \frac{2{,}640}{0.3199} = 8{,}250$$

$$\overline{V}_2 = \frac{1.091 \times 4{,}670}{\log\left[\frac{7{,}000 + 1.091 \times 4{,}670}{7{,}000}\right]} = 9{,}320$$

$$\overline{V}_3 = \frac{1.091 \times 5{,}340}{\log\left[\frac{7{,}000 + 1.091 \times 5{,}340}{7{,}000}\right]} = 9{,}620.$$

VERTICAL WELL VELOCITIES

In September, 1939, some two years after the completion of the refraction-reflection profile, it was possible to lower an instrument into a well and obtain vertical velocities, the well Guayabo No. 1 having been drilled in the meantime. The measurements were made in the usual manner by lowering the instruments in the well and shooting at at least two different points on the surface. It was not possible to lower the instrument to the depths reached by the refractions, but harder and denser formations were encountered in the lower part of the hole, suggesting higher velocities as indicated by the seismic velocity calculations.

COMPARISON BETWEEN VELOCITIES

In Fig. 5 are plotted the previously calculated velocities from the refraction and reflection profiles, and the well velocities as determined afterwards. The maximum deviation between the calculated velocities and those directly measured is only 5%. At a depth of 4,000′, which is the point of greatest interest, the variation is practically zero. The good agreement between the two suggests that this method of approach may be used in areas where well shooting is not possible and where, otherwise, velocities must largely be conjectures.

NETWORK ADJUSTMENT BY LEAST SQUARES—ALTERNATIVE FORMULATION AND SOLUTION BY ITERATION*

M. O. GIBSON†

ABSTRACT

Given a network, as in a gravity survey, comprising observed differences in the values of adjacent points, any adjustment of the network, however obtained, is shown to be a least square adjustment if (1) the sum of the corrected observations around any circuit is zero and (2) the sum of the weighted corrections at any junction is zero. This principle provides a means of controlling necessary approximations such as the subdivision of a large network, and simplifies subsequent adjustments made necessary by extension or revision of the observations. It also serves in some cases to reduce the number of equations and in others to eliminate the equations entirely. The paper outlines a time-saving trial and error method of solving network equations, applicable to electric circuits as well as observational network problems.

INTRODUCTION

A common task of those who analyze certain types of observational data is the adjustment of a network such as that represented in Fig. 1. The difference in some quantity such as gravity or elevation between adjacent stations A, B, C, $\cdots$ is observed. Because of observational error the sum of the measurements around any circuit ordinarily will not be zero but will be some finite quantity q. Assuming that the observations contain only random errors, the most probable values of the observed quantities are determined by the principles of least squares. As explained in various textbooks[1] the method involves the formulation of a series of normal equations.

For each independent circuit of the network there is a normal equation and an unknown correlate x which is in effect a partial correction to be applied to each observation in the circuit. As the coefficients of the normal equations are the reciprocals of the weights of the observations, we find it convenient to use the term "adjustability" to denote the reciprocal of weight. Thus, a doubtful observation which should have a relatively large correction is given a large adjustability a.

The normal equations are of the form:

* Presented at the Annual Meeting, Chicago, Ill., April 11, 1940.

† Shell Oil Company, Inc., Houston, Texas.

[1] Leland, O. M., *Practical Least Squares*, McGraw-Hill, 1921.

$$\begin{aligned}
\textstyle\sum a_1x_1 + \quad a_{12}x_2 + \quad a_{13}x_3 + \cdots + \quad a_{1n}x_n + q_1 &= 0\\
a_{21}x_1 + \textstyle\sum a_2x_2 + \quad a_{23}x_3 + \cdots + \quad a_{2n}x_n + q_2 &= 0\\
a_{31}x_1 + \quad a_{32}x_2 + \textstyle\sum a_3x_3 + \cdots + \quad a_{3n}x_n + q_3 &= 0\\
\cdots\cdots\cdots

Hence, at any junction of the network the corrections sum to zero. (In the algebraic solution of the normal equations x_0 becomes 0).

Thus it is shown that for any network adjusted by least squares two conditions are satisfied.

1.) The sum of the corrected observations around any circuit is zero.

2.) The sum of the corrections at any junction is zero.

Conversely, for any arbitrary set of corrections at a junction we may build up a set of correlates for the adjoining circuits thus:

Let x_1 be any number

$$x_2 = x_1 + k_{12}$$

$$x_3 = x_2 + k_{23}$$

. . . . . .

$$x_n = x_{n-1} + k_{nn-1}$$

$$x_1 = x_n + k_{1n} + C.$$

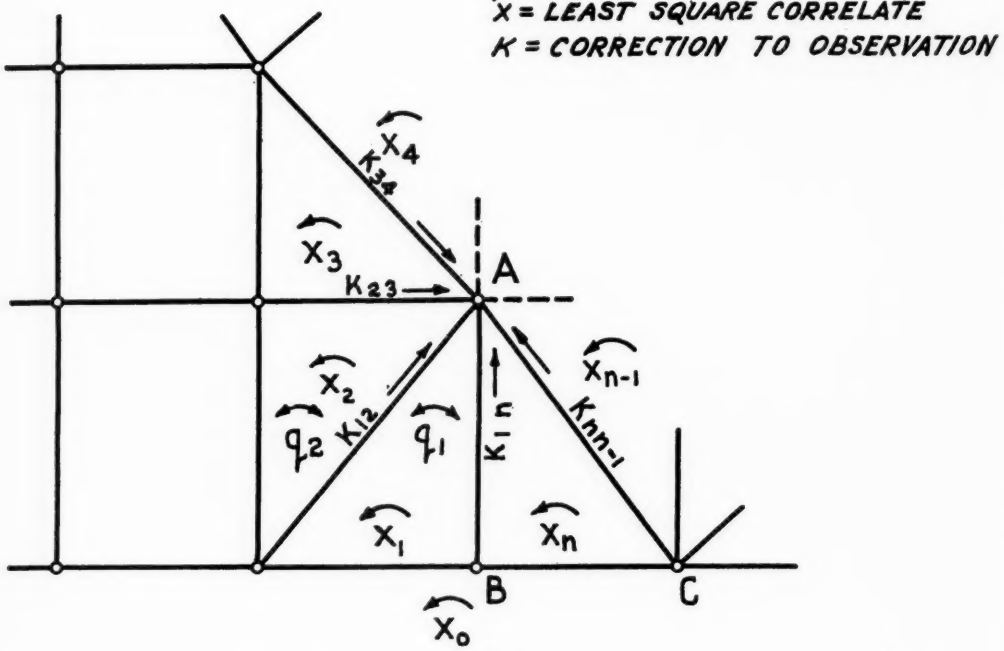

FIG. 1

These equations may be transposed into

$$k_{12} = x_2 - x_1$$
$$k_{23} = x_3 - x_2$$
$$\cdots\cdots\cdots$$
$$k_{nn-1} = x_n - x_{n-1}$$
$$k_{1n} = x_1 - x_n - C.$$

If we now impose the condition that the corrections make the junction balance, that is, if

$$k_{12} + k_{23} + k_{34} + \cdots + k_{1n} = 0$$

then

$$x_2 - x_1 + x_3 - x_2 + \cdots + x_n - x_{n-1} + x_1 - x_n - C = 0$$

or

$$C = 0.$$

Thus it is shown that at any junction where the sum of the corrections is zero, there can be written for the adjoining circuits a set of correlates which will produce the given corrections. Also, it is obvious from equations (1) that a constant may be added to each correlate of a set without changing the corrections derived therefrom; hence the correlates at one junction may be raised or lowered to agree with the correlates of an adjacent junction. Therefore, for a complete network, proceeding from one junction to another, if the corrections at each junction sum to zero, a set of network correlates can be derived which will produce the given corrections. If the given corrections also balance the closing error of each circuit, then the correlates derived therefrom must be the least square correlates, for the normal equations indicate that there is only one set of correlates which serves to balance the network.

Thus it is shown that the two conditions stated above are not only necessary but sufficient and that any corrections, however obtained, which balance the closing errors of the circuits and sum to zero at the junctions are least square corrections.

In the above proof it was assumed that all ties had unit adjustability. This assumption does not limit the application of the method because any observation or line of observations whose adjustability is n may be represented by a line of n ties each of unit adjustability. In that case the total correction to the line must be divided among n

ties; hence the correction at each terminal junction is the total correction divided by n or the "unit correction" of the line.

ELECTRIC CIRCUIT ANALOGY

A gravity network such as shown in Fig. 1 is analogous to an electrical network in which impressed voltages correspond to observed gravity differences, and resistances to adjustabilities.[3] The current in each branch corresponds to the unit correction, and the current times the resistance, or the voltage drop across the resistance, is analogous to the unit correction times the adjustability, or total correction for the line.

In the electrical network the currents will be such that the power, that is

$$\sum i^2 r = \text{minimum.}$$

In the observational network the unit correction k will be such that

$$\sum k^2 a = \text{minimum}$$

where a is the adjustability.

In the electrical network the currents are found by means of Kirchoff's law which are:

1) The sum of the e.m.f.'s around any circuit is zero.

2) The sum of the currents at any junction is zero.

The principles established above for observational networks may be put in the same form, thus:

1) The sum of the adjusted observational differences around any circuit is zero.

2) The sum of the unit corrections at any junction is zero.

In the electrical network, points separated in space but joined by a bus-bar whose resistance is zero are treated as a single junction. Similarly, in the observational network, stations joined by fixed sides (whose adjustability is zero) are treated as a single junction.

These definitive conditions for a least square adjustment may be utilized in the following ways.

REDUCTION OF NUMBER OF EQUATIONS

In any network it is possible to arrive at a least square adjustment by (1) adjusting the sides arbitrarily so that the circuits close, (2)

[3] Cowles, Laurence G. loc. cit.

adding up the corrections at the junctions, (3) writing normal equations for the junctions in the same manner as is ordinarily done for the circuits, and (4) solving the normal equations for junction correlates. The correction for each side is then the arbitrary correction plus the sum of the correlates of the adjacent junctions.

Since this process requires extra steps it is used to advantage only when it substantially reduces the number of equations. That will usually be the case when the network has a number of fixed sides or jump ties. A jump tie is one that on a network diagram *must* be represented as crossing another tie. For example, the network shown in Fig. 2 has 13 adjustable circuits but has only five adjustable junctions. The surrounding ring of fixed sides or "bus-bar" is in effect one junction. Adjustment by the circuit method would require 12 equations while adjustment by the junction method would require only 4 equations. Furthermore, with the circuit method, the jump tie would complicate the mathematics by introducing off-diagonal plus terms

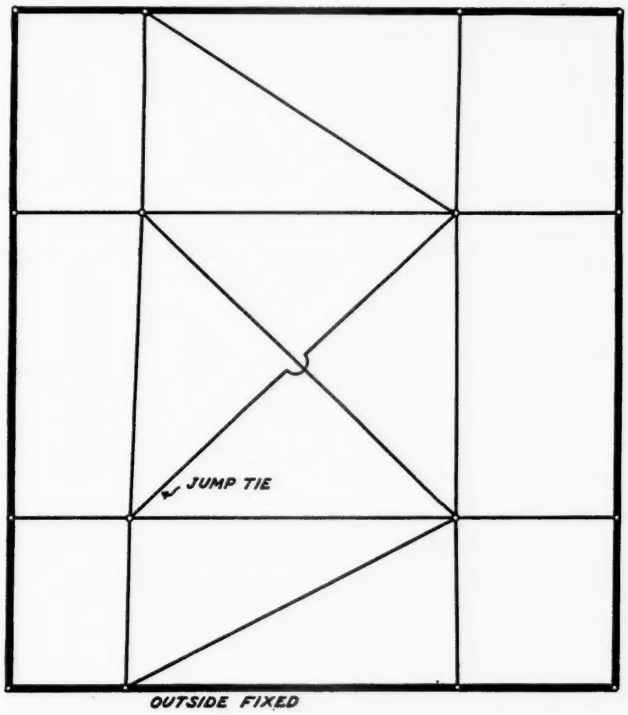

FIG. 2

in the normal equations and placing some sides in more than two circuits; whereas with the junction method any number of jump ties can be handled without increasing the number of changing the form of the equations.

On the other hand, if the enclosing sides in Fig. 2 were not fixed and the jump tie were omitted, the junction method would require 15 equations against 12 for the circuit method. In general, the circuit method is preferable, because with the junction method (1) a preliminary step of arbitrary adjustment is required, and (2) in the final check, junctions as well as circuits must be summed. If a wrong correlate is set down at a junction the circuits will still balance, hence in checking the final result, it is not sufficient to sum the corrections around each circuit. However, where the network is enclosed by fixed sides or contains a number of jump ties, the number of equations can often be substantially reduced by using the junction method.

NETWORK ADJUSTMENT BY SECTIONS

The requirement that both the circuits and the junction shall balance affords a check on networks that must be adjusted in sections; that is, networks which are growing by continued field work, and networks that are so large that an adjustment as a whole is impracticable. Such networks may be adjusted by dividing into overlapping sections. The adjusted values for the outside lines of the first section are taken as fixed sides for the second section. After the sections are adjusted separately, the corrections at each border station are summed and, if necessary, re-adjusted. In the same manner, where new data are added to an old network, only part of the old network need be re-adjusted. The amount that the sections should overlap cannot be rigidly defined. The greater the overlap the greater the number of equations, and the less the overlap the more the border junctions must be re-adjusted. Where the network consists chiefly of single ties, overlapping two lines of stations has generally been found satisfactory. In detail work, where there are long lines of stations and base control, overlapping one line of stations is usually sufficient.

CORRECTION OF ORIGINAL DATA

Occasional mishaps in network adjustment are the omission or misplacement of observations in the network diagram. More frequently, some belated data appear from the field after an adjustment is completed. Ordinarily the addition or revision of even one observa-

tion would require repeating the whole process of adjustment. However, by summing the corrections at the junctions it is possible to tell how much disturbance the new data will cause and it is usually possible to limit the re-adjustment to a small area.

SMALL NETWORKS

Small networks (about 10 circuits or less) may be adjusted by trial and error without forming equations. One method is to make alternate arbitrary adjustments of the circuits and the junctions. Usually it is sufficient to make in turn a circuit adjustment, a junction adjustment, and then another circuit adjustment. Another method is to choose a group of adjoining circuits with a large total error, divide the error equally among the enveloping sides, thus keeping the junctions in balance, compute the revised error of each circuit, choose a new group of circuits and so on until the residual errors are negligible. For large networks the interaction of circuits is so complex that it is usually advantageous to set up equations.

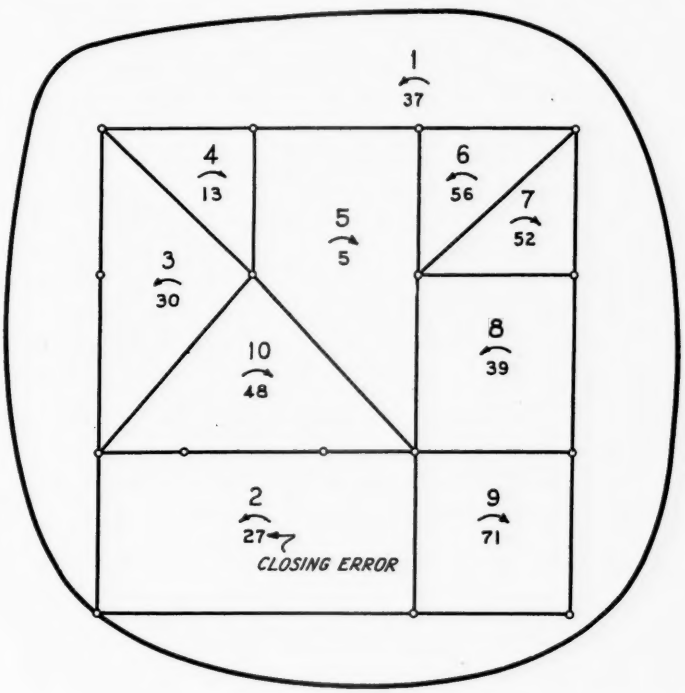

FIG. 3

TRIAL AND ERROR METHOD OF SOLVING NORMAL EQUATIONS

A trial and error method of solving the normal equations has been developed which saves from half to three-quarters of the time required for an algebraic solution. In brief, the method consists of choosing a set of approximate correlates, applying those correlates to the observed values to find new closing errors (residual errors), choosing a second set of approximate correlates, applying the second set of correlates to the residual errors of the first set, and continuing the process until the residual errors are small enough to be adjusted arbitrarily without loss of accuracy. A detailed explanation of the method would be too cumbersome to be presented here in toto* but a brief illustration will be given by applying the first step of the method to the network shown in Fig. 3.

Although the detailed explanation may appear complicated, most of the arithmetic can be done mentally; hence, with a little experience, the work can be performed quickly. As the sole objective of the method is to find a set of correlates which will balance the network, any means or device used is justified if it produces the desired result.

TABLE 1

B A	o	o +5	+7 +8	−1 −2	+2 −1	+15 +18	−10 −11	+3 +7	−15	−5
	1	2	3	4	5	6	7	8	9	10
1	+11	−2	−2	−1	−1	−1	−1	−1	−2	
2	−2	+6							−1	−3
3	−2		+4	−1						−1
4	−1		−1	+3	−1					
5	−1			−1	+5	−1		−1		−1
6	−1				−1	+3	−1			
7	−1					−1	+3	−1		
8	−1				−1		−1	+4	−1	
9	−2	−1						−1	+4	
10		−3	−1		−1					+5
11	+37	+27	+30	−13	−5	+56	−52	+39	−71	−48
12										
13	o	o	+7	−1	+2	+15	−10	+3	−15	−5
14										
15	+30	−3	−4	−1	−3	+3	−4	+4	−8	−14
16	+3									
17										
18	−3	+3	+2	+2	o	+6	−1	+7	−2	−14

* An exposition of the method with step by step instructions and examples has been prepared which the author will be glad to supply on request.

It is assumed that the adjustability of each side of the network is proportional to the number of observations. For example, the side between circuits two and ten has an adjustability of three. The normal equations are written by inspection and arranged as shown in Table 1. (For example, the total adjustability of circuit 2 is 6. Hence +6 is placed in column 2, line 2. Circuit 2 has in common with circuits 1, 9 and 10 adjustabilities of 2, 1 and 3. Hence these figures with the negative sign are put in columns 1, 9 and 10 on line 2. The closing error +27 is placed below the equations in column 2.) These equations are in the same form as for the algebraic solution except that for the algebraic solution the terms to the left of the diagonal would be omitted, and the constant terms or closing errors would be written in their respective lines rather than columns. Also the check terms of the algebraic solution are replaced by a summation circuit. In Fig. 3, the error in circuit 1 is the negative sum of the errors in the other circuits and equation 1 is the negative sum of the other equations. By using this circuit, the coefficients in each line and each column sum to zero and throughout the solution the sum of the closing errors must always be zero.

We now wish to find a set of trial correlates which, when substituted in the equations with the corresponding closing error subtracted from the original, will yield a small residual error. The simplest method would be to divide each error by the total adjustability of its circuit and use the quotient as a trial correlate. However, by this process convergence is slow and the trial correlates often oscillate between positive and negative. The following method is designed to speed up convergence, particularly where adjacent circuits have errors of the same sign.

For convenience we take the trial correlate of the enclosing circuit 1 to be zero. For circuit 2 we divide the closing error +27 (line 11, col. 2) by the total adjustability +6 (line 2, col. 2) and place the result, +5, in line A above the equations. Throughout the solution divisions are carried only to the nearest integer. The remainders are included in the residual errors. For circuit 3 we divide the closing error, +30 (line 11, col. 3), by the total adjustability, +4 (line 3, col. 3), and place the result +8 on line A, col. 3. For circuit 4, since it links with circuit 3, we multiply the common adjustability −1 (line 4, col. 3) by the trial correlate for circuit 3(+8, line A, col. 3) subtract the result from the error for circuit 4, divide the difference (−13+8=−5) by the total adjustability +3 (line 4, col. 4) and place the quotient −2 in line A,

col. 4. This process is continued through circuit 10 for which the trial correlate is

$$\frac{(3 \times 5) + (1 \times 8) - (1 \times 1) - 48}{5} = -5 \text{ (line A, col. 10).}$$

The trial correlates are then revised by applying a similar process to the circuits in descending order. Circuits 9 and 10 do not link with higher numbered circuits. Therefore, beginning with circuit 8, we multiply -1 (line 8, col. 9) by -15 (line A, col. 9), divide the result by the total adjustability $+4$ (line 8, col. 8), change sign, and add the quotient $-15/4 = -4$ to the previous correlate $+7$ (line A, col. 8). The sum $+3$ is placed in a new line B. This process is continued through circuit 2 for which the correlate becomes

$$\frac{(-3 \times 5) - (1 \times 15)}{6} + 5 = 0 \text{ (line B, col. 2).}$$

The uppermost figures in lines A and B are taken as the trial correlates for the first step, are written in line 13 below the equations and substituted in the equations. For circuit 1, each adjustability in line 1 is multiplied by the corresponding correlate in line 13 and subtracted from the error in line 11.

$$37 - (11 \times 0) - (2 \times 0) - (2 \times 7) + (1 \times 1) - (1 \times 2)$$
$$- (1 \times 15) + (1 \times 10) - (1 \times 3) + (2 \times 15) = +30.$$

The residual error, $+30$, is placed in line 15. When the trial correlates have been similarly substituted in all of the equations the residual errors will be those on line 15. Their sum is zero.

We now consider circuit 1 alone, divide its error, $+30$, by the total adjustability, $+11$, place the result, $+3$, in line 16 and substitute that value in all of the equations. For circuit 1, the new error will be

$$30 - 11 \times 3 = -3 \text{ (line 18, col. 1).}$$

For circuit 2 the new error will be

$$-3 + 2 \times 3 = +3 \text{ (line 18, col. 2) etc.}$$

As a check the errors in line 18 sum to zero.

It will be noted that by the above process the maximum error has been reduced from 71 to 14. By applying the same process to the residual errors of line 18, computing new errors and so on, the final error

of each circuit could be reduced to no greater than half the adjustability of the circuit. The final reduction can be obtained more quickly by means of variations in the method which are described in a supplement to this paper which those interested can obtain from the author.

The following table shows the time required for the trial and error method compared to the algebraic method. The figures given are for difficult conditions (bottle necks, jump ties, etc.). Under favorable conditions (large adjustabilities, adjacent errors opposite in sign, etc.) the time for the algebraic method is about the same, but the time for the trial and error method is substantially reduced.

TIME REQUIRED TO SOLVE NORMAL EQUATIONS*

	Algebraic Method (forward & backward solution)	*Trial & Error Method*
15 equations	2½ hours	1½ hours
20 equations	3½ hours	2 hours
30 equations	6 hours	3 hours
50 equations	12 hours	5 hours
70 equations	24 hours	7 hours

* The time for setting up the equations and for applying the solution to the network was not included because it is substantially the same for both methods.

CONCLUSIONS

Any adjustment, no matter how obtained, of a network comprising observed differences in the values of adjacent points, is a least square adjustment if it satisfies the following conditions: 1) the sum of the corrected observations around any circuit must be zero, and 2) the sum of the corrections at any junction must be zero.

The above principle provides a means of controlling necessary approximations such as the subdivision of a large network and simplifies subsequent adjustments made necessary by extension or revision of the data. It also serves in some cases to reduce the number of equations and in others to eliminate the equations entirely.

THE CALCULATION OF GRAVITY ANOMALIES DUE TO BODIES OF FINITE EXTENT*

S. LEVINE†

ABSTRACT

A new method for calculating the gravity anomalies due to mass distributions of finite extent and simple geometrical form has been developed. The principle of the method is the construction, in a plane, of curves which represent the boundaries of the body, such that the gravity effect is directly proportional to the area enclosed by such curves. The advantage of this method for bodies of considerable extent is emphasized. This approach is more rapid than that of the sector or graticule diagrams commonly employed.

This paper develops a simple, quick method for calculating the gravity effect due to sub-surface masses of finite extent and simple geometrical form. It was found that the graticule method proposed by Hedstrom[1] for solving gravity problems was cumbersome and hence a more rapid method was considered desirable. The results presented here are of use in determining the location and form of local lenses, dykes, zoned, faulted or folded geological structures from the experimental results of a gravimeter survey; they may also be extended to apply to torsion balance and magnetic experiments. It is assumed that the topographical, Bouguer, free air and necessary latitude corrections have already been applied to the field measurements.[2]

From a consideration of the gravity effects for plate-like masses, Jung[3] has indicated how the location of a two dimensional anomalous body (infinite in strike direction) may be determined from a study of the variation in gravity across the body.‡ Jung's is the direct method of interpretation, as contrasted to the more usual indirect procedure where various mass distributions are tested until the calculated anomalies resemble the field results.

Schwinner[5] and Ansel[6] have derived formulae for the gravitational anomaly due to a group of tabular bodies, into which most irregularly shaped geological bodies may be broken up. However, the application of their results to bodies of finite extent is a cumbersome process.

* Manuscript received August, 1940.

† McLennan Laboratory, Department of Physics, University of Toronto, Toronto, Canada.

[1] Numbered references refer to list at end of paper.

‡ Jung's results are not complete and can be extended. A fairly comprehensive study of curvature values and gradients, measured by the Eötvös torsion balance, has also been made by him.[4]

Consequently a graphical method is developed here whereby, for a given body, planimetrically measured areas are directly proportional to the gravitational effect.[7] This should present a relatively rapid and simple aid to the indirect interpretation of corrected gravimeter field observations.

PRINCIPLE OF AREA METHOD

Consider a prismatic body (Fig. 1a) extending at right angles from the (x, z) plane to a distance y, with its base in the (x, z) plane, bounded by the two radial lines making angles α_1 and α_2 with the z

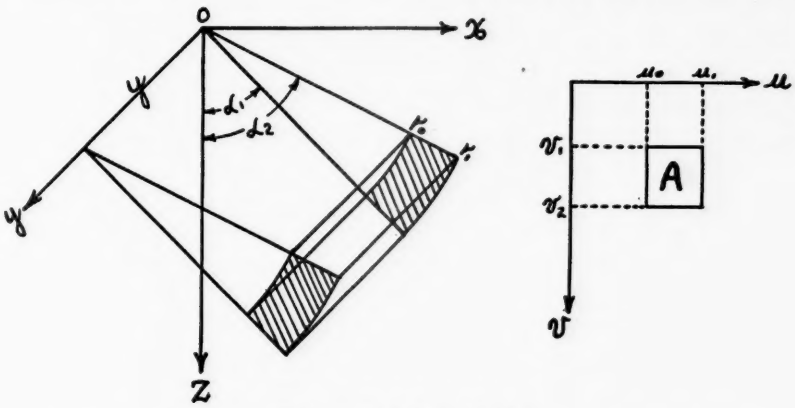

FIG. 1a. Rod-shaped body.
FIG. 1b. Rectangle in (u, v) plane corresponding to base in (x, z) plane in Fig. 1a.

axis and the two circles having the origin O and radii r_0 and r_1. The vertical component of the gravitational force at O caused by this body is readily found to be

$$\Delta g = G\sigma y(\sin \alpha_2 - \sin \alpha_1) \ln \left[\frac{r_1 + \sqrt{r_1^2 + y^2}}{r_0 + \sqrt{r_0^2 + y^2}}\right], \qquad (1)$$

where G = gravitational constant $= 6.66 \times 10^{-8}$ c.g.s. units and σ = density difference with respect to the surrounding medium. Let us compare the (x, z) plane with the (u, v) plane, where

$$\begin{aligned} u &= \ln (\bar{r} + \sqrt{\bar{r}^2 + 1}), \qquad v = \sin \alpha, \\ \bar{r} &= r/y, \qquad r^2 = x^2 + z^2, \qquad \tan \alpha = x/z. \end{aligned} \qquad (2)$$

In the (u, v) plane, the region in the (x, z) plane, forming the base of the prismatic body, is transformed into a rectangular area bounded by the lines

$$u = u_0 = \ln(\bar{r}_0 + \sqrt{\bar{r}_0^2 + 1}), \qquad u = u_1 = \ln(\bar{r}_1 + \sqrt{\bar{r}_1^2 + 1}),$$
$$v = v_1 = \sin \alpha_1$$

and $v = v_2 = \sin \alpha_2$ (Fig. 1b). The area of this rectangle is given by

$$(u_1 - u_0)(v_2 - v_1)$$
$$= (\sin \alpha_2 - \sin \alpha_1) \ln \left[\frac{\bar{r}_1 + \sqrt{\bar{r}_1^2 + 1}}{\bar{r}_0 + \sqrt{\bar{r}_0^2 + 1}} \right] = \frac{\Delta g}{G\sigma y}, \qquad (3)$$

according to (1). Now these regions in the (u, v) and (x, z) planes can be made arbitrarily small and there is a one-to-one correspondence between the points in the two planes. It follows that for any closed curve in the (x, z) plane, defining the base of a body of uniform cross section and horizontal length y, the corresponding closed curve in the (u, v) plane is such that the area A enclosed yields the gravity effect of this body at O, namely

$$\Delta g = G\sigma y A. \qquad (4)$$

To treat bodies with rectangular cross-sections we need to draw families of curves which correspond to $x = \text{constant}$ and $z = \text{constant}$ in the (x, z) plane. This can be carried out in the following manner. We shall work in units of the body length y, so that

$$\bar{x} = x/y, \qquad \bar{z} = z/y, \quad \text{and} \quad \bar{r}^2 = \bar{x}^2 + \bar{z}^2.$$

Then

$$|\bar{x}| = \bar{r} \sin \alpha = \bar{r} v, \qquad \bar{z} = \bar{r} \cos \alpha = \bar{r}\sqrt{1 - v^2}, \qquad (5)$$

where, according to (2)

$$\bar{r} = (e^{2u} - 1)/2e^u. \qquad (6)$$

These equations define the functional relations between $(\bar{x}, \bar{z})$ and (u, v). In the (u, v) plane, the curves representing constant values of $\bar{x}$ and $\bar{z}$ (which are the parameters in the two families of curves) are given by

$$\{(e^{2u} - 1)/2e^u\}\sqrt{1 - v^2} = \bar{z}, \quad \{(e^{2u} - 1)/2e^u\}v = |\bar{x}|. \qquad (7)$$

However, in plotting these curves in the (u, v) plane, it is more convenient to retain the forms (5) and (6) and proceed as follows. In one quadrant of the $(\bar{x}, \bar{z})$ plane (Fig. 2) we have drawn the set of radial lines representing given values of v, namely $v = 0.05, 0.10, \cdots, 0.80, 0.825, \cdots, 0.975$ and also the set of circular arcs with O as origin, of

radius representing given values of u, namely $u=0.05, 0.10, 0.15, \cdots, 0.25$. To determine the curve in the (u, v) plane which corresponds to a given value of $\bar{x}$ (or $\bar{z}$), say $\bar{x}_0$ (or $\bar{z}_0$), the values of u at the points of

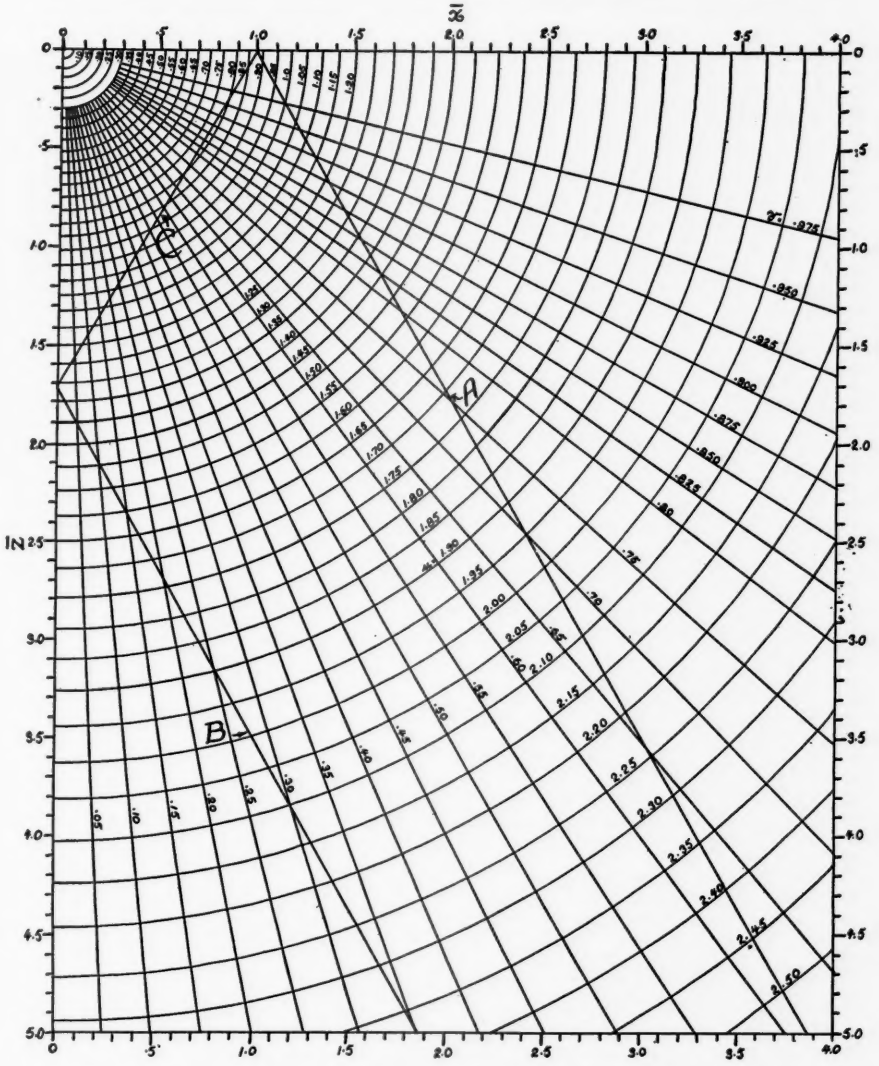

FIG. 2. In $(\bar{x}, \bar{z})$ plane, radial lines and circular arcs represent fixed values of of $v=\sin\alpha$ and $u=\ln(\bar{r}+\sqrt{\bar{r}^2+1})$ respectively. Equation of line A is $\bar{z}=\sqrt{3}(\bar{x}-1)$, that of B, $\bar{z}=\sqrt{3}(\bar{x}+1)$ and that of line C, $\bar{z}=-\sqrt{3}(\bar{x}-1)$, equivalent to the continuation of line B into quadrant $\bar{x}<0$.

intersection of the line $\bar{x}=\bar{x}_0$ (or $\bar{z}=\bar{z}_0$) with the radial lines representing fixed v's are found, thus giving a series of (u, v) values for fixed $\bar{x}$ or $\bar{z}$.

This graphical method is not the most convenient when $\bar{r}\ll 1$ or when $\bar{r}\gg 1$ (actually it is sufficient that $\bar{r}>8$) since the formulae (5) and (6) can be simplified as follows. When $\bar{r}\ll 1$, then according to (2), $u\approx\bar{r}$ so that (5) becomes

$$u \approx |\bar{x}|/v, \qquad u \approx \bar{z}/\sqrt{1-v^2}, \tag{8}$$

from which we readily compute the curves for constant $\bar{x}$ and $\bar{z}$. When $\bar{r}\gg 1$, then (2) or (6) becomes $u\approx\ln 2r$ or $r\approx e^u/2$ respectively, and (5) may be written as

$$u \approx \ln 2\,|\bar{x}| - \ln v, \quad u \approx \ln 2\,|\bar{z}| - \ln\sqrt{1-v^2}, \tag{9}$$

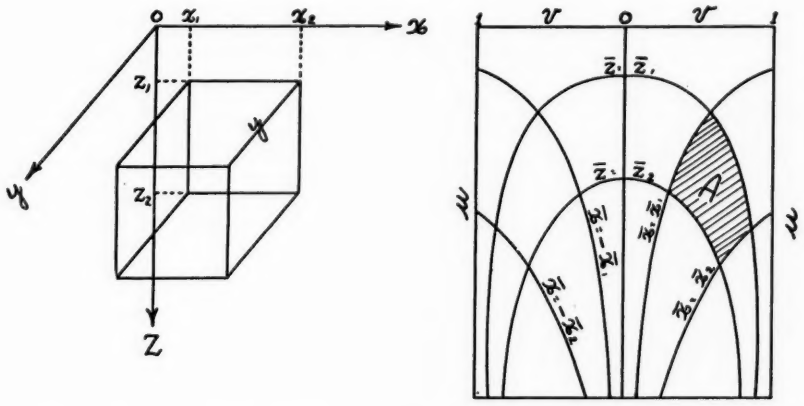

FIGS. 3a and 3b. Gravity anomaly due to rectangular body. At O, $\Delta g=G\sigma yA$, where σ=density difference, G=gravitational constant, y=length of body in y direction, A is shaded area, $\bar{x}_1$, $\bar{x}_2$, $\bar{z}_1$ and $\bar{z}_2$ are measured in units of y, i.e., $\bar{x}_1=x_1/y$, $\bar{x}_2=x_2/y$, $\bar{z}_1=z_1/y$ and $\bar{z}_2=z_2/y$.

which again is convenient for numerical computation. Actually, in Fig. 3c, where the $\bar{x}$ and $\bar{z}$ curves in the (u, v) plane are shown, equations (9) were employed in the lower half of the diagrams, equations (8) in a narrow strip at the top, and Fig. 2 in the remaining part.

The following special properties of the $\bar{x}$ and $\bar{z}$ curves were also used in drawing Fig. 3c. When $v=0$, $u=\ln(\bar{z}+\sqrt{\bar{z}^2+1})$; when $v=1$, $u=\ln(|\bar{x}|+\sqrt{|\bar{x}|^2+1})$. When $v=\epsilon\ll 1$, then $\epsilon\approx|\bar{x}|/\bar{z}$ and when $v=1-\epsilon$, $|\bar{x}|\approx\bar{z}/\sqrt{2\epsilon}$. The line $v=1$ is an asymptote to the $\bar{z}$ curves

and the line $v=0$ an asymptote to the $\bar{x}$ curves. The symmetry of the two families of curves about the u axis is to be expected. All these properties are readily checked by examining equations (2), (5) and (6).

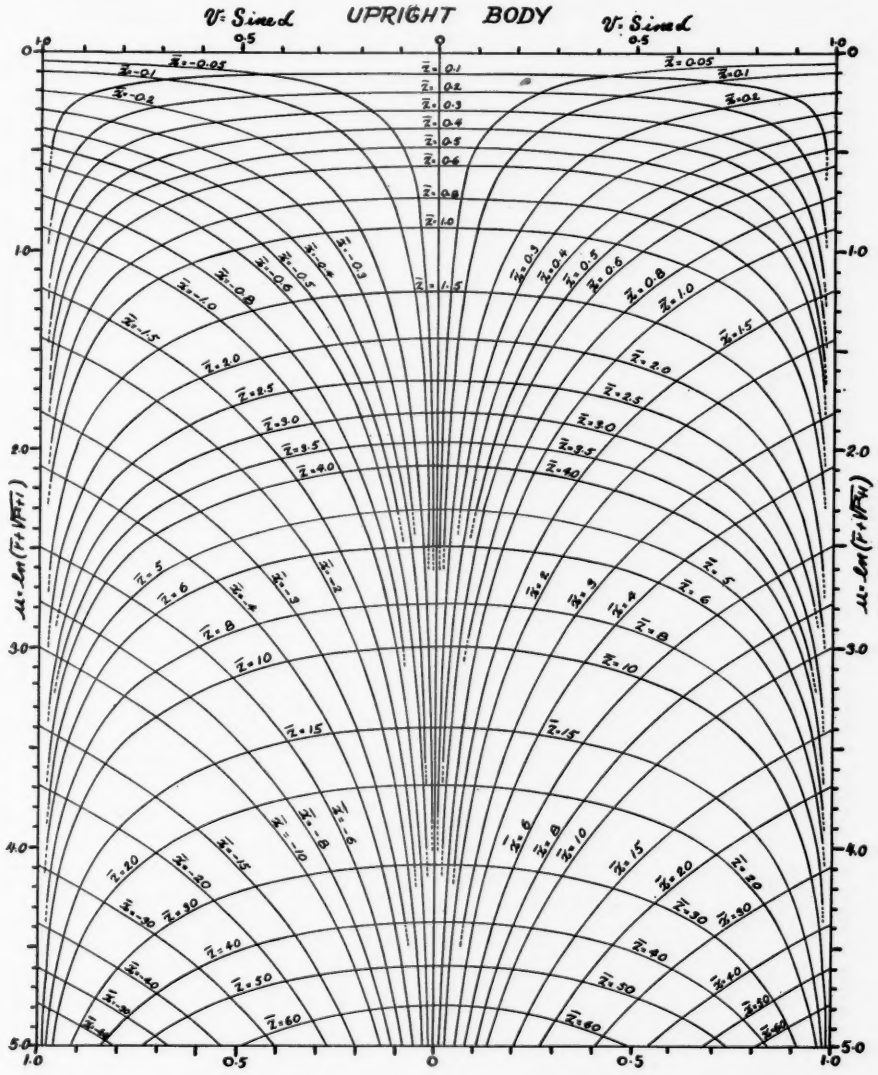

FIG. 3c. Reproduction of actual diagram used to determine gravity anomaly due to rectangular body. In original, $\Delta u=0.1$ or $\Delta v=0.05$ corresponds to 1 cm. Then $\Delta g=0.005\,G\sigma yA=1.015\times10^{-3}A$ milligals for $y=100$ feet and $\sigma=1$, where A is measured in sq. cm.

The application of Fig. 3c in calculating the gravity anomalies of rectangular upright bodies will now be explained. Suppose that we are given a rectangular body bounded by the planes $x=x_1$, $x=x_2$, $z=z_1$, $z=z_2$, $y=0$ and $y=y$ (Fig. 3a). To the rectangular base of this body in the (x, z) plane there will correspond in the (u, v) plane, an area bounded by the four curves $\bar{x}=\bar{x}_1=x_1/y$, $\bar{x}=\bar{x}_2=x_2/y$, $\bar{z}=\bar{z}_1=z_1/y$ and $\bar{z}=\bar{z}_2=z_2/y$ enclosing an area A, say (Fig. 3b). Then the gravity anomaly at the origin O due to the body will be given by (4) which becomes

$$\Delta g = 0.005 G\sigma y A = 1.015 \times 10^{-3} A \text{ in milligals,} \qquad (10)$$

taking $y=100$ feet, $G=6.66\times10^{-8}$ and $\sigma=1$, A being measured in sq. cm. The factor 0.005 enters because in the original (u, v) plane $\Delta u=0.1$ or $\Delta v=0.05$ corresponds to 1 cm. Since Δg is proportional to y, if the length of the body is, say, 1,000 feet, we need only multiply (10) by the factor 10, remembering, of course, that the values of $\bar{x}_1$, $\bar{x}_2$, $\bar{z}_1$ and $\bar{z}_2$ are divided by the same factor 10. To find the variation in the gravity anomaly as we move across the body at right angles to its strike (length y) we need only shift the values of $\bar{x}_1$ and $\bar{x}_2$ always remaining in the region bounded by the two curves $\bar{z}=\bar{z}_1$ and $\bar{z}=\bar{z}_2$ and keeping the difference $\bar{x}_2-\bar{x}_1$ constant. In this way, we see that by observing the change in area, it is possible to estimate quickly the relative change in the gravity effect with position of observation. Formula (4) or (10) applies to the gravity effect along one edge of the body. If we require the effect across the centre of the body, then we need to assume a length $y/2$ ($=50$ feet) in (10) and double the value of Δg obtained, since a body extending from 0 to $y/2$ gives the same contribution as one extending from 0 to $-y/2$.

Similarly it is possible to find the gravity variation across any section at right angles to the strike direction (parallel to the x axis). Thus for a body of length y, if the effect is required across a section at a distance y' from one end, we need only divide the body into two parts of lengths y' and $y-y'$, apply the method described above to each part separately and then add the two contributions. In the case where $y'>y$, that is, the body is no longer directly underneath the line of observation, the difference and not the sum of the two contributions is taken.

We next turn our attention to bodies with different dips. Consider a body of length y, and of uniform cross section, the base in the (x, z) plane being a parallelogram bounded by four lines of the type $z=z_1$,

$z=z_2$, $z=m(x-a_1)$ and $z=m(x-a_2)$ (Fig. 4a). Here $m=\tan(\pi/2-\alpha)$ is the slope of the two parallel inclined lines, a_1 and a_2 being their intercepts on the x axis. To treat such a body, we need to draw the two

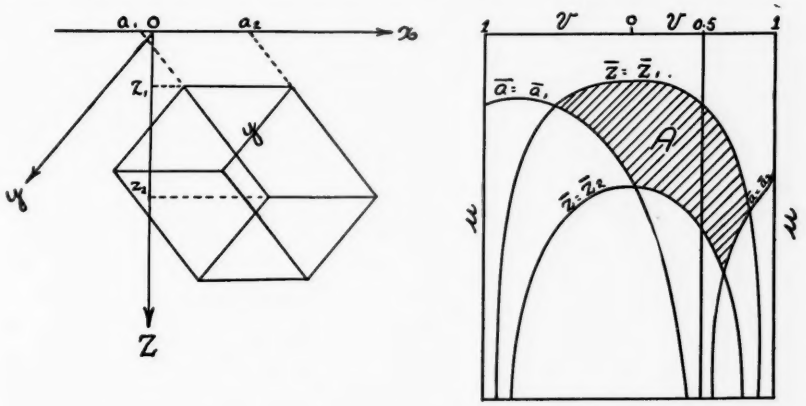

FIGS. 4a and 4b. Gravity anomaly due to dipping body. At o, $\Delta g=G\sigma yA$, where σ=density difference, G=gravitational constant, y=length of body in y direction, A is shaded area, $\bar{a}_1$, $\bar{a}_2$, $\bar{z}_1$ and $\bar{z}_2$ are measured in units of y, i.e., $\bar{a}_1=a_1/y$, $\bar{a}_2=a_2/y$, $\bar{z}_1=z_1/y$ and $\bar{z}_2=z_2/y$.

families of curves in the (u, v) plane, represented by the horizontal line, $\bar{z}$=constant; that is

$$\bar{z} = \bar{r}\sqrt{1 - v^2}, \tag{11}$$

and by the inclined line

$$\bar{z} = m(\bar{x} - \bar{a}) \quad \text{or} \quad \bar{r}\sqrt{1 - v^2} = m(\pm\, \bar{r}v - \bar{a}), \tag{12i}$$

which may be written as

$$\bar{r} = \left|\frac{m\bar{a}}{\sqrt{1 - v^2} + mv}\right|, \qquad \bar{x} < 0;$$
$$\bar{r} = \left|\frac{m\bar{a}}{\sqrt{1 - v^2} - mv}\right|, \qquad \bar{x} > 0; \tag{12ii}$$

where (6) defines $\bar{r}$ in terms of u and $\bar{a}=a/y$. These two sets of contours are shown in Fig. 4c, taking the dip $\pi/2-\alpha=60°$, so that $m=\sqrt{3}$. The set representing constant values of $\bar{z}$ is identical with the one in Fig. 3c.

The parameter in the family of curves (12i) in the (u, v) plane is

the intercept $\bar{a}$. The upper half of Fig. 4c (excluding a narrow strip at the top) is again treated by first drawing (12i) in the $(\bar{x}, \bar{z})$ plane,

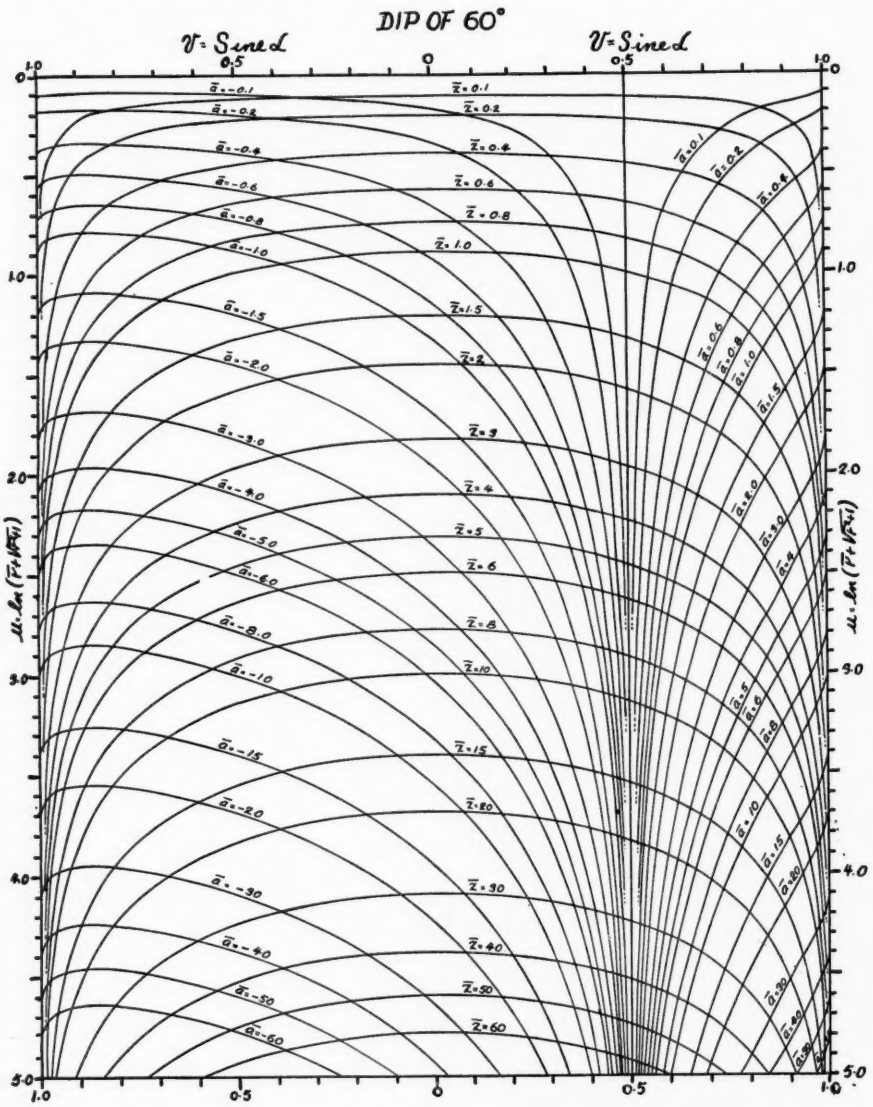

FIG. 4c. Reproduction of actual diagram to determine gravity anomaly due to body with uniform cross section dipping at 60°. In original, $\Delta u = 0.1$ or $\Delta v = 0.05$ corresponds to 1 cm. Then $\Delta g = 0.005\, G\sigma y A = 1.015 \times 10^{-3} A$ milligals for $y = 100$ feet and $\sigma = 1$, where A is measured in sq. cm.

in Fig. 2. Here we need to consider two quadrants in the $(\bar{x}, \bar{z})$ plane, namely $\bar{x}>0$ and $\bar{x}<0$ (with $\bar{z}>0$), but it is possible to restrict oneself to the one quadrant shown in Fig. 2 ($\bar{x}>0$) by the following device. When $\bar{a}>0$, then (12i) lies inside $\bar{x}>0$, as illustrated by line A in Fig. 2 for the case $\bar{a}=1$, $m=\sqrt{3}$. When $\bar{a}<0$, then part of the line (12i) lies inside $\bar{x}>0$ (as illustrated in Fig. 2 by the line B for the case $\bar{a}=-1$, $m=\sqrt{3}$) and part inside $\bar{x}<0$. On account of the symmetry of the radial lines (fixed v's) about the $\bar{z}$ axis in the $(\bar{x}, \bar{z})$ plane, the latter part can be replaced by the line $\bar{z}=-m(\bar{x}+\bar{a})$ in the quadrant $\bar{x}>0$, as illustrated in Fig. 2 by the line C for the case $\bar{a}=-1$, $m=\sqrt{3}$. Then, in Fig. 2 a series of (u, v) values for the curve in the (u, v) plane corresponding to the line (12i) with $\bar{a}=1$ and $m=\sqrt{3}$, is determined by reading off the values of u at which line A intersects the radial lines (fixed v's). When $\bar{a}=-1$, the intersections along lines B and C are considered. In a similar fashion, we obtain curves for a whole series of $\bar{a}$ values, both positive and negative.

Again this graphical method is not convenient when $\bar{r}\ll 1$ or when $\bar{r}\gg 1$. In the narrow strip at the top of Fig. 4c, where $\bar{r}\ll 1$, (12ii) becomes

$$\begin{aligned} u &\approx \left|\frac{m\bar{a}}{\sqrt{1-v^2}+mv}\right|, \qquad \bar{x}<0; \\ u &\approx \left|\frac{m\bar{a}}{\sqrt{1-v^2}-mv}\right|, \qquad \bar{x}>0; \end{aligned} \tag{13}$$

since $u\approx\bar{r}$. In the lower half of Fig. 4c where $\bar{r}\gg 1$, (12ii) reduces to

$$\begin{aligned} u &\approx \ln\left|\frac{2m\bar{a}}{\sqrt{1-v^2}+mv}\right|, \qquad \bar{x}<0; \\ u &\approx \ln\left|\frac{2m\bar{a}}{\sqrt{1-v^2}-mv}\right|, \qquad \bar{x}>0; \end{aligned} \tag{14}$$

substituting $u\approx\ln 2r$. Other properties of (12ii) which are useful are the following. When $v=0$, $u=\ln(|m\bar{a}|+\sqrt{|m\bar{a}|^2+1})$; when $v=1$, $u=\ln(|\bar{a}|+\sqrt{|\bar{a}|^2+1})$. The line $v=1/\sqrt{1+m^2}$ is an asymptote to all the curves (12ii) in the (u, v) plane. In Fig. 2, lines of the type A ($\bar{a}>0$, $\bar{x}>0$) correspond to the region $1/\sqrt{1+m^2}\leqq v\leqq 1$, in the right-hand half of Fig. 4c; lines of type B($\bar{a}<0$, $\bar{x}>0$), to the region $0\leqq v\leqq 1/\sqrt{1+m^2}$, in the same half; and lines of type C ($\bar{a}<0$, $\bar{x}<0$) to the

left-hand half of Fig. 4c, $0 \leqq v \leqq 1$. In the immediate vicinity of the asymptote we have used the formula $u = \ln(\bar{r} + \sqrt{\bar{r}^2+1})$, where $\bar{r} = \left| m^2\bar{a}/\epsilon(m^2+1) \right|$ with $\left| v - 1/\sqrt{1+m^2} \right| = \epsilon$. The ordinate $v=1$ is a tangent to the curves (12ii), since $du/dv = \infty$ when $v=1$, and a maximum is exhibited at $v = m/\sqrt{|m^2+1|}$ when $\bar{x}<0$, since $du/dv=0$. All these results are readily verified by examining (2) and (12ii).

The application of Fig. 4c is similar to that of Fig. 3c. The area bounded by the four curves in the (u, v) plane (Fig. 4b), corresponding

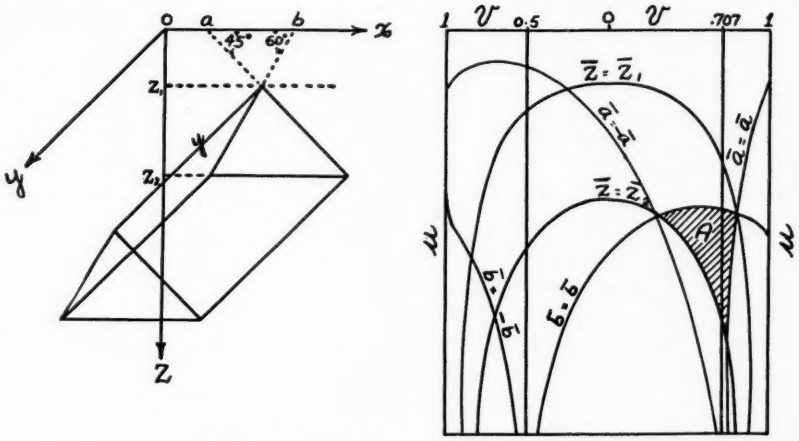

FIGS. 5a and 5b. Gravity anomaly due to body of triangular cross section shown. At 0, $\Delta g = G\sigma y A$, where σ = density difference, G = gravitational constant, y = length of body in $\bar{y}$ direction, A is shaded area, $\bar{a}$, $\bar{b}$, $\bar{z}_1$ and $\bar{z}_2$ are measured in units of y, i.e., $\bar{a} = a/y$, $b = b/y$, $\bar{z}_1 = z_1/y$ and $\bar{z}_2 = z_2/y$.

to the sides of the parallelogram in Fig. 4a, yields the gravity effect at O according to (4) or (10). When we move across the mass in the x direction, $\bar{a}_1$ and $\bar{a}_2$ change, but $\bar{a}_2 - \bar{a}_1$ remains fixed. Figures for dips of 75°, 45°, 30°, and 15°, have not been included.*

It is quite simple to draw the three families of contours in the (u, v) plane, which will yield the gravity effect of a body in the form of a triangular prism (uniform triangular cross section). In Figs. 5b and 5c, we have carried this out for a prism, two of whose sides are dipping at 45° and 60°, the third side being horizontal (Fig. 5a). The three families of curves in the (u, v) plane for this particular case are defined by $\bar{z} = \text{constant}$, $\bar{z} = (\bar{x} - \bar{a})$ and $\bar{z} = -\sqrt{3}(\bar{x} - \bar{a})$. To obtain

* The reproductions of such figures, as illustrated by Figs. 3c, 4c, and 5c, are of little value for applications because of their reduced size. On request prints of the original large-scale diagrams can be furnished by the author.

the last set of curves, Fig. 4c need only be drawn on transparent paper which is then turned over to give the equivalent mirror image with respect to the axis $v=0$.

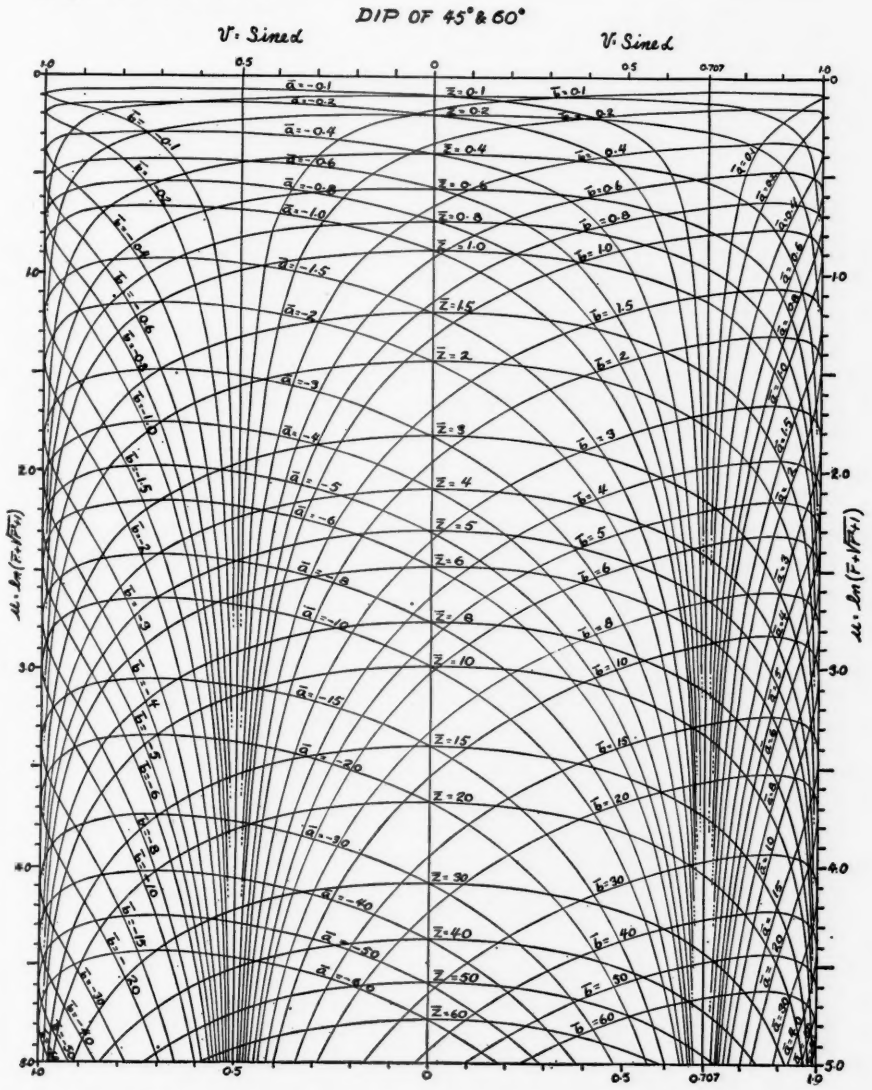

FIG. 5c. Reproduction of actual diagram used to determine gravity anomaly due to body of triangular cross section shown. In original $\Delta u=0.1$ or $\Delta v=0.05$ corresponds to 1 cm. Then $\Delta g=0.005\,G\sigma yA=1.015\times10^{-3}A$ milligals for $y=100$ feet and $\sigma=1$, where A is measured in sq. cm.

APPLICATIONS AND DISCUSSIONS

The area method was applied to the results of a gravimeter survey in Chibougamau Property, Rouyn Area, Noranda, Quebec carried out by Hans Lundberg Ltd., Geophysicists. The gravity variation across

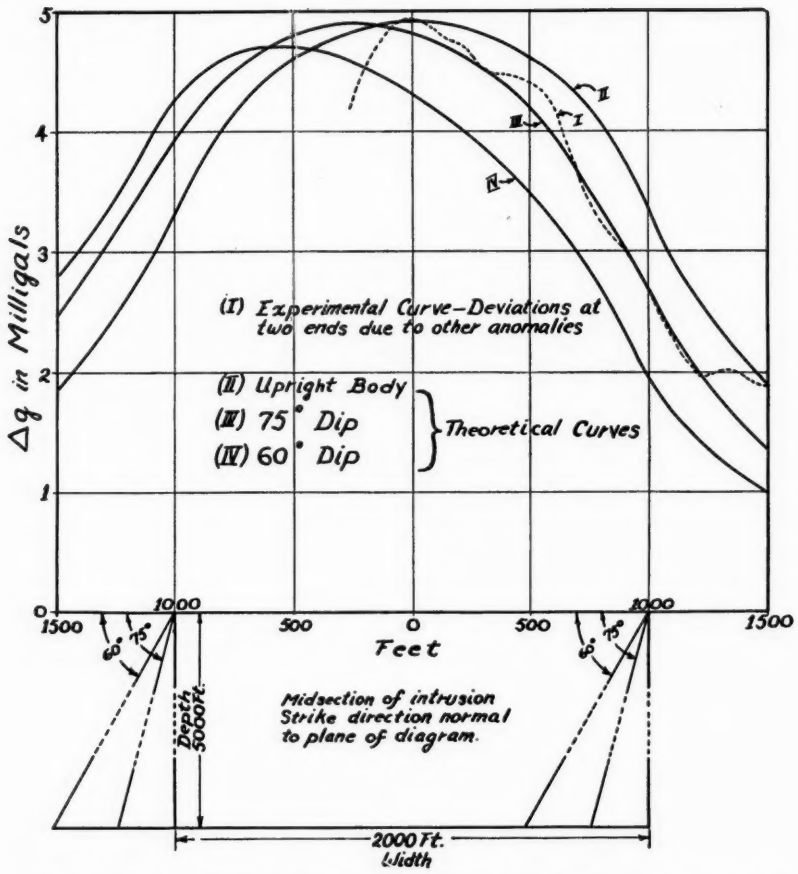

FIG. 6. Gravimeter profile across intrusion of gabbro in rhyolite in Rouyn Area, Noranda, Que. Theoretical curves for dips of 60°, 75°, and 90° shown, assuming strike length 4,000 ft., width 2,000 ft., $z_1=0$, $z_2=5{,}000$ ft. and $\sigma=0.3$. Gravity readings have been corrected for the topographical, Bouguer, free air and latitude effects.

the mid-section of an intrusion of gabbro in rhyolite is shown in Fig. 6. Assuming a strike length of 4,000 ft., width 2,000 ft., depth 5,000 ft. and density difference $\sigma=0.3$, the theoretical curves for dips of 60°,

75° and 90° have been drawn in Fig. 6. It is seen that the dip 75° gives the closest agreement with experiment.

Another method of computing the gravity anomalies caused by mass distributions has been suggested by Hedstrom,[1] who also begins with equation (1). If we put

$$G\sigma(\sin \alpha_2 - \sin \alpha_1) = \text{constant} = c, \text{ say,}$$

and $r_0 = 0$, (1) may be written as

$$\lambda_1 = e^{\Delta g/c y} = (r_1 + \sqrt{r_1^2 + y^2})/y = \bar{r}_1 + \sqrt{\bar{r}_1^2 + 1},$$

or

$$\bar{r}_1 = r_1/y = (\lambda_1^2 - 1)/2\lambda_1. \tag{15}$$

Let us assume a given gravity anomaly, $\Delta g = 0.01$ milligal (1 milligal $= 10^{-3}$ gal $= 10^{-3}$ cm.sec.$^{-2}$), take certain divisions of angle, say 0°, 10°, 20°, · · ·, 80°, 90° so that $\alpha_2 - \alpha_1 = 10°$, and put $y = 100$ meters and $\sigma = 1$. Then the values of λ_1 are known and (15) will yield the radii $\bar{r}_1$, in units of the length y of the prismatic body. To obtain the radii $\bar{r}_n$ which will correspond to a gravity anomaly of $n\Delta g$, where n is some integer, we observe that $e^{n\Delta g/cy} = \lambda_1^n$, so that

$$\bar{r}_n = r_n/y = (\lambda_1^{2n} - 1)/2\lambda_1^n. \tag{16}$$

Introducing this simplification to Hedstrom's calculations, we have constructed a sector diagram similar to the one shown by Hedstrom (Fig. 7). Each field in the diagram represents the base surface of a body of length $y = 100$ metres, that increases the gravity force at the origin by 0.01 milligal, assuming the density difference σ to be unity. With the aid of this diagram gravity anomalies caused by bodies of horizontal length 100 metres and a certain cross-section can be computed, by plotting the cross-section of the body in Fig. 7 and then counting the number of fields covered.

The advantages of the area method developed may be listed as follows:

(1) By means of a planimeter, the areas in the (u, v) plane can be obtained quite rapidly with fair accuracy.

(2) Bodies which extend to considerable depths or which have considerable lateral (horizontal) dimensions are readily treated. The diagrams in the (u, v) plane read to values of $\bar{r}$ greater than 60, i.e., to distances 60 times the strike length. The convergence of the areas with distance from the origin is a very useful feature, the diminishing con-

tribution to the gravity effect from distant parts of the body being elegantly demonstrated in the (u, v) plane.

(3) It is possible to obtain a rapid visual estimation of the variation of the gravity effect both with depth and lateral extension. The gravity anomaly is directly proportional to the area, a property which is very convenient.

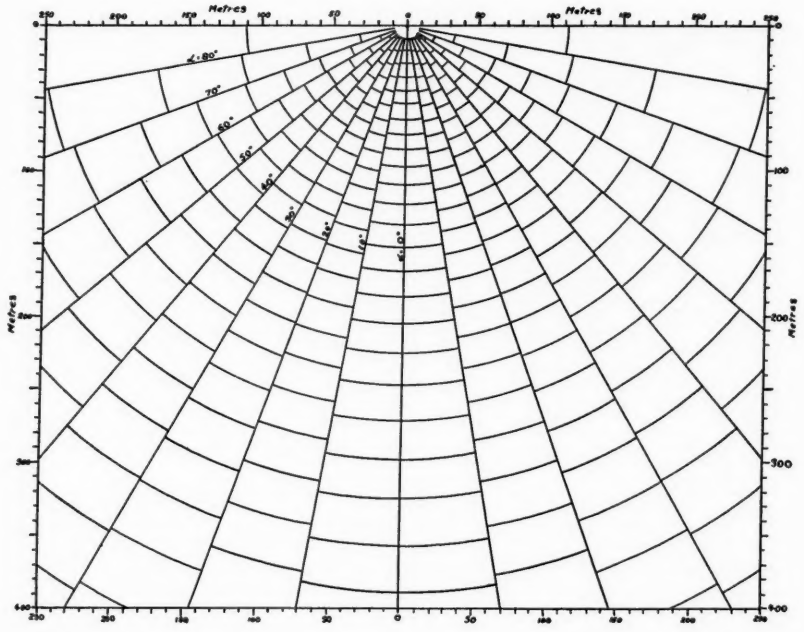

FIG. 7. Sector diagram for computation of gravity anomalies, each field = 0.01 milligal. Longitudinal extension of body at right angles to plane of paper = 100 m. in one direction.

(4) There is no difficulty when the length of the body is changed. One need only remember that the values of $\bar{x}$ and $\bar{z}$ in the (u, v) plane are always measured in units of y (that is, in units of the strike length) and that y enters as a multiplicative factor in the expression for Δg.

(5) The gravity effect due to bodies of simple geometrical form and any dip can be computed, although a separate diagram for each dip is required. Since ordinarily the exact shape of a geological structure is unknown, it is necessary to assume various simple shapes and ascertain by trial and error which form is the nearest to the true one.

Rapidity is essential in this process and is attained by means of our area method.

The following remarks on Hedstrom's graticule method are relevant.

(1) The counting of fields in Fig. 7 requires estimations of fractions, which is awkward and tedious. This is particularly true for a body with a long narrow cross-section. Moreover, the determination of the variation in gravity across a body necessitates a repetition of the counting process for each point on the curve.

(2) Fig. 7 extends only to the distance $\bar{r} \approx 4$. It may be said that the range covered by our (u, v) diagrams could only be realized by a series of diagrams of the Hedstrom type.

(3) For large $\bar{r}$, the fields in the sector diagram become very large and the estimation of small fractions is clumsy. This can be overcome, of course, by taking a smaller angle division $\alpha_2 - \alpha_1$, but this increases the number of graticules, thereby making the counting even more tedious and lengthy.

(4) Hedstrom's method can also be applied to any strike length y but this involves a change of the scale along the x axis, which is a little awkward.

(5) The only significant advantage of Fig. 7 is that it is applicable to a body of irregularly shaped cross-section. However, it is customary to break up an irregular structure into a number of bodies of simple geometrical form, so that even this advantage is not important in actual practise.

A preliminary investigation shows that our area method can also be adopted to find the curvature values and gradients due to the same forms of bodies as considered above, from measurements with the torsion balance. Since the magnetic intensity due to magnetic bodies can also be expressed in terms of the second derivatives of the gravity potential, this also permits the construction of area diagrams leading to the computation of magnetic anomalies. Work in this direction is now being carried on.

ACKNOWLEDGMENTS

This problem was suggested to me by Mr. Hans Lundberg and I am indebted to him for financial assistance, enabling the work to be carried out. I also wish to express my gratitude to Dr. A. A. Brant for his valuable help and numerous suggestions during the preparation of the paper.

REFERENCES

(1) H. Hedstrom, Amer. Inst. Min. & Met. Eng., Tech. Pub. No. 953, 1938.
(2) S. Hammer, GEOPHYSICS, Vol. IV, No. 3, p. 184, July 1939.
(3) K. Jung, Zs. f. Geophys. 13, 45, 1937.
(4) K. Jung, Zs. f. Geophys. 3, 257, 1927; 5, 238, 1929.
(5) R. Schwinner, Gerlands Beitr. z. Geophys. 23, 35, 1929.
(6) E. A. Ansel, Beiträge z. angewand. Geophys. 5, 263, 1936; 6, 141, 1936.
(7) See also Handbuch der Experimentalphysik, Vol. 25, Part 3, pp. 169, 176–177, 182–183, discussing the fundamental idea. (Editor)

PATENTS*

ELECTRICAL PROSPECTING

U. S. No. 2,230,803, P. W. Klipsch, S. S. West, S. Bilinsky, and W. G. McLarry. Iss. 2/4/41, Appl. 8/25/38.

Wave Synthesizing Network—Transient-synthesizer for making comparisons with "eltran" waves. Square-wave generator output is applied to a complex network which combines voltages from various resistive and reactive elements to obtain complex transients.

U.S. No. 2,231,013, P. W. Klipsch and S. S. West, Iss. 2/11/41, Appl. 11/1/37. Assign. E. E. Rosaire.

Electrical Prospecting with Alternating Current—Alternating current transmitted through the earth is measured for phase shift and attenuation at different frequencies.

U.S. No. 2,231, 048, C. C. Beacham, Iss. 2/11/41, Appl. 11/22/35.

Process or Method of Geophysical Prospecting—Electrical prospecting with two potential electrodes, one remote current electrode, and two nearby current electrodes used alternately so that variations of the resistivity near the electrodes may be compensated by comparison of the data obtained.

GRAVIMETRIC PROSPECTING

U.S. No. 2,225,566, J. McD. Ide, Iss. 12/17/40, Appl. 1/22/38. Assign. Shell Development Company.

Gravity Meter—Torsion Gravimeter achieves linear scale with astatization by means of two radial weight arms mounted about 90 degrees apart at two points on a horizontal torsion filament. The weight arms may be eccentrically weighted spheres submerged in liquid of just sufficient density to support their weight and having their centers of buoyancy lying on the torsion wire axis.

U.S. No. 2,225,582, J. L. Bible, Iss. 12/17/40, Appl. 3/9/40. Assign. Stanolind Oil and Gas Co.

Gravity Meter Clamp—Moving system of a gravimeter is clamped between three or more adjustable points on one side and a single adjustable point on the other side. The points make contact simultaneously to hold the moving system in approximate operating position.

U.S. No. 2,232,177, J. McD. Ide, Iss. 2/18/41, Appl. 6/10/39. Assign. Shell Development Co.

Optical System—Image deflections in a gravimeter or similar instrument are magnified by multiple reflections between a partially-transmitting mirror and a totally-reflecting mirror.

GEOCHEMICAL PROSPECTING

U.S. No. 2,228,223, G. S. Bays, Iss. 1/7/41, Appl. 11/14/39. Assign. Stanolind Oil and Gas Co.

Geochemical Prospecting—Conductivity of soil sample is measured in place usually

* Quarterly listings provided by Gary Muffly, Gulf Research & Development Co.

in a shallow drill hole. Sample is wetted to varying degrees or saturated with water. Measurements taken over an area show changes in mineral content, which are used to locate hydrocarbon deposits.

U.S. No. 2,229,884, C. R. Chalkley, Iss. 1/28/41, Appl. 2/12/38.

Oil and Gas Detector Apparatus—Part of the sludge from a well being drilled is placed on a conveyor and heated to distill off any hydrocarbons whose presence is indicated by means of a combustion chamber.

U.S. No. 2,230,593. G. L. Hassler, Iss. 2/4/41, Appl. 10/31/38. Assign. Shell Development Co.

Apparatus for Analyzing Gaseous Mixtures—Gas-analyzing cell contains electrolyte which changes upon reaction with gas. Liquid circulation through the cell is broken to insulate a part of the liquid for measuring electrodes.

SEISMOGRAPH PROSPECTING

U.S. No. 2,224,565, J. W. Flude, Iss. 12/10/40, Appl. 8/31/37. Assign. Hercules Powder Co.

Casing for Bore Holes—Shot-hole casing of partially water-proofed cardboard or the like keeps the hole open for several shots and thereafter becomes water-soaked and disintegrates.

U.S. No. 2,229,191, H. C. Schaeffer and R. A. Peterson, Iss. 1/21/41, Appl. 7/28/39. Assign. Consolidated Engineering Corp.

Method of Making Weathering Corrections—Wave paths between bottoms of shot holes are used in addition to the customary refracted-wave paths to determine weathering.

U.S. No. 2,230,002, J. P. Minton, Iss. 1/28/41, Appl. 11/17/37. Assign. Socony-Vacuum Oil Co., Inc.

Method of Calibrating Field Timing Systems—Frequency of a seismograph timing device is compared with a laboratory frequency standard via telephone or radio by means of a carrier wave of an audible frequency which can be effectively transmitted over the system.

U.S. No. 2,231,575, L. W. Gardner, Iss. 2/11/41, Appl. 11/20/39. Assign. Gulf Research & Development Co.

Seismograph Prospecting—Velocity measuring set-up uses at least two pairs of shot-detector spans arranged to cancel errors by using reflection points and detectors in common.

U.S. No. 2,232,612, P. W. Klipsch, Iss. 2/18/41, Appl. 5/1/37. Assign. fifty per cent to E. E. Rosaire.

Recording Seismic Waves—Detector arrays are laid out so that the array lengths are in effect greater than half a wave length with respect to disturbing waves and less than a quarter wave length with respect to reflected waves.

U.S. No. 2,232,613, P. W. Klipsch, Iss. 2/18/41, Appl. 10/1/40. Assign. fifty per cent to E. E. Rosaire.

Seismic Prospecting—A multiple shot array is spread by less than a quarter wave length with respect to reflected waves, but by more than a half wave length with respect to surface noise waves. Shots and detectors may both be spread in arrays such that the combined length of one detector array and the shot array will fall within the limits specified above.

WELL LOGGING

U.S. No. 2,224,635, E. Lipson, Iss. 12/10/40, Appl. 11/28/39. Assign. Casolog, Inc.

Alternating Current Method and Apparatus for Logging Wells—A.C. is applied between a well electrode and a surface electrode. Resultant D.C. due to rectification between the well casing and earth strata is measured between the casing and a grounded electrode.

U.S. No. 2,225, 668, P. Subkow and L. Dillon, Iss. 12/24/40, Appl. 8/28/36. Assign. Union Oil Co.

Method and Apparatus for Logging Drill Holes—Frequency of an oscillator in a well is varied by conditions, and the variations are transmitted to the surface by means of spaced well electrodes and a tuned receiver connected to spaced surface electrodes.

U.S. No. 2,229,604, D. Silverman, Iss. 1/21/41, Appl. 8/19/40. Assign. Stanolind Oil and Gas Co.

Electrical Logging—Phase and amplitude relationships of A.C. picked up in a well logging set-up are indicated by combining the varying A.C. picked up with constant A.C. from the A.C. supply, and rectifying and recording the combined A.C.

U.S. No. 2,230, 502, J. M. Pearson, Iss. 2/4/41, Appl. 8/2/38. Assign. Sperry-Sun Well Surveying Co.

Electrical Prospecting Method and Apparatus—Well is logged with an exploratory coil whose inductance is continually recorded by connecting it in an oscillator circuit, repeatedly adjusting the circuit over a limited range and indicating the point at which oscillations start or stop.

U.S. No. 2,230,999, H. G. Doll, Iss. 2/11/41, Appl. 2/25/39. Assign. Schlumberger Well Surveying Corp.

Methods of Indicating Spontaneous Potentials in Shallow Wells—Shallow wells traversing strata containing liquid of low ion concentration are logged by adding electrolyte and measuring self e.m.f.s.

U.S. No. 2,231,243, R. F. Beers, Iss. 2/11/41, Appl. 6/19/39.

Method of and Means for Analyzing and Determining the Geologic Strata below the Surface of the Earth—Seismic velocities are measured in bore holes by using a sound source of varying frequency and observing the frequency difference between the source and a receiver to determine the transmission time.

U.S. No. 2,231,577, Don. G. C. Hare, Iss. 2/11/41, Appl. 5/29/40. Assign. Texaco Development Co.

Locating Cement—Cement treated with a neutron-absorbing compound is placed in a well and is located by passing a neutron source and detector through the well.

REVIEW

Fourier Series and Boundary Value Problems. Ruel V. Churchill. McGraw-Hill Book Company (1941) 206 pp., $2.50.

This book is an introduction to the mathematical method used in solving boundary value problems in linear partial differential equations of physics and engineering. Careful attention is given to the parts of the theory of orthogonal sets of functions which are necessary in obtaining an expansion of a given function in an infinite series whose terms are the orthogonal set and to the solution of boundary value problems with the aid of these expansions. The treatment of the subject is given from a mathematician's point of view. Theorems are given and in most cases proved, utilizing modern ideas and notation. Emphasis is placed on the general methods for obtaining solutions and on the necessity of formulating the mathematical conditions of a given physical problem in such a manner that a unique solution is obtained.

Chapter I gives a discussion of linear equations and an introduction to the boundary value problem. In Chapter II brief derivations of the partial differential equations for gravity (Laplaces equation), heat, the vibrating string and vibrating membrane are given. The Fourier series is introduced in a problem of the vibrating string.

An excellent discussion of orthogonal functions is presented in Chapter III. A brief discussion of orthogonal vectors leads to the concept of functions as vectors with a condition for orthogonal functions analogous to that for orthogonal vectors. Several theorems concerning the generalized Fourier series are stated and proved.

Fourier series are defined and the conditions for convergence are given in Chapter IV. Chapter V is a continuation of Chapter IV discussing differentiation and integration of Fourier series, and the definition and properties of the Fourier integral.

"Solution of Boundary Value Problems by the Use of Fourier Series and Integrals" is the title of Chapter VI. Emphasis is placed on the fact that a solution to a boundary value problem is only "formal" until it is shown to be unique. Problems of the vibrating string, heat flow, temperatures, vibrating membrane and potential are given. These problems are used to illustrate the method and their variety is rather limited. Chapter VII is devoted to a discussion of the uniqueness of the solutions with theorems given for temperature and potential problems.

The derivation and properties of Bessel Functions are given in Chapter VIII. Solucions are obtained for the temperature in an infinite cylinder, radiation at the surface of the cylinder, and for the vibrations in a circular membrane. Legendre polynomials are defined and discussed in Chapter IX. Solutions for the potential about a spherical surface and for the potential due to a circular plate are given.

At the end of each section numerous problems are given (with answers), and at the end of each chapter a convenient bibliography of reference books is listed.

The reviewer feels that this book is excellent to obtain a clear understanding of the Fourier method for obtaining the solution of boundary value problems. A clear picture is given of the necessity for a complete mathematical statement of the problem so that a unique solution will be obtained, a fact overlooked in many discussions of the subject. However, the book is mathematical in nature rather than physical, and hence the variety of problems actually solved is limited. Thus to the applied physicist or geophysicist, the book is a textbook showing the general methods for solving boundary value problems rather than a reference book for solutions of various problems.

THOMAS BARDEEN

THE SOCIETY ROUND TABLE

MEMBERSHIP APPLICATIONS APPROVED FOR PUBLICATION

The Executive Committee has approved for publication the names of the following candidates for membership in the Society. This publication does not constitute an election, but places the names before the membership at large. If any member has information bearing on the qualification of these nominees, he should send it to the Secretary within thirty days. (Names of sponsors are placed beneath the name of each nominee.)

ACTIVE

Harm Hindrik Brons
P. M. Schoorel (Article III-C-1)

Harry M. Buchner
George E. Wagoner, A. B. Bryan, P. S. Williams

Terence Edwin Dennis
Frank Ittner, R. B. Moran, Jr., Walter A. English

Henri Georges Doll
E. G. Leonardon, E. F. Stratton, R. Henquet

Ardris Haig
Vincent Miller, A. J. Hintze, William Henry Courtier

Thomas Ola Hall
F. Goldstone, G. W. Carr, P. M. Konkel

Henry H. Happel
John D. Marr, F. F. Reynolds, F. L. Bishop

William Bayard Heroy
E. E. Rosaire, Eugene McDermott, L. W. Blau

Robert Campbell Herron
B. Perkins, Jr., M. D. Butler, E. A. Eckhardt

Ward Kelley
Cyril B. Smith, Edward L. De Loach, Richard Williams

Martin Cyrus Kelsey
J. D. Pernell, Darwin S. Renner, Jack R. Cooper

Gustave John Kohler
O. T. Lawhorn, George Augustat, J. E. Jonsson

Frederic Henry Lahee
D. M. Collingwood, H. W. Rose, L. G. Ellis

Robert Wesley Lindsey
C. A. Swartz, E. A. Eckhardt, B. Perkins, Jr.

Federico Luchsinger Centeno
(Article III-C-1)

Charles Conrad Ludwick
F. Goldstone, G. W. Rulfs, Jr., M. O. Gibson

Lowell Kendall Mower
F. Goldstone, W. Hafner, Robert D. Miller

Walter Sigfrid Olson
Alexander Wolf, George D. Mitchell, Jr., Roy L. Lay

Fredrik W. Oudt
F. Goldstone, G. W. Rulfs, Jr., M. O. Gibson

Loyal Davis Palmer
E. A. Eckhardt, V. Vacquier, J. C. Heggblom

Raymond G. Piety
William Henry Courtier, Vincent Miller, R. L. Doan
Duwain Lafayette Scott
R. D. Wyckoff, B. Perkins, Jr., E. A. Eckhardt
Ralph Harold Theis
George B. Lamb, J. E. Gunn, W. J. Osterhoudt
John Bradley Tomlinson
E. A. Eckhardt, W. J. Osterhoudt, G. B. Lamb
Lynn Burdeaux Trombla
Frank Ittner, R. B. Moran, Jr., Walter A. English
Edmond William Westrick
R. D. Wyckoff, E. A. Eckhardt, J. C. Heggblom

ASSOCIATE

Charles Hugh Broussard
W. E. Steele, Jr., R. S. Jackson, J. W. Flude
Herman H. Chanowitz
Jack Desmond, J. M. Maxwell, T. P. Ellsworth
Benjamin Bedinger Cooper
H. Wayne Hoylman, E. A. Eckhardt, J. C. Heggblom
Harry McAllister Cooper, Jr.
B. Perkins, Jr., Charles A. Swartz, E. A. Eckhardt
Eugene Joseph Cronin
John A. Gillin, J. D. Pernell, Paul Farren
John McCullagh
John H. Crowell, A. L. Smith, D. F. Broussard
Chesley Benjamin Pickle
Hugh M. Zenor, G. F. Kaufmann, Thomas R. Warrick
William Wesley Ramsay
H. Wayne Hoylman, E. A. Eckhardt, J. C. Heggblom
John Lawrence Robinson, Jr.
Charles A. Swartz, C. H. Dresbach, E. A. Eckhardt
Samuel Eberle Sims
J. P. Black, Wilton W. La Rue, Homer I. Henderson
Andres Lopez Vasquez
F. L. Bishop, Kenneth Burg (Article III-C-1)

STUDENT

Joseph Gilbert Hatheway
C. A. Heiland, J. E. Hawkins, Dart Wantland
Howard Edward Itten
Dart Wantland, C. A. Heiland, J. E. Hawkins
Walter Eli Martin
J. E. Hawkins, C. A. Heiland, Dart Wantland
George Nelson Meade
C. A. Heiland, Dart Wantland, J. E. Hawkins
Billy Edward Richards
W. S. Levings, Dart Wantland, J. E. Hawkins
Harrison EdFred Stommel
Dart Wantland, C. A. Heiland, J. E. Hawkins

THE ELEVENTH ANNUAL MEETING OF THE SOCIETY OF EXPLORATION GEOPHYSICISTS, HOUSTON, TEXAS, APRIL 1-3, 1941

The Eleventh Annual Meeting of the Society of Exploration Geophysicists was held in Houston, Texas, at the Rice Hotel, April 1–3, 1941. The meeting was held concurrently with those of the American Association of Petroleum Geologists and the Society of Economic Paleontologists and Mineralogists. On Tuesday, April 1, the technical sessions were held in the Main Ballroom, while on Wednesday, April 2, and Thursday afternoon, April 3, sessions were held in the South American Room. Thursday morning a joint session was held with the other two associations, again in the Main Ballroom.

It was by far the most successful meeting ever held by the Society. Despite the failure of some to register, 704 were registered as being in attendance. This number included 305 members, 240 non-members, and 159 wives.

An excellent program of papers was arranged by members of the Program and Arrangements Committee working under Chairman H. B. Peacock. A copy of the program is to be mailed to each member who was unable to attend, and a few extra copies are available for others who may desire them. The majority of papers listed in the program will be published in GEOPHYSICS during the coming year.

MEMBERS REGISTERED AT THE ELEVENTH ANNUAL MEETING

The following members registered at the Eleventh Annual Meeting of the Society of Exploration Geophysicists, Houston, Texas, April 1-3, 1941: Joseph L. Adler, Frank T. Allen, T. L. Allen, Manuel Alvarez, Jr., John F. Anderson, Leland L. Antes, M. A. Arthur, L. F. Athy, Glen E. Bader, H. E. Banta, L. A. M.Barnette, A. J. Barthelmes, Joseph W. Bastian, W. O. Bazhaw, C. B. Bazzoni, A. F. Beck, H. C. Becker, M. L. Benke, Roy F. Bennett, A. C. Bertram, John L. Bible, R. N. Bills, F. L. Bishop, J. P. Black, L. W. Blau, W. T. Born, Merle C. Bowsky, R. M. Bradley, James A. Brooks, Jr., David F. Broussard, C. H. Broussard, Hart Brown, Leon D. Brown, Jr., A. B. Bryan, Carl L. Bryan, M. R. Budd, J. H. Burney, R. H. Burton, W. W. Butler, F. F. Campbell, Wm. R. Campbell, D. P. Carlton, Ray Carter, Harvey Cash, Jr., Lyman Chandler, Jr., V. E. Child, R. W. Clark, R. Clare Coffin, Paul Conrad, Jack R. Cooper, Henry C. Cortes, Laurence G. Cowles, A. P. Crary, John H. Crowell, Drexler Dana, Edward, L. DeLoach, Alexander Deussen, Arthur E. Dietert, R. L. Doan, John Doering, Chester J. Donnally, Norvel Douglas, Charles A. Durham, Karl Dyk, E. A. Eckhardt, A. N. Eby, J. Brian Eby, Joseph D. Eisler, Dan F. Elam, L. G. Ellis, H. M. Evjen, H. M. Falkenhagen, L. Y. Faust, Kenneth H. Ferguson, John L. Ferguson, Craig Ferris, John W. Flude, F. Julius Fohs, Edward S. Foster, Jr., L. I. Freeman, Alex Frosch, Ewin D. Gaby, J. F. Gallie, Derry H. Gardner, G. A. Garrett, C. H. Gerdes, H. A. Gibbon, M. O. Gibson, Andrew Gilmour, John M. Golden, F. Goldstone, J. S. Gomez, Martin J. Gould, I. M. Griffin, Jr., J. E. Gunn, W. Hafner, A. B. Hamil, Willis W. Hardy, W. J. Harkey, T. I. Harkins, G. H. Harrington, Sidon Harris, J. E. Hawkins, C. J. Haynes, E. I. Head, M. E. Hibbler, Herbert F. Hieatt, Ray H. Hillyer, A. J. Hintze, Malvin G. Hoffman, W. B. Hogg, C. W. Horton, H. M. Houghton, Chas. E. Houston, Leo Horvitz, Lynn G. Howell, Darrell S. Hughes, John F. Imle, A. I. Innes, R. S. Jackson, J. E. Jett, Curtis H. Johnson, Sidney A. Judson, F. M. Kannenstine, J. C. Karcher, G. D.Kendall, J. M. Kendall, W. B. Kendall, Paul W. Klipsch, A. L. Ladner, G. B. Lamb, Wilton W. La Rue, O. T. Lawhorn, Roy L. Lay, W. B. Lee, O. C. Lester, Jr., Edward Lipson, J. M. Lohse, J. B. Lovejoy, C. R. Lowe, M. M. McCaleb, Geo. C. McGhee, E. V.

McCollum, H. J. McCready, Eugene McDermott, John E. McGee, A. E. McKay, Ethel Ward McLemore, C. T. MacAllister, J. B. Macelwane, O. B. Manes, W. H. Mannes, John D. Marr, E. Maxwell, C. G. McBurney, Ben S. Melton, J. C. Menefee, H. W. Merritt, Robert D. Miller, J. P. Minton, Geo. D. Mitchell, Jr., George P. Montgomery, Jr., James A. Moore, James L. Morris, Arthur A. Moore, Jr., Marion J. Moore, L. M. Mott-Smith, Morton Mott-Smith, Whitman D. Mounce, D. S. Muzzey, Jr., Paul E. Nash, L. L. Nettleton, W. W. Newton, R. G. Nisle, Willard North, Decatur O'Brien, W. J. Osterhoudt, J. E. Owen, Geo. L. Parkhurst, J. H. Pernell, H. B. Peacock, R. A. Peterson, H. Hart Partley, Wm. R. Ransone, Robert H. Ray, Cecil E. Reel, Darwin S. Renner, F. F. Reynolds, E. R. Rice, Jr., Norman Ricker, O. F. Ritzmann, Antonio Garcia Rojas, J. F. Rollins, Frederick Romberg, E. E. Rosaire, H. W. Rose, Charles M. Ross, W. W. Ruhlen, G. W. Rulfs, Jr., W. M. Rust, Jr., R. B. Rutledge, C. W. Sanders, L. W. Sanders, W. G. Saville, Hugh C. Schaeffer, Sidney Schafer, David Scharf, Henry Schoellhorn, J. P. Schumacher, A. T. Schwennesen, Frank Searcy, A. L. Selig, W. A. Seyffert, Joseph A. Sharpe, E. S. Sherar, Stuart Sherar, H. F. Shore, T. R. Shugart, Daniel Silverman, Harry H. Sisson, M. M. Slotnick, W. G. Smiley, Jr., Neal Smith, George B. Somers, Louis Statham, Noel H. Stearn, William E. Steele, Jr., Elisabeth Stiles, H. W. Straley, III, G. Stubbe, Olaf Francis Sundt, Albert Taylor, Josiah Taylor, M. C. Terry, Virgil W. Teufel, Earl Thomas, J. W. Thomas, R. R. Thompson, Erik Thomsen, John B. Tomlinson, E. J. Toomey, Frederick A. Tompkins, E. E. Unger, R. J. Urick, F. A. Van Melle, Jack Van Valkenburgh, E. H. Vallat, R. F. Van Cleave, Stefan Von Croy, Geo. E. Wagoner, J. S. Watt, B. B. Weatherby, S. P. Weatherby, Paul Weaver, John F. Weinzierl, Wm. M. Wells, S. S. West, G. H. Westby, George S. Wheaton, Rex H. White, P. S. Williams, Darrell Williams, John H. Wilson, R. M. Wilson, J. R. Winnek, Alexander Wolf, R. D. Wyckoff, B. B. Zavoico.

MINUTES OF THE ANNUAL BUSINESS MEETING OF THE SOCIETY OF EXPLORATION GEOPHYSICISTS, HELD IN THE MAIN BALLROOM OF THE RICE HOTEL, HOUSTON, TEXAS, APRIL 1, 1941

The meeting was called to order by President W. T. Born in the Main Ballroom of the Rice Hotel, Houston, Texas, at 9:45 A.M., April 1, 1941. The minutes of the business meetings held at Chicago in 1940 were read by the Secretary-Treasurer, Andrew Gilmour. Upon motion being made and seconded, the minutes were unanimously approved.

The Secretary-Treasurer read a brief report of the financial position of the Society as of December 31, 1940. The Society showed an increase in assets of $1,800.56 over 1939. The membership was given as 892.

President Born thanked the retiring officers for their cooperation and assistance in administering the affairs of the Society. He also announced the results of the balloting, as follows:

President, H. B. Peacock
Vice-President, Frank Goldstone
Editor, R. D. Wyckoff
Secretary-Treasurer, W. M. Rust, Jr.

On motion being duly made, seconded, and passed, the meeting was adjourned.

Respectfully submitted,

ANDREW GILMOUR, *Secretary-Treasurer*

NOTE ON THE BALLOT FOR THE ELECTION OF OFFICERS OF THE SOCIETY OF EXPLORATION GEOPHYSICISTS FOR THE YEAR APRIL, 1941–APRIL, 1942

In the 1941 election of officers 415 members mailed ballots to the Secretary-Treasurer. Of these 43 had to be discarded because the voting member had not paid his dues at least ten days before the Annual Meeting, as required by the Society Constitution, and 1 arrived too late. Six others had to be discarded because the voting member neglected to write his name on the outside of the ballot envelope. Attention of members is called to the provision in the Constitution that: "Ballots to be valid must be enclosed in an envelope carrying on the outside the written signature of the member submitting the ballot, and must be received by the Secretary-Treasurer at his officially recognized address not later than ten days prior to the Annual Meeting. Only ballots received from members in good standing as of a date ten days prior to the Annual Meeting shall be valid."

Respectfully submitted,

ANDREW GILMOUR, *Secretary-Treasurer*

ANNUAL REPORT OF THE SECRETARY-TREASURER OF THE SOCIETY OF EXPLORATION GEOPHYSICISTS

The increase in membership in the Society of Exploration Geophysicists is indicated in the following figures, compiled as of December 31, 1940:

Year	*Honorary*	*Active*	*Associate*	*Total*	*Increase*
1930	0	34	5	39	
1931	2	68	11	81	42
1932	2	83	11	96	15
1933	2	91	10	103	7
1934	2	141	23	166	63
1935	2	156	31	189	23
1936	4	195	34	233	44
1937	4	367	112	483	250
1938	4	510	158	672	189
1939	4	632	185	821	149
1940	4	700	188	892	71

In addition to the assets shown on the balance sheet which follows, as of December 31, the Society had on hand approximately 5600 copies of past publications. At a minimum value of $2 each, the cost to members, these total $11,200.

The financial condition of the Society of Exploration Geophysicists as of December 31, 1940, is shown in the following report, reproduced from the annual audit:

BALANCE SHEET—DECEMBER 31, 1941

ASSETS

Current			
Cash			
In Banks		$8,962.18	
Accounts Receivable			
Membership Dues	$457.50		
Advertising	777.80		
Reprints	457.51		
Back Numbers	109.40		
Subscriptions	76.50	1,878.71	$10,840.89
Office Equipment			
Steel File and Bookcase		$ 31.50	
Less: Allowance for Depreciation		7.80	23.70
			$10,864.59

LIABILITIES

Current			
Accounts Payable			
For Expenses, etc.			$ 227.17
Deferred Income			
Prepaid Advertising, Dues and Subscriptions			306.85
Surplus			
Balance January 1, 1940		$8,530.01	
Add			
Increase from Current Year Operations—Per Statement of Income and Expense		1,800.56	10,330.57
			$10,864.59

INCOME AND EXPENSE—DECEMBER 31, 1940

INCOME

Membership Dues			
Dues	$4,322.50		
Reinstatements	8.00	$4,330.50	
Publications			
Advertising	$2,595.25		
Subscriptions	1,221.78		
Back Numbers	739.70		
Reprints	365.61	4,922.34	
Other Income			
Interest Received	$ 86.46		
Credit Balance Written Off	9.10		
Commissions on Publications	2.50	98.06	
		$9,350.90	
Less Discounts to Colleges, etc.			
On Subscriptions and Back Numbers		82.20	$9,268.70

COSTS AND EXPENSES

Publication Costs				
Geophysics:				
Vol. V No. 1—140 Pages		$ 799.32		
No. 2—122 Pages		753.38		
No. 3—134 Pages		984.68		
No. 4—166 Pages		1,081.38		
		$3,618.76		
Reprints		362.31	$3,981.07	
Expenses				
Salary—Business Manager		$1,200.00		
Commissions:				
Advertising:				
Business Manager	$273.81			
Agencies	306.90			
Subscriptions, etc.				
Agencies	77.80	658.51		
Bad Debts		390.02		
Annual Meeting Expense:				
Programs, Circulars, and Registration Cards	$161.26			
Telephone and Telegraph	59.86			
Stenographers and Typewriter Rent	40.00			
Signs, Badges, etc.	31.30			
Luncheon—Net	15.28	307.70		
Postage and Box Rent		289.71		
Stationery and Office Supplies		200.12		
Traveling Expense		145.17		
Auditing		104.50		
Telephone and Telegraph		98.33		
Binding		50.35		
Society Card—A.A.P.G.		15.00		
Express and Freight		13.06		
Bond Premium		10.00		
Depreciation		3.15		
Bank Charges		1.45	3,487.07	7,468.14
Excess of Income over Costs and Expenses				$1,800.56

Respectfully submitted,
ANDREW GILMOUR, *Secretary-Treasurer*

PERSONAL ITEMS

(Members are requested to send material for inclusion herein to J. F. Gallie, P. O. Box 777, Austin, Texas.)

LYMAN CHANDLER, JR., of the National Geophysical Company, has been transferred from Longview to Rosenberg, Texas, where his postal address is P. O. Box 112.

J. H. NEIDERT is returning from Venezuela, where he has been in the employ of the Standard Oil Company of Venezuela, and will be located at 1231 Camden Street, San Antonio, Texas.

R. H. DANA may be addressed c/o Stanolind Oil and Gas Company, P. O. Box 148, Mangum, Oklahoma.

The Times-Mirror Press advises that the first edition of *Exploration Geophysics*, by J. J. JAKOSKY, has been exhausted, but that the second impression is now available.

ERNEST DISSLER is now seismograph computer for the Indian Territory Illuminating Oil Company, P. O. Box 1251, Bartlesville, Oklahoma.

LAWRENCE A. GOEBEL, of the Carter Oil Company, has been transferred from Many to P. O. Box 23, Monroe, Louisiana.

JOHN C. HOFFMAN may be addressed at P. O. Box 255, Durant, Oklahoma.

J. P. FARIS, JR., is now First Lieutenant with the Corps of Engineers, Fort Sam Houston, Texas.

KENNETH K. KENNEDY has returned from New Zealand and may be addressed c/o Carter Oil Company, Many, Louisiana.

The Independent Petroleum Association of America recently published a booklet on "The Independent Oil Producer and His Problems."

S. P. WEATHERBY announces that he is no longer associated with the Seismograph Service Corporation, having returned to work for the Independent Exploration Company as District Representative in Tulsa, Oklahoma. His office address is 407 National Bank of Tulsa Building.

Captain GEORGE B. KAISER is located at 148 Cedar Avenue, Long Branch, New Jersey.

H. M. HORTON has his office at 521 Citizens Bank Building, Evansville, Indiana.

The first edition of *Geophysical Prospecting for Oil*, by L. L. NETTLETON, was soon sold out, but a second printing is now available.

HARRY L. THOMSEN may be addressed c/o Shell Oil Company, Incorporated, P. O. Box 999, Bakersfield, California.

J. W. THOMAS, JR., of the Stanolind Oil and Gas Company, has been transferred from Garden City to Hays, Kansas.

GEORGE H. HAZEN may be addressed c/o I. A. Manning, Socony-Vacuum Oil Company of Colombia, Barranquilla, Colombia.

C. T. MACALLISTER is now Gravity Meter Supervisor for the Independent Exploration Company, 2011 Esperson Building, Houston, Texas.

A. V. HARGIS is studying Petroleum Engineering at the University of Texas in Austin, and is located at 2802 Rio Grande.

WALTER T. WELLS, Chairman of the Board of Directors of the Lane-Wells Company, announces the election of M. E. MONTROSE as a Vice-President.

LYNN D. ERVIN is on leave of absence from the Stanolind Oil and Gas Company and may be addressed c/o Company H, Candidates' Class, Marine Corps School, M. B., Quantico, Virginia.

STANLEY W. WILCOX has transferred from Jackson, Mississippi, to Wichita, Kansas, where he has opened a District Office for Seismograph Service Corporation. The postal address is P. O. Box 1503.

L. H. WISE, formerly with the National Geophysical Company, is now with the Stanolind Oil and Gas Company, P. O. Box 591, Tulsa, Oklahoma.

DWIGHT E. WARD, of the Carter Oil Company, has moved from Holdrege to Lexington, Nebraska, where his address is P. O. Box 585.

MORRIS BRENNER, formerly with the Independent Exploration Company, is now Field Engineer for Molson and Company of Tucson, Arizona. He may be addressed c/o R. C. Munguia, Casa B-4, Empalme, Sonora, Mexico.

R. DAVIES may be addressed c/o D'Arcy Exploration Company, Burgage Manor, Southwell, Notts, England.

WILLIAM R. CAMPBELL, of the Stanolind Oil and Gas Company, has been transferred to the geological department, and is serving as a scout in the Houston area. He may be addressed at P. O. Box 3092, Houston, Texas.

PAUL V. HENDERSON, formerly with the Geotechnical Corporation, is now with the General Geophysical Company, 2513–14 Gulf Building, Houston, Texas.

B. G. HUBNER, JR., has returned from Cuba and is located at P. O. Box 299, Forest, Mississippi, c/o National Geophysical Company.

LOUIS J. SMITH, of the Shell Oil Company, Incorporated, has been transferred from Centralia, Illinois, to P. O. Box 238, Stroud, Oklahmoa.

PAUL H. BOOTS has advised the Society of his change of address from Barcelona, Venezuela, to c/o Gulf Research and Development Company, P. O. Box 2038, Pittsburgh, Pennsylvania.

DONALD R. BROWN has left Karachi, India, and may be addressed c/o Bataafsche Petroleum Maatschappij, Batavia-Centrum, Java, Netherlands East Indies.

DAVID M. WEBER is on the Interpretation Staff of the Gulf Research and Development Company, P. O. Box 2038, Pittsburgh, Pennsylvania.

MARION H. GILMORE, Assistant Magnetic and Seismological Observer with the United States Coast and Geodetic Survey, is now located at 1426 United States Post Office and Court House, Los Angeles, California.

MAYNARD H. JAMESON is a student in the Graduate School of Business Administration of Harvard University. His address is Mellon Hall B44, Soldiers Field Station, Boston, Massachusetts.

J. C. KARCHER is serving on the standing committee of the Independent Petroleum Association of America.

L. O. SEAMAN should be addressed c/o Sinclair Prairie Oil Company, P. O. Box 521, Tulsa, Oklahoma.

VINCENT EMANUEL returned to the United States from Italy in January, and may be addressed c/o Geophysical Laboratory, Stanolind Oil and Gas Company, P. O. Box 591, Tulsa, Oklahoma.

F. O. MORTLOCK is on leave of absence from the Gulf Research and Development Company and is serving with the Bureau of Ordnance, United States Navy. Until June 30, and possibly later, he may be addressed c/o Commanding Officer, Sixteenth Naval District, Cavite, Philippine Islands.

JAMES C. TEMPLETON, Managing Director of the Geophysical Prospecting Company, Limited, announces a change in address from 9/11 Copthall Avenue to 2a, Guildhall Chambers, Basinghall Street, London, E. C. 2, England.

J. C. HEGGBLOM has been transferred from Fresno to P. O. Box 1062, Modesto, California.

Well Surveys, Incorporated, announce the election of S. A. SCHERBATSKOY as Vice-President. He has been with the Company for the past five years.

WAYNE H. DENNING, of the United Geophysical Company, is currently in Brazil. He may be addressed as before, 1255 East Green Street, Pasadena, California.

The Lane-Wells Company has issued a well-illustrated bulletin on the "Lane-Wells Electrolog," and announce that copies are available through any Branch Office. The bulletin describes the electrical logging of uncased hole.

JACK R. COOPER is now serving as a Geophysical Research Engineer with the Stanolind Oil and Gas Company. His address is 1527 South Atlanta Avenue, Tulsa, Oklahoma.

E. T. NICHOLS is returning to the States from Sumatra and will be located at 4499 Eleventh Street, Riverside, California.

H. W. STRALEY, III, advises that he spent most of last summer in the Interior Basins in the Appalachian Plateau for the Worthington Development Association. He is now located in Waco, Texas, where his address is P. O. Box 363.

R. H. WOODWARD, formerly with the Schlumberger Well Surveying Corporation, is acting as Research Associate at the Massachusetts Institute of Technology. His address is Apartment 25, 19 Everett Street, Cambridge, Massachusetts.

HENRY SCHOELLHORN, III, of the Gulf Research and Development Company, may be addressed at P. O. Box 31, Gretna, Louisiana.

JOHN S. IVY is located at 3247 Inwood Drive, Houston, Texas.

G. E. HIGGINS is serving as geologist with Trinidad Leaseholds, Limited, at Pointe-a-Pierre, Trinidad, British West Indies.

L. M. MOTT-SMITH has sold out his interest in the Mott-Smith Corporation to V. J. MEYER. For the present Dr. Mott-Smith may be addressed at 1012 Shadder Way, Houston, Texas.

F. H. AGEE is located at P. O. Box 608, Morgan City, Louisiana.

CHESTER J. DONNALLY, of the Western Geophysical Company, is located in Dallas, Texas, at 902 Southland Life Building.

FRANCIS H. CADY may be addressed c/o Carter Oil Company, P. O. Box 252, Aberdeen, Mississippi.

DARRELL S. HUGHES, W. M. RUST, JR., W. D. MOUNCE, L. G. HOWELL, LEO HORVITZ, and M. M. SLOTNICK have addressed the Geophysical Prospecting Methods class at the University of Texas at various times during the current semester.

C. E. WILLIAMS has been transferred from La Dorada to Barranquilla, Colombia, where he may be addressed c/o T. F. Roche, Tex. Pet. Co., with the air mail box number being Apartado Aereo 32.

J. M. KILBORN, Magnetometer Operator with the Gulf Research and Development Company, has been transferred from Columbus to Cuero, Texas, with his postal address being P. O. Box 534.

H. M. EVJEN is now with the Elflex Company in Houston, Texas. His residence address is 3423 Robin Hood Street.

SAM ZIMERMAN, of the Carter Oil Company, may be addressed at P. O. Box 270, Waurika, Oklahoma.

The Post Office Department has advised that R. F. ACKER is now located at 541 North Gerona Avenue, San Gabriel, California.

C. H. DIX has moved from New York to 1455 North Los Robles Avenue, Pasadena, California.

Engineering Laboratories, Incorporated, announce the election of R. P. GREEN, Chief Engineer, as Vice-President, and the election of W. R. COLEMAN, formerly General Manager, as Secretary and Treasurer.

JACK MASON may be addressed at 3430 Elliott, San Diego, California.

J. W. DE BRUYN has left Karachi, India, and is with B. P. M., Pladjoe, Netherlands East Indies.

R. B. MORAN, JR., has moved from La Canada to 1412 Flower Street, Bakersfield, California.

LOUIS J. PADDISON is with the Stanolind Oil and Gas Company, P. O. Box 711, Tyler, Texas.

V. T. DONNELLY is Gravity Meter Party Chief with the Land and Geological Department of the Arkansas Fuel Oil Company, Shreveport, Louisiana.

J. B. JACKSON, of B. P. M., has been transferred from Burma to Bandjermasin, Borneo.

HARRY H. SISSON is with the General Geophysical Company, 2513–14 Gulf Building, Houston, Texas.

D. C. BLEVINS, III, has returned from the Netherlands East Indies to his position with Geophysical Service, Incorporated, 1311 Republic Bank Building, Dallas, Texas.

E. I. HEAD has been transferred from Columbus to 1010 North Gonzales, Cuero, Texas.

JOHN H. WILSON, of the Independent Exploration Company, will henceforth supervise the interpretation of all gravity work.